

SPECIAL PAPERS IN PALAEOLOGY

Number 7

SHELL STRUCTURE OF
THE CRANIACEA AND
OTHER CALCAREOUS
INARTICULATE
BRACHIOPODA

BY

A. WILLIAMS AND A. D. WRIGHT

PUBLISHED BY
THE PALAEOLOGICAL ASSOCIATION
LONDON

Price £1.50

SPECIAL PAPERS IN PALAEOLOGY NO. 7

SHELL STRUCTURE OF
THE CRANIACEA AND
OTHER CALCAREOUS
INARTICULATE
BRACHIOPODA

BY
A. WILLIAMS
AND
A. D. WRIGHT

With 15 plates

THE PALAEOLOGICAL ASSOCIATION
LONDON

© THE PALAEOLOGICAL ASSOCIATION, 1970

PRINTED IN GREAT BRITAIN

CONTENTS

	<i>Page</i>
Abstract	5
Introduction	7
Materials and methods	8
Shell structure of living <i>Crania</i>	9
The mantle edge	9
Secretion of the brachial valve	9
Secretion of the pedicle valve	18
Microstructure of the muscle scars	25
Growth and morphology of caeca	30
Shell structure of fossil craniaceans	33
<i>Isocrania</i>	33
<i>Danocrania</i>	34
<i>Ancistrocrania</i>	35
<i>Craniscus</i>	36
<i>Philhedra</i>	38
<i>Acanthocrania</i>	38
<i>Petrocrania</i>	39
<i>Pseudocrania</i> and <i>Orthisocrania</i>	42
Shell structure of the Craniopsidae	43
Shell structure of the Obolellida	44
Conclusions	45
Acknowledgements	50
References	51

ABSTRACT. The brachial valve of living *Crania* is triple-layered with an outer periostracum consisting of a mucopolysaccharide layer bounded by protein membranes and protected by an impersistent, external film of mucopolysaccharide, a primary calcareous layer made up mainly of acicular crystallites and a secondary calcareous layer composed of laminae of calcite ensheathed in protein sheets. In the pedicle valve, the secondary layer is not developed and the external mucopolysaccharide film acts as an adhesive by which the valve is attached to the substrate. The myotest in both valves is differentiated as a series of calcitic blades disposed more or less normal to the internal surface. Branched caeca permeate both valves and act as storage centres for polysaccharides and proteins but are not connected to the periostracum by a brush as in the articulate brachiopods. Studies of fossil craniaceans have shown that the structure of the pedicle valve, unlike that of the brachial valve, has changed repeatedly during the evolution of the group. Such variation includes a fully developed succession in the unattached *Pseudocrania* which is identical with that of the brachial valve, the loss of punctation in *Petrocrania*, the secretion of coarse crystallites instead of laminae in the thick secondary shell of certain Mesozoic craniaceans like *Ancistrocrania* and *Isocrania*, and the lack or negligible deposition of calcareous shell in some early stocks like *Philhedra* and *Acanthocrania*.

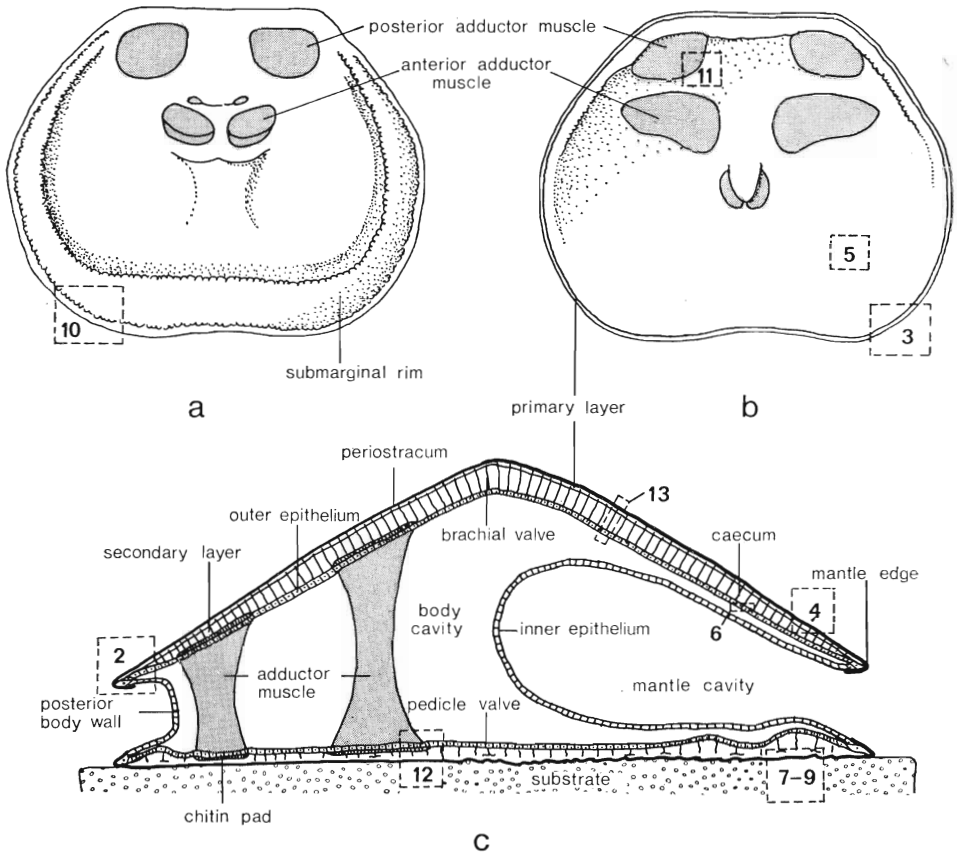
A laminar secondary layer is also characteristic of two other groups of calcareous-shelled inarticulates, the Craniopsidae and Obolellida, but is not regarded as indicating any close relationship between them and the Craniacea.

INTRODUCTION

THE Craniacea are unusual inarticulate brachiopods in that their shell is composed not of protein, chitin, and calcium phosphate but of protein and calcium carbonate, the diagnostic ingredients of the articulate skeleton. The superfamily is all the more remarkable because, having first appeared in the Ordovician after basic divergences within the phylum had led to the establishment of the Articulata, it has survived to the present day; and, although it includes only fourteen living species assigned to three genera, representatives of the commonest genus, *Crania*, are widely distributed in all oceans. Other inarticulates with calcareous shells were much less successful. The Obolélida appeared briefly in the Lower and Middle Cambrian. The Craniopsidae and the Trimerellacea are first recorded in the Ordovician only slightly later than the earliest undoubted craniacean. Yet the Trimerellacea became extinct before the end of the Silurian and the Craniopsidae before the end of the Carboniferous. As will be shown later, the craniopsid shell is like the craniacean in its ultrastructure and possibly reflects a closer connection between the two stocks than is currently favoured. Even the shell of the obolélide *Trematobolus* bears a resemblance to that of *Crania*. The crystal form and fabric of the trimerellacean shell, however, are quite different. Jaanusson (1966, p. 279), considering the long-known fact that the trimerellacean shell is invariably either recrystallized or dissolved away, concluded that the mineral component of the exoskeleton must have been aragonite. His novel interpretation certainly explains why a gross drusy mosaic has replaced the shells of contemporaneous trimerellaceans and molluscs from the Silurian Slite and Hemse beds of Gotland but not those of articulate brachiopods taken from the same assemblages, the fabric of which mostly survives in an identifiable form. Our own perfunctory search for signs of a relict ultrastructure in sections of *Trimerella lindstroemi* (Dall) from the Slite Beds at Lärbro, where they occur with well-preserved fragments of cryptostomatid bryozoans, has confirmed Jaanusson's findings; and we accept his explanation of the anomaly, as the only observed traces of original growth surfaces seen in our sections were a few sporadic trails of impurities parallel with the valve outlines. Consequently, the Trimerellacea will not be considered further.

The shell of *Crania*, the general structure of which (text-fig. 1) is known through the classic studies of Blochmann (1892), is much more complex than that characteristic of even the punctate Articulata. Apart from basic similarities like the presence of caeca permeating an exoskeleton which is greatly modified in the regions of the muscle bases, the calcareous succession of the brachial valve is fully differentiated into primary and secondary layers whereas the mineral part of the pedicle valve consists exclusively of primary shell. Consequently, the shell structure of *Crania* is discussed in four sections: that of the brachial valve which has proved to be standard throughout craniacean history, that of the pedicle valve, the modification effected by the emplacement of muscle bases, and the nature and growth of caeca in relation to the shell. Only the fabric of the pedicle valve and, less importantly, the variation in development of ventral caeca have changed significantly in the course of craniacean evolution. They are, however, important enough to warrant a section devoted to consideration of every genus for which specimens were

SHELL STRUCTURE OF THE CRANIACEA



TEXT-FIG. 1. Diagrammatic representation of the interiors of the pedicle (*a*) and brachial (*b*) valves, and a submedial section of a complete shell through the adductor muscles (*c*) to show the principal morphological and anatomical features referred to in the text, and to indicate areas (enclosed in broken lines) that are illustrated in more detail in the numbered text-figures.

available, before describing the shell fabric of the Craniopsidae and the Obolellida and concluding with comments on the evolution of the calcareous-shelled Inarticulata.

Materials and methods. Detailed studies of the mantle and shell of living *Crania* required the removal of the respective mineral or organic parts of specimens. For electron microscope study of the mantle, animals were fixed in 4% glutaraldehyde made up in 3% sodium chloride buffered to pH 7.2 with phosphate buffer. They were subsequently decalcified in 10% EDTA, washed in sucrose and treated for 1 hour with 2% osmic acid; all these solutions were buffered to pH 7.2 with phosphate buffer. Following dehydration, specimens were embedded in an epoxy resin and the sections stained with aqueous uranyl acetate and aqueous lead citrate. For histochemical studies under the light microscope, specimens were fixed in Bouin's fluid, and after decalcification in 5.5% EDTA and embedding in Ester wax, sections were stained with Haemalun and subjected to a periodic acid-Schiff test.

For the study of sections of fossil shells, specimens in the rock were preferred to those free of matrix which may have suffered significant though microscopic fabric changes through weathering. When examination of fossil surfaces became necessary, they were first cleaned ultrasonically in a weak detergent followed by acetone. Removal of the periostracum, mantle, and caecum for the scrutiny of exoskeletal surfaces or sections of living *Crania* was best effected by leaving specimens in a papain

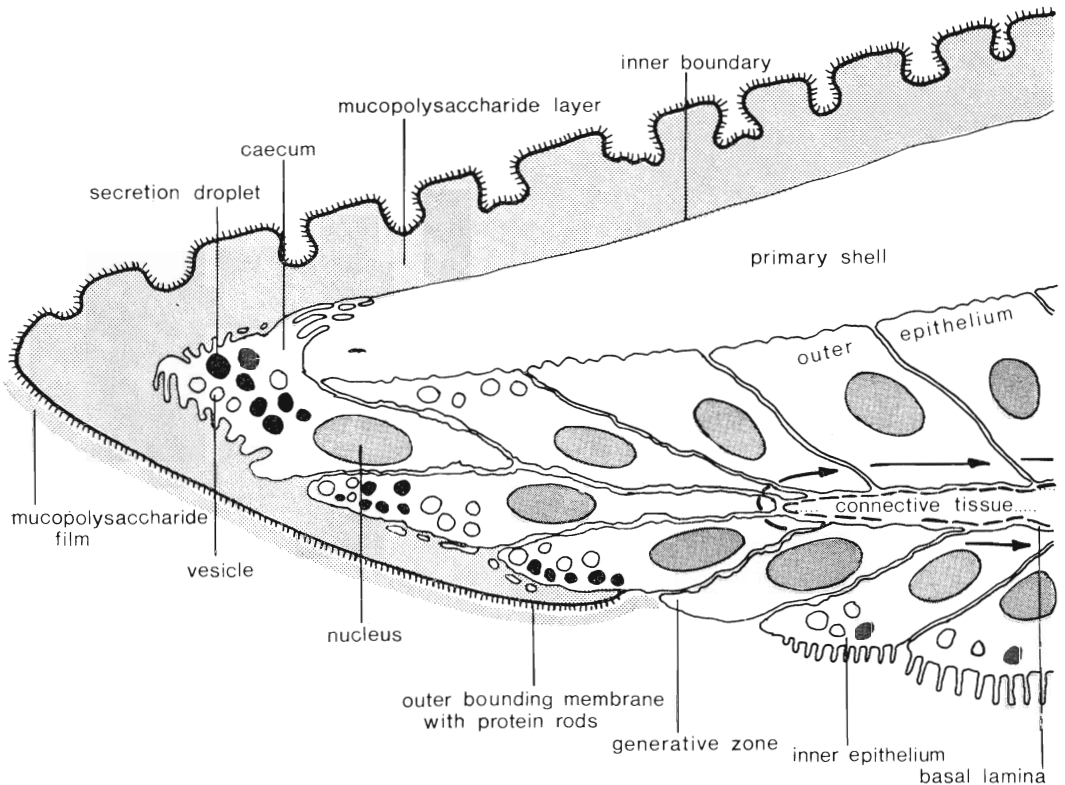
solution (0.1 gm. per ml.) overnight at 37 °C, and then cleaning in an ultrasonic tank in a weak detergent followed by acetone. For study under the scanning electron microscope (the Cambridge 'Stereoscan'), shell surfaces and polished sections of shells, the latter having been etched in 2% EDTA for between 20 minutes and 1 hour according to geological age, were coated with gold-palladium.

SHELL STRUCTURE OF LIVING *CRANIA*

The mantle edge. The processes governing secretion of the exoskeleton of *Crania anomala* (Müller) are essentially the same as those controlling deposition of the articulate shell (Williams 1968), but there are important differences in the morphology of the edge of the mantle lining the valves, and in the constitution of the shell (Pl. 1, fig. 1). Particularly striking is the absence of setae as well as the mantle lobes and grooves accommodating them, although this does not affect the dual nature of the epithelium which makes up the mantle. As in articulates, both outer and inner epithelia are immediately identifiable on either side of a narrow generative zone (Pl. 1, fig. 2). This zone, which forms a continuous strip just within the circular edge of each valve, is also highly distinctive with its small cells separated from one another by anastomosing intercellular spaces, and packed with relatively large nuclei and granular endoplasmic reticulum. Within the intercellular spaces of the generative zone a median sheet of connective tissue develops concomitantly with the proliferation of cells. Hexagonally stacked microvilli with more widely spaced filaments appear on the external surfaces of those cells which are produced internal to the generative zone to become part of the inner epithelium (Pl. 3, fig. 1, lower half). Cells forming peripherally to the generative zone push one another around the epithelial fold constituting the edge of the mantle, to become incorporated within the outer epithelium. Thus each outer epithelial cell can be thought of as part of a 'conveyor belt' moving around an axis represented by the connective tissue hinge. In this way the free surface of each cell always faces outwards while it is rotated through 180°, and is responsible for the secretion of a succession of organic and mineral substances, which explains the high frequency of vesicles and secretion droplets within the rotating cells (text-fig. 2). Such secretory sequences or regimes have so far proved to be constant for groups of brachiopods up to ordinal status. In *Crania*, however, there are differences even between the development of the valves; and although these differences are minor and are related to cementation of the pedicle valve to a substrate, they prompt separate consideration of each valve. One other point should be noted about *Crania* because it has a bearing on the presentation of evidence concerning the ultramicroscopic growth of the shell. The junction between the periostracum and the epithelial surface which secretes it, is weak and was invariably disrupted by decalcification of the shell during the preparation of animals for sectioning. Consequently the first-formed part of the periostracum has not yet been seen *in situ* although its correct position on the inner surface of the mantle edge of either valve is easily reconstructed, and the account given below must be substantially correct.

Secretion of the brachial valve. Deposition of the brachial valve proceeds in the following manner (text-fig. 2). When an outer epithelial cell is first differentiated from the generative zone, it starts secreting an impersistent mucopolysaccharide film up to 50 nm. thick. The mucopolysaccharide is permeated by an open network of fibrils which extend outwards as much as 70 nm., but more usually about 25 nm., from a series of

protein rods. These rods, like their homologues in the shell succession of articulate brachiopods, are the first durable constituents of the periostracum to be assembled beneath the mucopolysaccharide by the migrating outer epithelial cell. They are disposed in closely packed rows about 15 nm. apart and are connected with one another by laterally extending fibrils (Pl. 2, figs. 2, 4). Each rod is made up of a bulbous top about 15 nm. in diameter and a supporting pedestal up to 12 nm. high which is continuous



TEXT-FIG. 2. Stylized longitudinal section of the edge of the brachial valve of *Crania* showing the origin of the outer epithelium and a caecum in relationship to secretion of the periostracum and primary shell.

EXPLANATION OF PLATE 1

Transmission electron micrographs of decalcified shell and mantle of *Crania anomalia*; Recent, Firth of Clyde.

Fig. 1. Longitudinal section through the edge of the ventral mantle showing young outer epithelial cells with numerous vesicles disposed about a contorted strip of connective tissue to the left, and extending to the lower right-hand corner in association with periostracum which is attached to the substrate seen along the bottom of the micrograph ($\times 6500$).

Fig. 2. Longitudinal section through the generative zone of the dorsal mantle showing the junction in the top right-hand part of the micrograph between microvillous inner epithelium and outer epithelium. Both types of epithelia are vesicular, and the strip of connective tissue, about which the outer epithelium is disposed, is seen to extend to the right from about 2 cm. above the lower left-hand corner ($\times 11\ 000$).

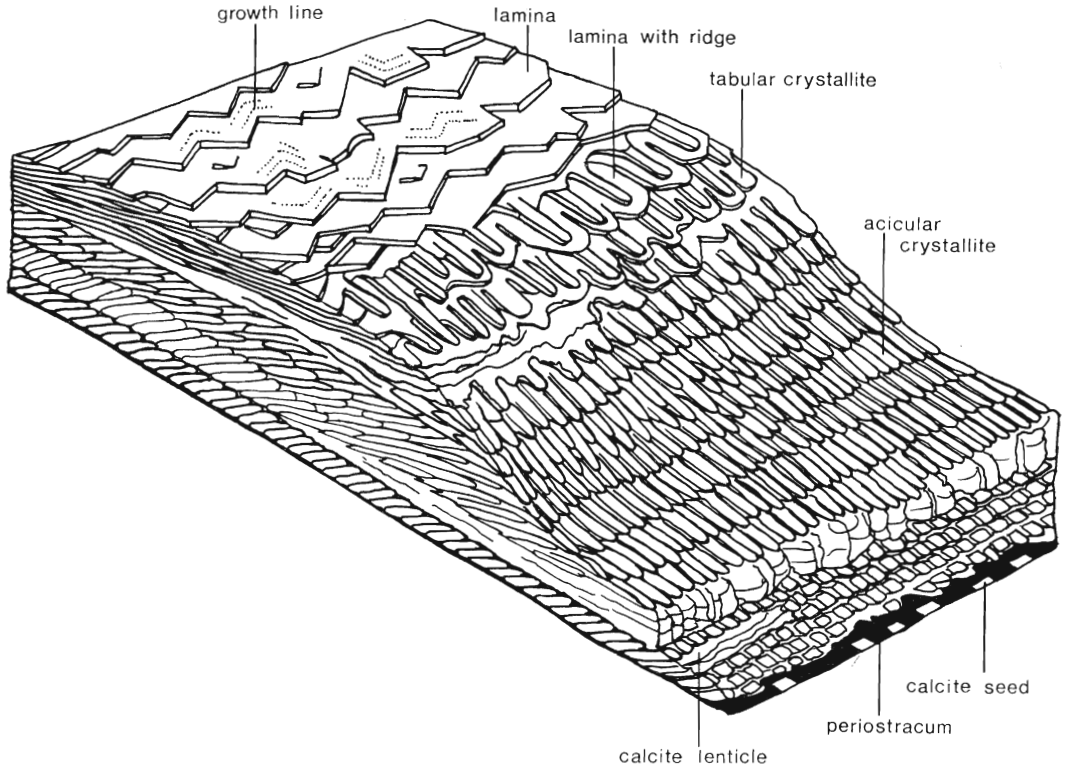
with a membrane about 12 nm. thick. No differentiation of the membrane has been seen even in those micrographs where the triple unit structure of the plasmalemmas of adjacent cells is discernible. Indeed similarities in electron density suggests that it is identical in composition to the external rods and fibrils and is also likely to be proteinous. Moreover, the cell continues to secrete the same substance in the form of fibrils or sheets because these extend from the inner surface of the membrane into the main layer of the periostracum. Thus the outer bounding membrane of the periostracum of *Crania* may be thought of as representing a change in the secretory regime of the cell, whereby fibrils are exuded temporarily to the exclusion of other substances to form a closely packed homogeneous mat.

The main layer of the dorsal periostracum of young *Crania* can vary from 2.5 to 5.5 μm in thickness because the external surface is thrown into a series of impersistent folds, with an amplitude of up to 3 μm , which are disposed more or less parallel to the shell margin. Judging from the strong PAS-positive reaction given by the periostracum in general, this layer is composed of a mucopolysaccharide partially segregated into lenticular masses, up to 9 μm wide, by proteinous fibrils and sheets which are continuous with those arising from the inner surface of the outer bounding membrane (Pl. 2, fig. 1, top half). This protein web extends throughout the layer to connect with an almost unbroken sheet of the same composition, up to 9 nm. thick, which forms the inner boundary to the periostracum. The regularity of deposition of the web, with a lineation more or less parallel to the inner bounding sheet, indicates that the arches were filled in first so that the outer folds in the periostracum are primary and do not result from differences in post-depositional shrinkage (Pl. 2, fig. 2).

The inner bounding sheet is not exuded until the secreting surface of the cell which is now greatly elongated, occupies the mantle edge and is already partly rotated to face dorsally. The appearance of the sheet marks the end of the wholly organic phase of shell secretion because it serves as a seeding surface for crystallites of calcite, the dominant constituent of the later-formed exoskeleton.

The mineral part of the exoskeleton of *Crania*, like that of the typical articulate brachiopod, is segregated into two layers although the distinction between them is much less striking. Calcitic seeds, which represent the first-formed part of the primary layer, must be deposited on the inner surface of the inner bounding sheet by outer epithelial cells while they are being rotated around the edge of the mantle to underlie the shell. Individual rhombohedra have not yet been seen in position of growth on the inner bounding sheet, but the great majority must always be aligned with the [10 $\bar{1}$ 1] cleavage surface normal to the mantle edge. Such an arrangement would explain how the dominant fabric of the primary layer is perpetuated during further carbonate secretion which causes the seeds to grow and amalgamate with one another and with the solid edge of the primary layer.

The characteristic fabric of the primary layer consists of crystallites, usually about 150 nm. thick, which are inclined at about 45° to the isochronous surfaces within the layer (text-fig. 3). In longitudinal section, the crystallites look like a finely but sporadically 'bedded' succession with the bedding indicating a rhombohedral cleavage direction (Pl. 5, fig. 2). There are also traces of a growth lineation with a periodicity of about 200 nm. and oblique intersections with other rhombohedral cleavage surfaces which lie parallel to the radius of the valve. In transverse section, these latter surfaces determine



TEXT-FIG. 3. Stylized block diagram showing the relationship of the periostracum, primary and secondary layers both in section and at the internal surface of the brachial valve of *Crania*.

the fabric and impart a needle-like aspect to the crystallites (Pl. 5, fig. 3), along which growth banding can still be seen; grosser surfaces of interruption in growth serve to segregate the needles into arcuate bundles. Internal surface views of some of the coarser crystallites, up to 800 nm. wide, show that their growth faces are concave and roughly

EXPLANATION OF PLATE 2

Transmission electron micrographs of decalcified shell and mantle of *Crania anomala*; Recent, Firth of Clyde.

Fig. 1. Longitudinal section through the edge of the shell showing caecal microvilli in association with an incomplete dorsal periostracum above, and folded ventral periostracum below ($\times 30\ 000$).

Fig. 2. Section through the fully developed dorsal periostracum showing the outer bounding membrane with protein rods beneath a bacterium in the top left-hand corner, and the inner bounding membrane in the bottom left-hand corner ($\times 40\ 000$).

Fig. 3. Section through a fully developed and folded ventral periostracum in relation to the outer epithelium above and the substrate in the bottom right-hand corner; to be compared with text-figs. 7-9 ($\times 22\ 500$).

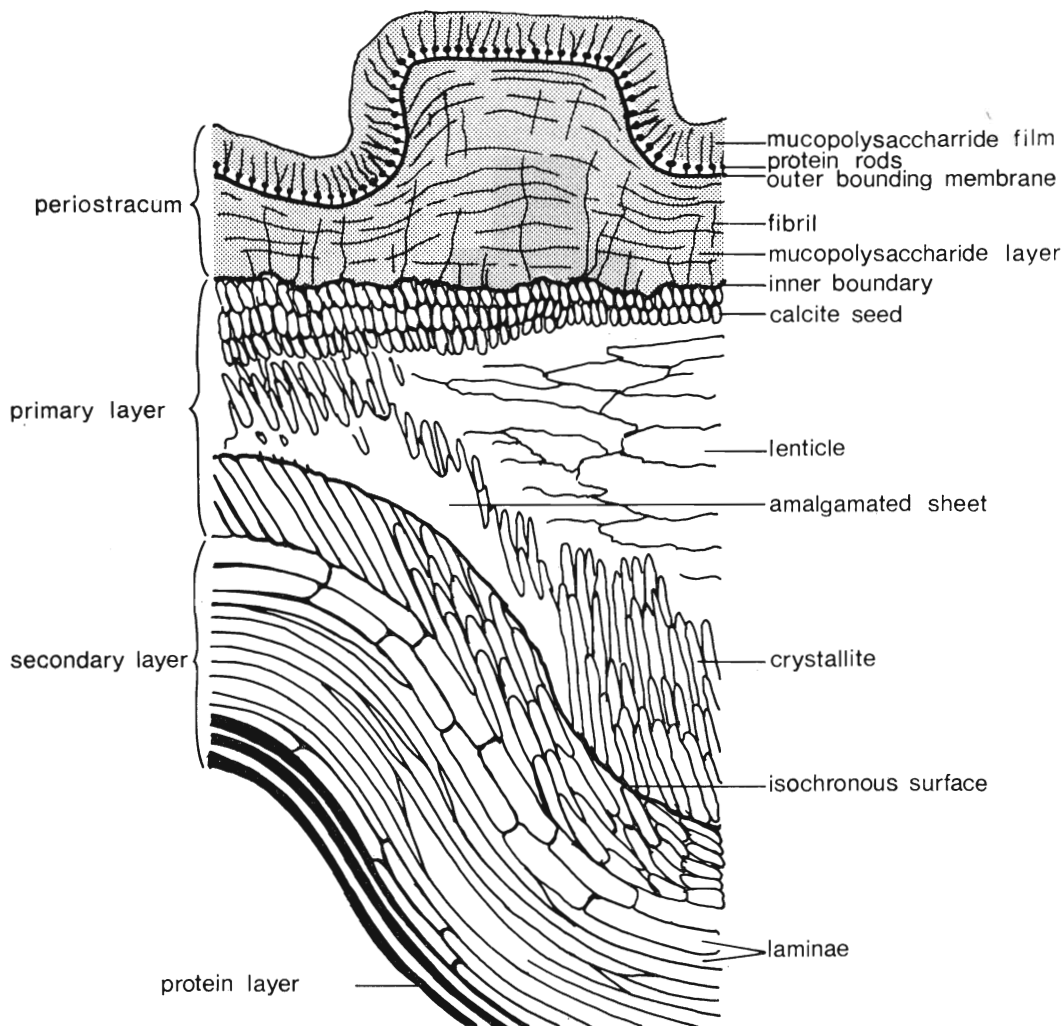
Fig. 4. Section through folded ventral periostracum between the secreting outer epithelium above and the substrate in the bottom right-hand corner showing, in particular, the protein rods of the outer bounding membrane and the fibrillar nature of the main mucopolysaccharide layer; no inner bounding membrane had been deposited at the time of death ($\times 68\ 750$).

rhombohedral in outline (Pl. 5, fig. 1). Presumably several centres of carbonate deposition can be maintained on the secretory surface of a single cell more or less throughout the deposition of the primary layer. Here and there, however, premature amalgamation of crystallites promotes the growth of impersistent lenticles of calcite, up to $5\ \mu\text{m}$ thick, the secretion of which may be terminated by reversion to the deposition of discrete crystallites (Pl. 5, figs. 1, 3). Segregation of crystallites is, to some degree, aided by the sporadic secretion of short strands of protein especially in the vicinity of the terminal branches of the caeca, but these never form the densely distributed, persistent sheets so characteristic of the secondary shell.

Each outer epithelial cell continues to secrete primary shell until the layer is about $40\ \mu\text{m}$ thick in the internal radial troughs containing the first-formed parts of the caeca, and about $60\ \mu\text{m}$ thick in the intervening crests. The cell now lies about $150\ \mu\text{m}$ within the edge of the adult shell which is undergoing almost continuous radial expansion as calcite nuclei, deposited by newly arriving cells, become amalgamated with the primary shell. At this stage in its development, the cell undergoes a profound change in its secretory habit which is reflected in the start of secondary shell deposition (text-fig. 4). The change from primary to secondary shell secretion is usually rapid, and is thus represented by a sharply defined junction in the skeletal succession; but a more gradual transition from one style of deposition to the other may also rarely occur.

The first indication of a change to secondary shell secretion is that the calcite crystallites are deposited as tabular rather than acicular aggregates (text-fig. 3). In section, these laminae are initially about $320\ \text{nm}$. thick (an average for 20 measured plates) and as much as $6\ \mu\text{m}$ long, and usually form a zone up to $5\ \mu\text{m}$ thick (Pl. 5, fig. 6). They grade inwardly into uniformly thinner laminae eighty-four of which averaged $260\ \text{nm}$. in thickness. At the primary-secondary junction, as seen on the internal surface of the valve, both types of laminae are usually arranged like a regular succession of overlapping tiles with their edges about $2\ \mu\text{m}$ apart and disposed more or less parallel to the commissure of the valve (Pl. 5, fig. 4). Such edges are normally scalloped by serrations subtending rhombohedral angles of 75° or 105° , with re-entrants between them emphasized by variably developed slots up to $150\ \text{nm}$. wide. The slots represent parts of aligned cleavage surfaces and partially segregate the exposed parts of laminae into strip-like laths about $1.5\ \mu\text{m}$ wide. Minute steps with a periodicity of about $140\ \text{nm}$. can be seen on many laminae and indicate how the entire inner surface grows incrementally at several different levels. Coarser steps, like impersistent scarps, also occur on the laminae to delineate locally developed surfaces grading into one another, and may extend across several laths.

Ridges, roughly rhombohedral in transverse section and bearing growth bands with a periodicity of $150\ \text{nm}$. frequently develop on the inner surfaces of laminae. They can be up to $0.5\ \mu\text{m}$ thick and are disposed parallel to one another at intervals of about $2\ \mu\text{m}$ to form the medial spines of laths or, when laminar deposition is in abeyance, groups of forward-pointing needles aligned with the radius of the valve (Pl. 5, fig. 5). In cross-section, adjacent ridges are seen to arise by accretion on the underside of one lamina and, later in their growth, to amalgamate with one another to form a continuous foundation for the succeeding lamina and a series of pits, up to $250\ \text{nm}$. in diameter, between the laminae. In the living animal, these pits almost certainly accommodate microvillous extensions of caeca.



TEXT-FIG. 4. Stylized section of the brachial valve of *Crania* showing the organic-mineral succession.

EXPLANATION OF PLATE 3

Transmission electron micrographs of decalcified shell and mantle of *Crania anomala*; Recent, Firth of Clyde.

Fig. 1. Section through the dorsal mantle showing the relationship between outer epithelium (with an intercellular vesicle to the left, as well as secretion droplets, vesicles and fibrils), a thin band of connective tissue and microvillous inner epithelium below ($\times 8000$).

Fig. 2. Section through the secreting plasmalemma of the outer epithelium showing the desmosomal attachments to a protein sheet of the secondary shell ($\times 40\,000$).

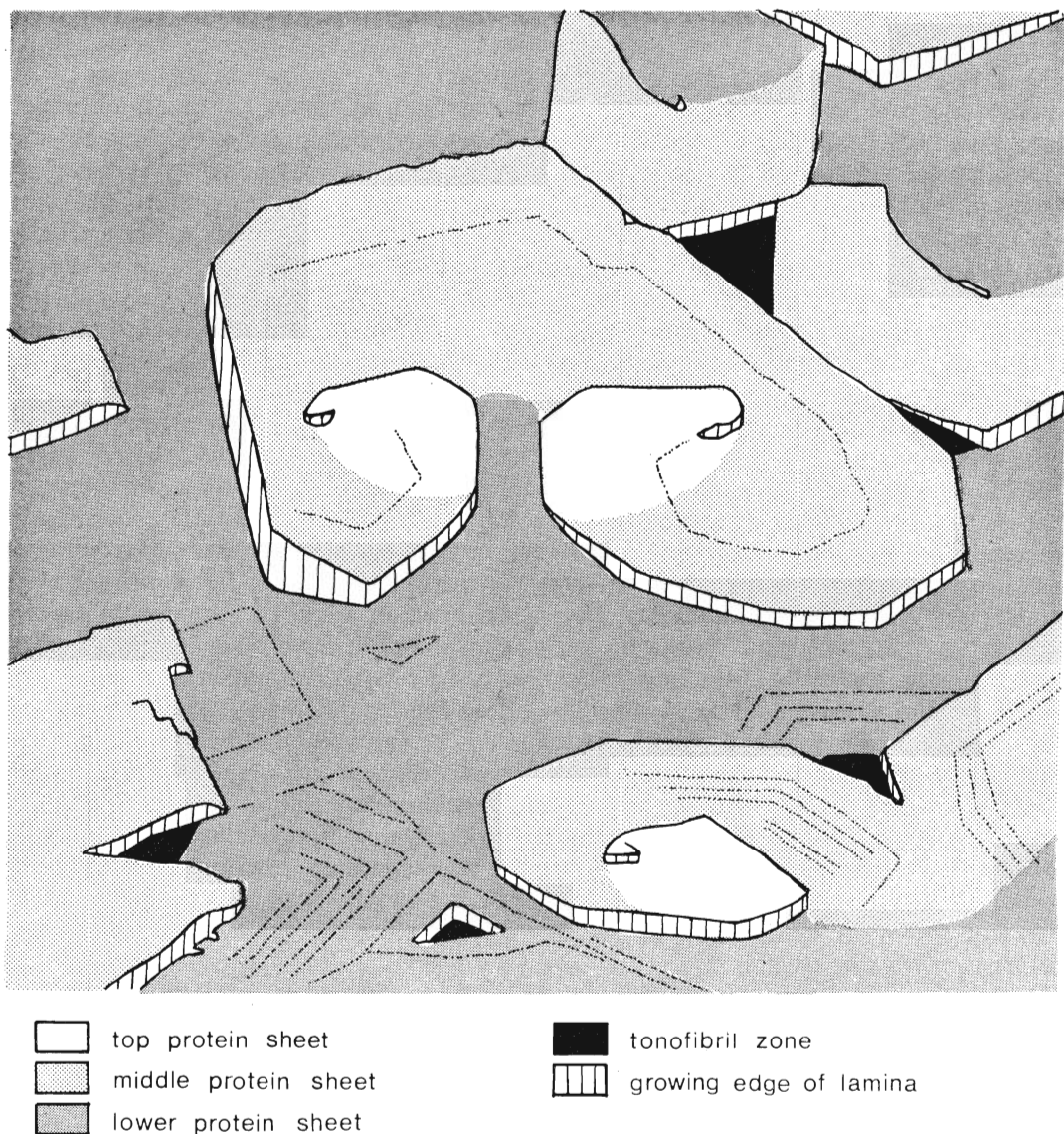
Fig. 3. Section through protein sheets of the secondary shell ($\times 20\,000$).

Fig. 4. Section below an adductor base through the ventral outer epithelium and decalcified shell substance (including folded periostracum seen just above the lower margin of the micrograph). The section shows the densely distributed tonofibrils within a cell and their relationship to the basal lamina above and the chitin pad below, and is the basis for text-fig. 12 ($\times 6000$).

Fig. 5. Section through the transition from normal outer epithelium (right side) to that underlying the dorsal adductor base showing the origin of the chitin pad and how it is penetrated by tonofibrils ($\times 12\,500$).

Internally away from the boundary with the primary layer, the secondary shell surface undulates as a series of rounded ridges between regularly spaced puncta, about $70\ \mu\text{m}$ apart. The ridges are ornamented by clusters of sub-circular tubercles up to $10\ \mu\text{m}$ in diameter and height, and are built up of regular laminae, about $250\ \text{nm}$ thick, which are separated from one another by protein sheets. The laminae with their organic coats are seen in section as a series of outwardly concave arcs, frequently with slightly stepped boundaries, subtended between the punctae (Pl. 6, figs. 1, 2). Individual laminae may be disposed at such acute angles to the main axis of a puncta as to form slightly projecting ledges along the wall, although these never develop into continuous partitions across the canal (Pl. 9, fig. 4). Surface views of the laminae show how they are built up on a protein sheet. They only rarely begin as perfect tabular rhombohedral seeds increasing evenly in area in all directions. Much more frequently, laminar crystallites nucleate along linear changes in the level of the protein foundation, and thereafter grow spirally from single or double screw dislocations (Pl. 6, figs. 3, 4). Perpetuation of the dislocation initially involves deposition of rhombohedral tablets with corner angles of 75° and 105° which are also subtended by concentric banding with a periodicity of about $200\ \text{nm}$ commonly preserved like faint steps on the surfaces of tablets. These angles usually increase suddenly from 120° or 135° to 150° as extra hexagonal or dihexagonal edges are built into the crystallite boundaries, and, in association with the spiral growth promoted by the original dislocation, impart a rounded outline to the crystallites. Although crystallites start off as isolated nuclei, two or three usually amalgamate, especially if the first-formed seeds were crystallographically aligned, and may even be ultimately circumscribed by surface banding. Junctions between adjacent crystallites, however, usually persist like fine cracks and can be as conspicuous as the notches that are formed between two convergent edges of non-aligned, adjacent crystallites. In a similar manner, the edges of three or more crystallites may meet to define a triangular or trapezoidal enclosure floored by the underlying protein sheet. As will be shown later, such enclosures act as areas for the temporary attachment of the outer epithelium to the shell surface. It is evident that the entire surface is unstable enough to promote the formation of superficial breaks even after a layer of carbonate has been deposited, because simultaneous growth from screw dislocations at three different levels are quite commonly exposed within a few square micrometres of one another (text-fig. 5). In any event, the amalgamation of contemporaneous crystallites and the addition of minor superficial spiral growths together provide a composite plate, normally between 200 and $250\ \text{nm}$ thick, which is the typical lamina of the secondary shell.

The differences between the primary and secondary shell really reflect an increasing orderliness in the secretory habits of the maturing cell with regular recurrent changes from organic to mineral deposition. In this respect, the primary shell is like a filling plastered over a pliable, irregular organic coat to form a stiff, smooth foundation for secondary deposition (text-fig. 4). Assuming the secretory surface of an immature cell depositing primary shell to be one-quarter that of a grown cell, estimated at $100\ \mu\text{m}$, there are about 16 centres of mineral accretion scattered over the plasmalemma of a young cell compared with only 3 or 4 sustained on an adult surface. Moreover, as has already been indicated, only the first-formed seeds are separated from one another by more or less continuous protein sheets; the rest of the primary shell away from the punctae is devoid of organic traces. The secondary layer, however, is immediately distinguishable

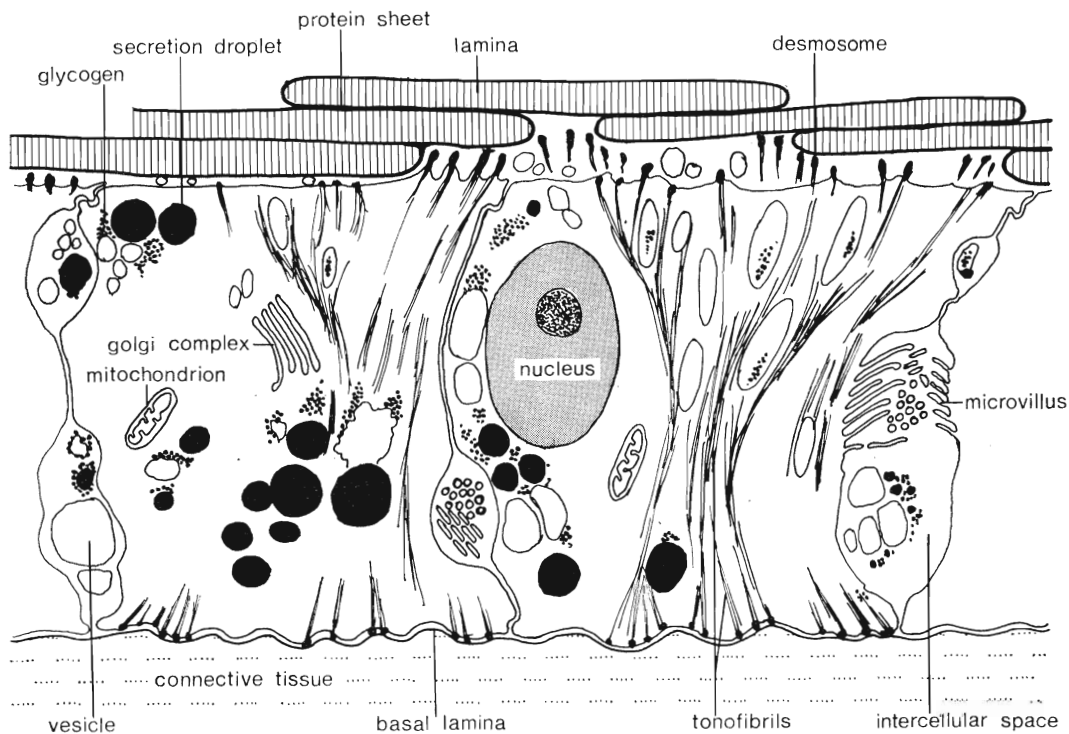


TEXT-FIG. 5. Diagrammatic view of the internal surface of the brachial valve of *Crania* to show the growth of laminae by screw dislocation.

because it is made up of laminae which are separated from one another by monolayers of protein (Pl. 3, fig. 3). Such alternation of organic and carbonate layers follows a set pattern and is accompanied by changes in the configuration of the plasmalemma of the secreting cell.

Even outside the principal muscle fields, outer epithelial cells can be greatly altered by the presence of large intercellular spaces accommodating microvilli, or by differential movement of adjacent cells in the vicinity of caeca. In general, however, the cells are

cuboidal in form; and, irrespective of morphology, contain numerous secretion droplets and conspicuous bundles of tonofibrils (Pl. 3, fig. 1; text-fig. 6). In the basal part of the cell, these tonofibrils are concentrated medianly and are attached to the underlying connective tissue by desmosomes. As they pass dorsally, the majority of tonofibrils become inclined towards one side or the other of the cell to connect with a lateral part of the outer plasmalemma. In this position, tonofibrils play an important part in



TEXT-FIG. 6. Stylized section of outer epithelial cells of the dorsal mantle of *Crania* showing their structure and their relationship to the secondary shell.

maintaining contact between the plasmalemma and the shell, and may even control the accretionary spread of laminae (Pl. 3, fig. 2). Thus as part of the organic-carbonate cycle of deposition, a protein sheet is first exuded by one (or more) cell(s) over an area which may exceed that of the secreting plasmalemma of a single cell. Concomitantly, the dorsal ends of the tonofibrils, which are segregated into groups accommodated by short microvilli about 200 nm. long and 100 nm. wide, become continuous through the plasmalemma with a series of desmosomal fibrils. The fibrils are connected to the protein sheet and pervade a moderately electron-dense zone, intervening between the plasmalemma and the sheet containing discarded vesicle membranes, which presumably represents secreted materials that were being used in the synthesis of the organic sheet at the moment of death (Pl. 3, fig. 2). Correlation between sections of the exoskeleton and of decalcified tissue shows that the carbonate laminae are deposited on the protein sheet lateral to the desmosomal zones where secretion of organic substances continues.

It may well be that, once calcite seeds establish themselves on a protein sheet, their lateral expansion only becomes possible because their growing edges intervene, like driven wedges, between the plasmalemma and the sheet simultaneously breaking the contact of any sporadically occurring desmosome. This would account for the concentration of tonofibrils, and the persistence of their desmosomal connections in zones which correspond to triangular or trapezoidal patches on the surface of deposition where the underlying protein sheet remains exposed between the encroaching edges of laminae. Indeed secretion of a protein cover to seal off a newly completed lamina usually begins at these centres where desmosomal connections with the organic sheet underlying a lamina persist. In a section covering $50 \mu\text{m}^2$ of decalcified secondary shell, 53 junctions between protein sheets were counted (Pl. 3, fig. 3) compared with only 7 points indicating sheets that had originated within laminae presumably at a dislocation. In this way, areas for the temporary attachment of cells are constantly being formed and then sealed off within the thickening laminar succession, as cells shift about on the protein sheets.

Optical examination of stained decalcified sections of the dorsal mantle and valve, shows that the spacing and thickness of protein sheets vary with the growth of the valve. In those parts of the valve where laminae are well developed and about 250 nm. thick, the protein sheets are, on average, 10 nm. thick. In others, the laminae are not more than 150 nm. thick but are more widely spaced because they are separated by coarse protein sheets, up to 300 nm. thick. The differences are clearly seasonal, with the former condition possibly reflecting deposition during the summer months and the latter secretion during the winter.

Secretion of the pedicle valve. Deposition of the pedicle valve, like that of the brachial valve, is controlled by outer epithelial cells rotating away from an intramarginal generative zone (Pl. 1, fig. 1). There are, however, differences in the morphology and succession of the pedicle valve, which results from its adhesion to the substrate. They arise in the following manner.

The first layer to be secreted binds the pedicle valve to the substrate (Pl. 2, fig. 4); and, although its adhesive characteristics may reflect some differences in composition from the corresponding layer in the brachial valve, its similar appearance under the

EXPLANATION OF PLATE 4

Transmission electron micrographs of decalcified shell and caecal extensions of the mantle of *Crania anomala*; Recent, Firth of Clyde (compare text-fig. 13).

Fig. 1. Section through the terminal branch of a caecum with associated tubules seen in transverse and longitudinal sections in the primary layer of the brachial valve; protein sheets of the secondary layer begin to appear at the bottom of the micrograph ($\times 15\ 000$).

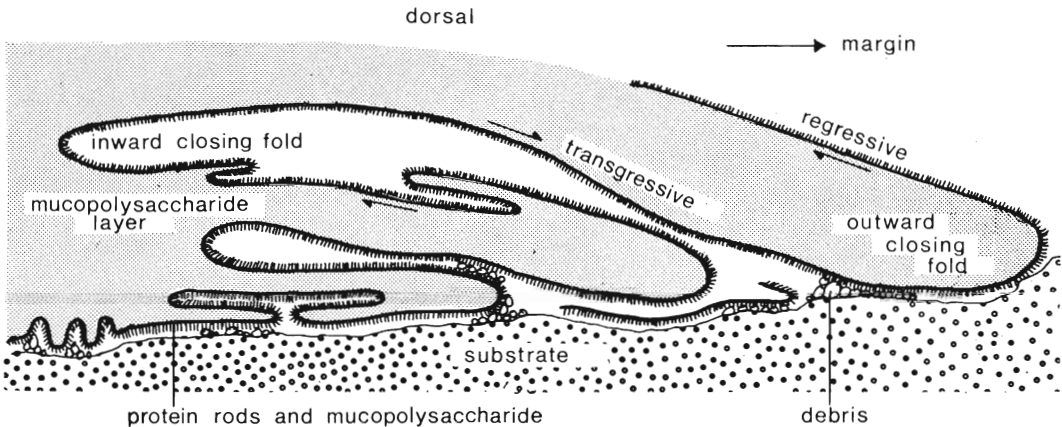
Fig. 2. Medial longitudinal section through a caecum in the secondary shell of the brachial valve showing the medial distribution of microvilli and the peripheral concentration of vesicles and secretion droplets ($\times 8250$).

Fig. 3. Transverse sections of microvilli found in the intercellular spaces of the caeca and mantle ($\times 150\ 000$).

Fig. 4. Transverse section of a caecal branch in the secondary shell of the brachial valve showing the highly folded intercellular boundaries of vesicular cells ($\times 8000$).

Fig. 5. Submedial section through part of the base of a caecum of the brachial valve, showing its relationship to outer epithelium to the left and connective tissue below ($\times 6000$).

electron microscope suggests that it is likely to be a mucopolysaccharide. This exudation is first applied to the substrate when it forms an external film to the outer bounding membrane of the periostracum, which must be rolled out over the substrate immediately after secretion by a highly extensible mantle edge. The film is squeezed against the substrate causing the fibrillar extensions of the outer bounding membrane, that permeate the layer, to flatten out. Yet the mucopolysaccharide must take some time to solidify because numerous folds develop in the periostracum in response to retractions and extensions of the mantle edge (Pl. 2, fig. 3; text-fig. 7). Such folds are usually flat-lying with their axial planes parallel to the oscillations of the mantle edge (Pl. 2, fig. 1 bottom half). They are commonly up to $2\ \mu\text{m}$ in amplitude but recumbent ones may extend for



TEXT-FIG. 7. Stylized section showing the folds developed by regression and transgression of the ventral periostracum in response to oscillations of the mantle edge of *Crania*.

$15\ \mu\text{m}$. Several may develop in vertical or lateral stacks and usually bear signs of having piled up as the periostracum was being spun out by an oscillating mantle edge. Thus no extraneous matter is trapped within the troughs of the folds while their limbs tend to be gummed together only along the crests. In other folds, however, debris, like that strewn on the substrate surface, can be found within the troughs. Such occurrences suggest that this part of the periostracum was at first rolled out over the substrate, but that, after the mucopolysaccharide had become sticky enough to pick up particles but not firm enough to act as a cement, the periostracum was peeled off the substrate by a retracting mantle edge and then folded. Indeed, the disposition of these periostracal folds afford a full record of the direction of movement of the mantle edge, and show how variable the rate and processes of growth by secretion can be (text-fig. 7).

At any stage in the spread of the pedicle valve over the substrate, accelerations in the advance of the mantle edge may occur. They are represented by either impersistent attenuations of the mucopolysaccharide layer on the inner surface of the outer bounding membrane; or, much more rarely, isolated patches of outer bounding membrane and mucopolysaccharide intervening between the periostracum proper and the substrate. These patches must have been quickly deposited well ahead of the continuous periostracal front during a rapid but briefly maintained advance of the mantle edge. In contrast, the radiating growth of the mantle edge may be interrupted by a general or

localized retraction. Retraction of the mantle involves a regression of the periostracum, while a later advance of the mantle causes the periostracum to be extended forward to define an inwardly closing fold (text-fig. 8). Thus reading a succession of folds dorsally from the substrate, all outwardly closing folds are bounded by transgressive-regressive limbs, and all complementary inwardly closing folds by regressive-transgressive segments of the periostracum.

Judging from the sequence in *Notosaria* as revealed by its better differentiated periostracum (Williams 1970) as well as evidence in *Crania*, the outer epithelium continues to secrete periostracum during mantle retraction. Thus, withdrawal of the mantle edge is accompanied by the rapid secretion of mucopolysaccharide and outer bounding membrane (*d-e* in text-fig. 8) by those newly formed cells that had only reached such stages in their secretory regime (cells 7 and 6). Older cells (5 to 2 inclusive) involved in retraction continue to secrete mucopolysaccharide as they move back, thereby filling up the core of an inwardly closing fold (*b-e-d*). The amount of mucopolysaccharide deposited on the extra strip of periostracum (*d-e*) depends on the speed of retraction. When all withdrawal has ceased, normal forward growth is resumed and defines a complementary outwardly closing fold (*c-d-e*). In this way, cells involved in mantle oscillation continue to secrete that part of the periostracal succession appropriate to their position in the regime at the time of retraction.

The only disposition which has been found to differ from that already described, occurs when a strip of periostracum is bent into two oppositely closing folds at the same level (text-fig. 9). Clearly the inwardly closing fold was formed during mantle retraction in the usual way; but *in situ* deposition of the outwardly closing fold would have required unlikely contortions of the mantle edge. It is, therefore, probable that the outwardly closing fold was originally an inwardly closing structure formed by the normal retreat and advance of the mantle edge, and originally stacked immediately above the inwardly closing fold. With continuing advance of the mantle edge, the fold could then have been rotated into its final outwardly closing position.

In comparison with the calcareous succession of the brachial valve, that of the pedicle

EXPLANATION OF PLATE 5

Scanning electron micrographs of the shell of *Crania anomala*; Recent, Firth of Clyde.

Fig. 1. View of the internal surface near the margin of the brachial valve (to the right) showing the concave, rhombohedral growth faces of primary crystallites ($\times 4000$).

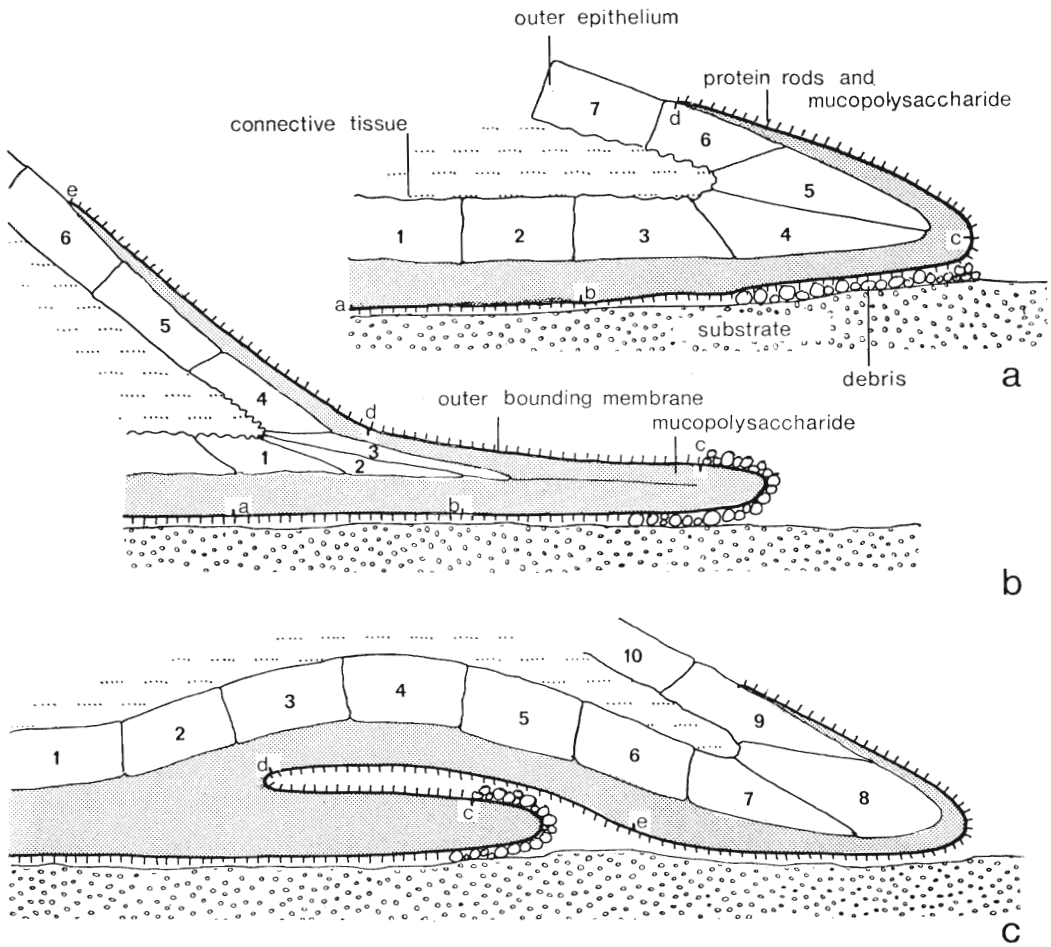
Fig. 2. Section of the brachial valve showing the disposition of primary crystallites in the vicinity of terminal branches of a puncta; valve margin to the right, exterior to the top ($\times 6500$).

Fig. 3. Section of the primary-secondary junction of the brachial valve showing calcite lenticles and more or less vertically disposed acicular crystallites of the primary layer overlying the laminar secondary layer in the bottom right-hand part of the micrograph; exterior of valve to the top ($\times 1400$).

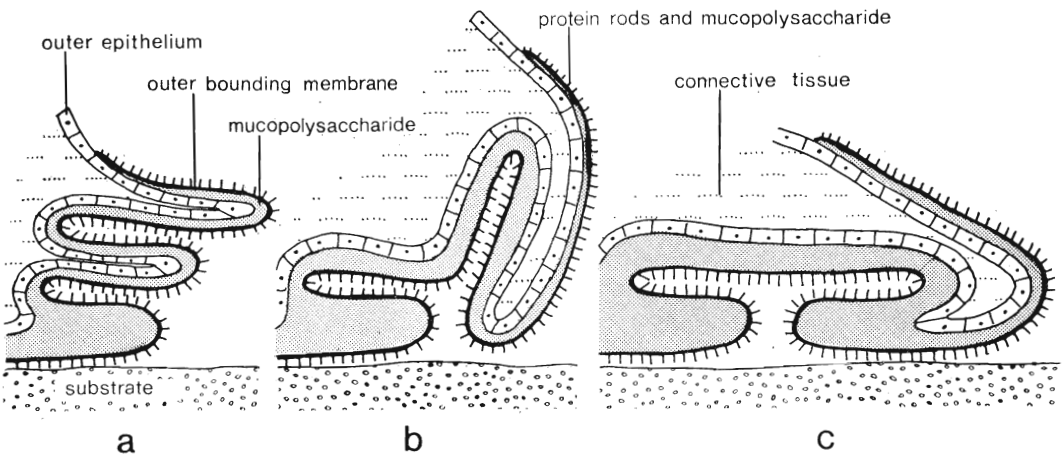
Fig. 4. View of the internal surface near the margin of the brachial valve (beyond the lower left corner) showing the overlapping arrangement of laminae just within the primary-secondary junction ($\times 4300$).

Fig. 5. View of the internal surface of the secondary shell of the brachial valve (with margin beyond the top of the micrograph) showing lath-like laminae with spines ($\times 6500$).

Fig. 6. Section of the primary-secondary junction of the brachial valve showing the acicular crystallites of the primary layer in the top right-hand corner passing into the thick tabular crystallites and then the thin laminae of the secondary layer in the bottom left-hand corner; exterior of valve beyond top right-hand corner ($\times 7000$).

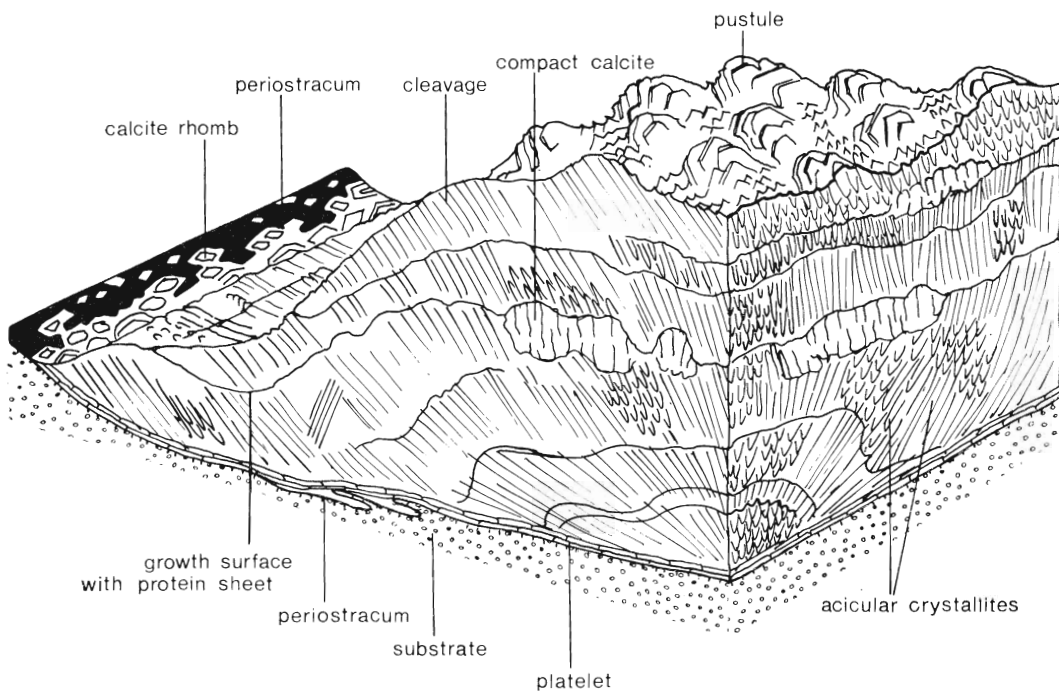


TEXT-FIG. 8. Three diagrammatic sections to illustrate the formation of folds of the ventral periostracum by temporary retraction of the mantle edge of *Crania*.



TEXT-FIG. 9. Three diagrammatic sections to illustrate the formation of oppositely closing folds at the same level within the ventral periostracum of *Crania*.

valve of *Crania* is incomplete. The mineral part of the ventral exoskeleton is generally very thin. In young shells of *C. anomala*, up to 5 mm. long, a negligible calcitic layer is sporadically secreted following a transitory post-larval phase when the pedicle valve is entirely organic (Rowell 1960, p. 41). Even in mature individuals, over 10 mm. long,



TEXT-FIG. 10. Stylized block diagram showing the relationship of the periostracum and primary shell both in section and at the internal surface of the pedicle valve of *Crania*.

a thickening exceeding 0.5 mm., is limited to an anterior arc which forms a dorsally convex submarginal rim so that a central area, between 3 and 5 mm. across, remains only partially covered by the merest mineral film. There is, however, a discernible pattern of shell deposition, which can be worked out by study of the internal surface of the valve as well as recourse to radial and tangential sections (text-fig. 10).

EXPLANATION OF PLATE 6

Scanning electron micrographs of the shell of *Crania anomala*; Recent, Firth of Clyde.

Figs. 1, 2. Sections of the laminar secondary shell of the brachial valve; exterior of valve beyond the top of the micrographs ($\times 6300$ and 7500 respectively).

Figs. 3, 4. Views of the internal surface of the brachial valve showing evidence for simultaneous growth of several laminae along screw dislocation edges (compare text-fig. 5) ($\times 6000$ and 7100 respectively).

Fig. 5. View of crystallite seeds of calcite scattered on the inner surface of the periostracum of the pedicle valve; margin of valve towards right ($\times 6500$).

Fig. 6. Section of the pedicle valve and the underlying substrate (along the bottom of the micrograph) showing the flat-lying platelets which form a basal pavement to the acicular crystallites of the primary shell ($\times 6500$).

The first constituents to appear are small calcite rhombs, about $1.5\ \mu\text{m}$ across and $0.3\ \mu\text{m}$ thick, which are secreted directly on to the inner surface of the periostracum (Pl. 6, fig. 5). The rhombs, which may grow into platelets up to $4\ \mu\text{m}$ in size, accumulate more or less parallel to the periostracal surface to form a pavement normally $2\text{--}3\ \mu\text{m}$ thick (Pl. 6, fig. 6).

With further secretion, this pavement of flat-lying platelets becomes the foundation for a series of needle-like crystallites set at high angles to the pavement and the secreting surface of the cell (Pl. 7, fig. 2). These crystallites may be up to $1\ \mu\text{m}$ thick and $40\ \mu\text{m}$ long, and disposition of their faces, in relationship to undulating surfaces of growth, can be likened to cleavage fans developed in folded rocks. In radial sections, the cleavage planes that define crystallites forming a dorsally convex mound, are seen to converge ventro-medially so that the long axes of the crystallites subtend angles with a convex growth surface, which do not usually deviate more than 20° from the vertical. A similar pattern of ventro-median convergence of cleavage characterizes tangential sections of such mounds. It seems, then, that the basic mineral fabric of the pedicle valve is determined by crystallites, deposited at very high angles to the secreting surfaces of the outer epithelium and, consequently, radiating outwards from any locus which may become the core of a calcitic mound.

Calcitic mounds may be enlarged radially or, more usually, concentrically; but in both types a strong radial cleavage develops in addition to that already described, and together they dominate the ultrastructure of the pedicle valve (text-fig. 10). Such cleavage surfaces are commonly accentuated by being clothed in proteinous sheets although these are more persistently and thickly developed as covers to the many growth surfaces. In all, despite these periodic alternations of prevalently organic or mineral phases of skeletal secretion, crystallites retain more or less the same habit throughout shell growth, being essentially acicular forms with acutely or broadly subrhombic outlines. Yet in any section of the pedicle valve, every variation in crystallite outline between those representing strictly longitudinal and transverse aspects can be found and indicate the topographic range of the internal growth surface.

Periodic changes in the proportion of protein and calcite secreted by the outer epithelium become most evident in the older part of the pedicle valve. The shell forming the outer slopes of the submarginal rim is almost invariably made up of normal crystallites. Here and there, however, small patches of more compact calcite occur (Pl. 7, fig. 3), in which individual crystallites are no longer sharply defined although general cleavage directions are aligned with those of adjacent contemporaneous crystallites. Hence these patches which are up to $15\ \mu\text{m}$ across are distinctive because they contain significantly smaller quantities of protein than is found interleaved with the surrounding crystallites. They represent localized centres of continuous calcite secretion; and because they accumulate faster than surrounding crystallites, they throw the terminating growth surfaces into undulations. Inwards from the valve edge, these patches become larger and commoner (Pl. 7, fig. 4) so that they make up the bulk of the calcareous layer beneath the crest and inner slopes of the submarginal rim. Here they can form groups of impersistent lenses arranged in levels one above another. In sections the lenses are seen to have variably wavy to planar bases and strongly convex dorsal surfaces. They bear traces of cleavage indicating the ventro-median convergence so typical of radiating growth, as well as sporadically preserved growth-lines about $300\ \text{nm}$. apart. They may

be more than 80 μm in size but rarely more than 30 μm thick, and are separated from one another by successions of crystallites up to 10 μm thick. The relationship between the lenses and the discrete crystallites surrounding them, reflects how shell differentiation takes place. In general, the base and sides of a lens constitute transitional zones into crystallites which are aligned with the cleavages within the lens. Thus, as with the patches occurring within the valve margin, lenses are centres characterized by a significant but gradual reduction in protein secretion. Their dorsal surfaces, on the other hand, are normally conspicuously abrupt junctions with crystallites which commonly form a basal pavement of flat-lying platelets overlapping one another across the lenses. Such junctions do not necessarily signify that each deposit is secreted by a distinctive group of cells which migrate over the internal surface. They are more likely to indicate abrupt secretory changes that take place repeatedly in the same cells which tend to be anchored to the same part of the valve by caeca.

Such alternations in secretion accord well with the succession characterizing the valve floor within the submarginal rim. Here the valve consists of a thinly banded succession in which predominantly organic layers alternate with those in which fine crystallites, disposed at high angles to the banding, are contained in an organic matrix. The banding is regular and continuous with more conspicuous zones of high organic content developed at intervals of 1–2 μm , and is not broken up into discrete plano-convex units as are found in the submarginal rim. Nonetheless, it is evident that the thinner organic bands within this succession can be correlated with the crystallite layers of the inner part of the submarginal rim and the thicker mineral bands with the lenses.

The growth of lenses with reduced organic content is reflected in the detailed topography of the submarginal rim. The crest as well as the upper parts of the flanking slopes of this feature, are greatly indented with punctae, between which arise tubercles and rounded eminences up to 0.5 mm. in diameter. The entire surface of this zone of the submarginal rim is further ornamented by a series of microscopic pustules up to 7 μm

EXPLANATION OF PLATE 7

Scanning electron micrographs of the shell of *Crania anomala*; Recent, Firth of Clyde and Raunefjord, Norwegian Sea.

Fig. 1. View of the pustulose internal surface of the subperipheral rim of the pedicle valve showing the 'scarp and dip slope' disposition of crystallites as illustrated in text-fig. 10; valve margin beyond the top of the micrograph ($\times 2600$).

Fig. 2. Section of the pedicle valve (and underlying substrate in bottom right-hand corner) to show the inclination of acicular crystallites within the calcareous layer; margin of valve towards the right ($\times 2400$).

Fig. 3. Section of the pedicle valve to show the presence of isolated lenses of more compact calcite within the calcareous layer; margin and internal surface of valve to the left and top respectively ($\times 2700$).

Fig. 4. Section of the pedicle valve to show the development of more continuous patches of relatively compact calcite in relation to the acicular crystallites of the calcareous layer; margin and internal surface of valve to the left and top respectively ($\times 2400$).

Fig. 5. View of internal surface of brachial valve showing a transition from the laminar secondary layer in the top right-hand corner to the polygonal areas with smaller crystallites representing an adductor muscle scar ($\times 2600$).

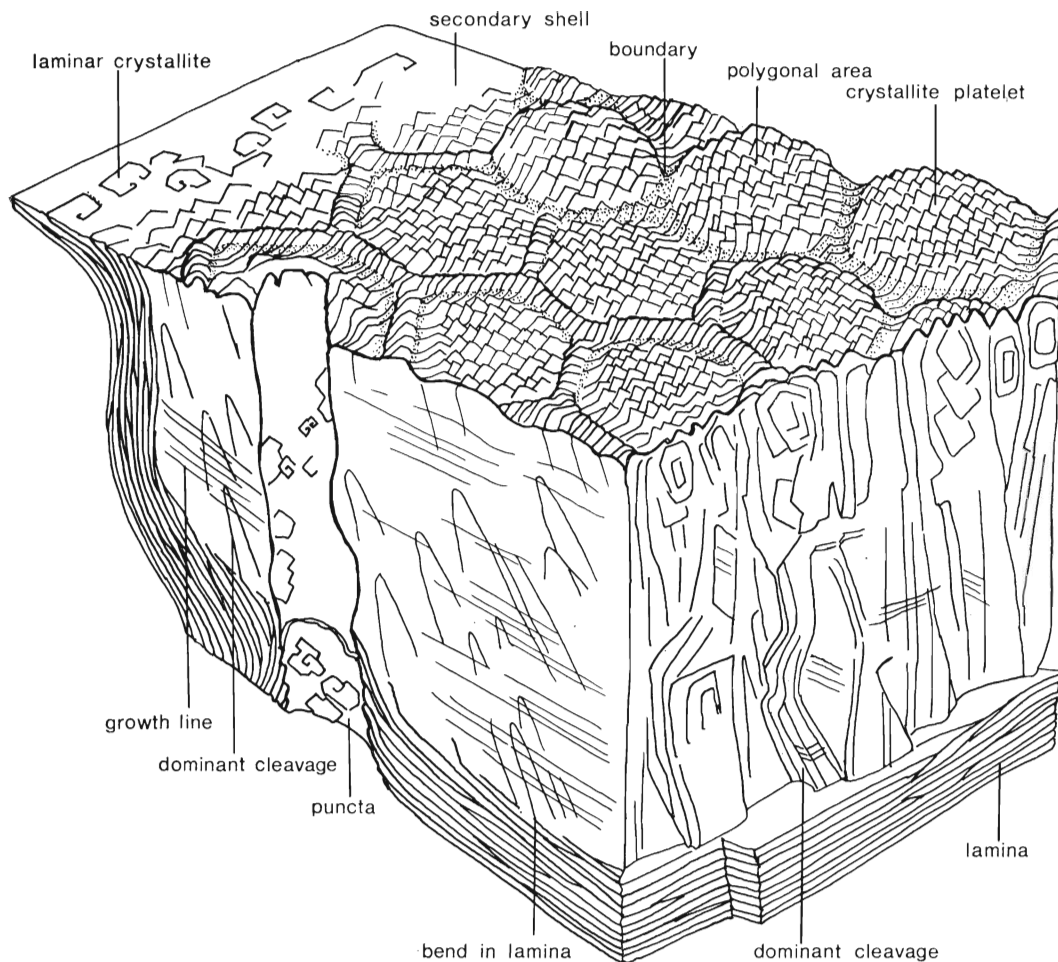
Fig. 6. View of the polygonal areas with raised boundaries found on the internal surface of the brachial valve in the medial area of a posterior adductor muscle scar ($\times 1300$).

across (Pl. 7, fig. 1). These pustules consist of platelets of calcite which dip inwards towards the middle line of the rim, so that platelets form externally facing scarps and internally dipping slopes in pustules on the outer slopes of the rim, and are oppositely arranged in pustules on the inner slopes. The areas between the pustules are occupied by crystallites which are similarly disposed but needle-like in habit and only about 100 nm. or so thick. The relationship between platelets and needles is transitional and it is clear that the pustules are surface manifestations of lenses as are the needles of the crystallites surrounding the lenses. Both internally and externally of this pustulose zone, crystallites are responsible for the detailed relief. Along the external margin of the rim, crystallite needles break the surface in orthodox alignment. Along the internal margin, platelets or needle-like crystallites can be seen to form a variably developed film over a protein layer, and correspond to the regularly banded part of the pedicle valve.

In summary, the ultrastructure of the pedicle valve is demonstrably complex. There is considerable variation in the disposition of crystallites and in the content of protein strands and sheets that partly segregate the crystallites. Such variation may lead to the formation of basal pavements of flat-lying platelets at one extreme or to the accretion of lenses of relatively pure calcite at the other. Yet the basic unit is a fine, prismatic crystallite generally highly inclined to the surface of secretion, and is similar in dimension and attitude to the essential constituent of the primary shell of the brachial valve. Indeed nothing in the ventral shell succession is comparable with the lamination characteristic of the secondary layer of the brachial valve, and we conclude that the pedicle valve is composed solely of periostracum and primary shell.

Microstructure of the muscle scars. The most profound alteration of the normal shell structure of *Crania* is brought about by the emplacement of muscles. A variety of muscles control the movement of the valves relative to one another; but only the insertion of the adductor and oblique muscle bases gives rise to conspicuous scars on the floors of the valves, although the attendant microstructure seems to be typical of all identifiable tracks.

The microtopography of the dorsal adductor scars is quite striking (text-fig. 11). It consists of a series of mounds or depressions essentially arranged in a hexagonal packing order, but varying from subcircular to pentagonal in outline (Pl. 7, fig. 6). The long and short axes of 11 of these polygonal areas averaged respectively 12.8 and 10.4 μm ; and they are separated by shallow troughs or low ridges, according to whether they form mounds or depressions, which averaged 2.8 μm wide in 7 measurements (Pl. 8, figs. 1, 2). The distinction between the polygonal areas and their boundaries, irrespective of whether they are raised or depressed, does not result from any realignment of crystallites because cleavage is invariably well developed, at intervals of 100–200 nm., and runs in continuity across boundary and polygon alike (Pl. 8, fig. 3). Indeed anteriorly dipping cleavage planes, with a constant strike parallel to the transverse diameter, have been traced across the right posterior adductor scar of an adult brachial valve. There are, however, differences in habit and size of crystallites forming a polygonal area and its boundary. The boundary typically consists of closely stacked platelets extending across its width, commonly with single rhombohedral faces forming the bottom of the trough or the crest of the ridge, whichever constitutes the boundary



TEXT-FIG. 11. Stylized block diagram showing the structure and features of the adductor myotest both in section and at the internal surface of the brachial valve of *Crania*.

EXPLANATION OF PLATE 8

Scanning electron micrographs of the shell of *Crania anomala*; Recent, Firth of Clyde and Raunefjord, Norwegian Sea.

Fig. 1. View of polygonal areas with depressed boundaries found on the internal surface of the brachial valve in the medial area of a posterior adductor muscle scar ($\times 1350$).

Fig. 2. Internal oblique view of a broken edge of a posterior adductor muscle scar of the brachial valve showing the disposition of crystallites in section and within polygonal areas ($\times 2700$).

Fig. 3. View of crystallites within polygons with raised boundaries found on the internal surface of the brachial valve in the medial area of a posterior adductor muscle scar, to show continuity of crystallite disposition across areas and boundaries ($\times 6500$).

Fig. 4. Section of the brachial valve showing a lens of cleaved calcite (myotest) surrounded by laminae of the secondary layer; dorsal i.e. external direction towards bottom left-hand corner ($\times 2600$).

Fig. 5. Section of the brachial valve showing the transition from the laminae of the secondary layer to the overlying myotest; dorsal i.e. external direction towards bottom left-hand corner ($\times 7000$).

Fig. 6. View of the internal surface of the pedicle valve showing impressions of posterior adductor muscle scar polygons on a thin layer of calcite ($\times 1400$).

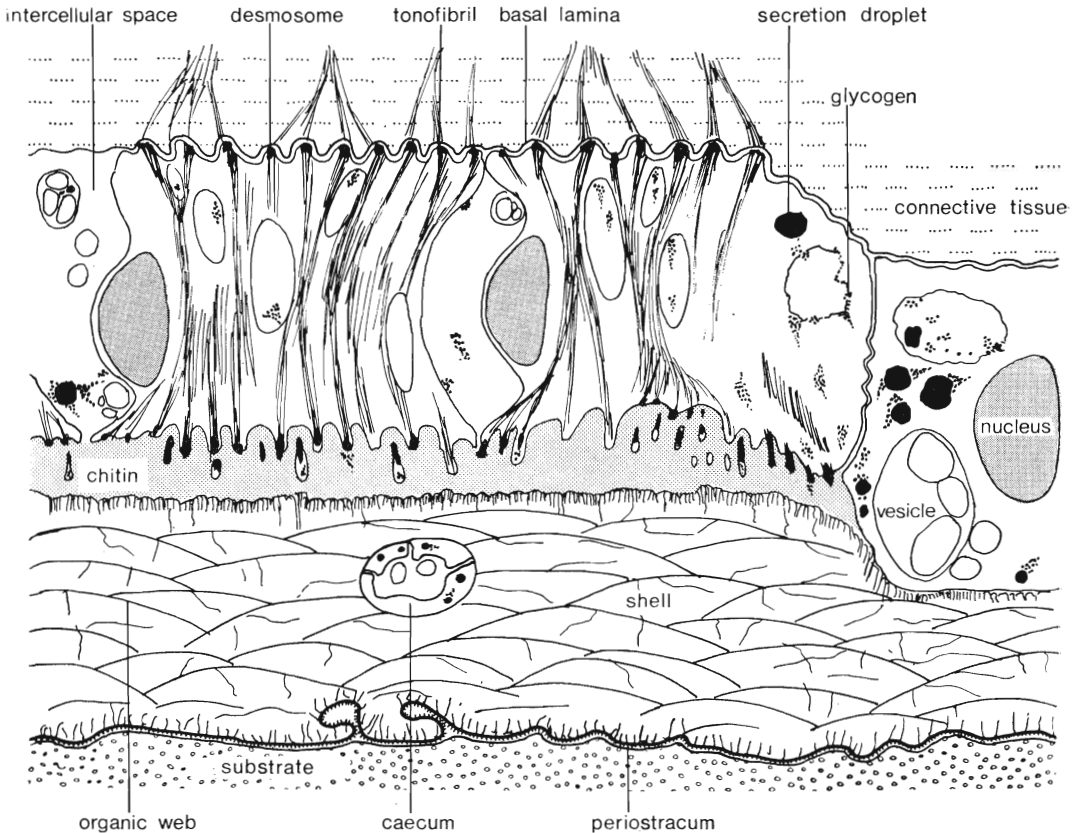
under scrutiny. In contrast, the crystallites of the enclosed area, whether it be raised or depressed, consist of significantly smaller rhombohedral units, up to $1\ \mu\text{m}$ across (Pl. 8, fig. 3). These are partly separated from one another by numerous slots and pits up to 100 nm. across which give the entire area a more open aspect than its boundary.

The difficulty of distinguishing between the microstructure of the polygonal areas and their boundaries is greater in section. Polished and etched sections of the brachial valve show that a muscle scar is underlain by a wedge of non-laminar calcite, which is outwardly flanked by impersistent lenses of similar texture generally with more or less planar dorsal surfaces and convex ventral ones. Such bodies constitute the myotest of Krans (1965, p. 95). They show a dominant cleavage at high angles to the ventral surface, and growth-lines with a periodicity of about 140 nm., but no differentiation consistent with the dimensions of the polygonal areas and their boundaries (Pl. 8, fig. 2). Broken sections of muscle scars confirm the impression that the calcite underlying the scar is disposed as a series of blades more or less normal to the growth surface, and that those beneath polygonal areas are narrower than those underlying the boundaries.

The relationship between muscle scars and the surrounding secondary shell is well displayed on a small scale by the outlying lenses which are neither discrete nodules nor lobate extensions of the main body of calcite forming the scar (Pl. 8, fig. 4). At first sight, the base or dorsal surface of a typical lens, i.e. that part which is first secreted, appears to overstep the underlying, gently inclined laminae. In detail, however, each lamina is seen to bend up sharply into alignment with the cleavage of the lens before it loses its identity (Pl. 8, fig. 5). Such realignment must involve a sudden acceleration in mineral deposition. Decalcified sections also show that the realignment of the calcitic blade is initiated and controlled by simultaneous exudation of protein sheets and strands in continuity with the organic layer beneath the lamina (Pl. 3, fig. 5). These sheets and strands fit into the slots and canals permeating the polygonal zones which must have been secreted by the same cells as deposited the underlying laminae. Differences in the composition and direction of deposition, therefore, reflect the onset of a physiological change in the outer epithelium as it comes to be overlain by growing muscle tissue. The realignment does not take place simultaneously along the entire base of a lens (text-fig. 11). Synchronous surfaces of growth as represented by growth-lines in section may be inclined at angles of up to 25° to the base so that one edge of a lens may be formed significantly later than the opposite edge. On the other hand the ventral surface of a lens, apart from the lateral extremities which grade into laminae, is a sharply defined, discontinuous junction with a series of transgressive laminae which are as likely to have been deposited by different cells from those responsible for the accretion of the lens as by the same cells subjected to secretory changes. On the inner surface of the valve, the junctions between normal secondary laminae and the muscle scar are usually well displayed (Pl. 7, fig. 5). Along the dorsal junction, the polygonal areas and their relatively smaller rhombohedral units are the first constituents of the muscle scar to appear. Their boundaries, which initially look like unmodified remnants of the normal secondary shell, become fretted into ridges or troughs later. The ventral junction is equally conspicuous as a wedge-like surface of laminar shell resting unconformably on the top surface of the lens.

The differentiation of the muscle scar surfaces into polygonal areas defined by wide boundaries, is, therefore, a surface phenomenon which must be related to the

configuration of the mantle cells. Outer epithelial cells underlying the muscle tissue are immediately distinguishable because they are crowded with tonofibrils which extend from the highly folded outer plasmalemma to the inner plasmalemma where fibrillar prolongations pass through both the cell and basement membranes to the muscle bases within the connective tissue (Pl. 3, fig. 4; text-fig. 12). They are also characteristically



TEXT-FIG. 12. Stylized section showing the modification of shell and outer epithelial cells of the ventral mantle which underlie the adductor bases of *Crania*.

biconcave in lateral view, being separated from one another by well-developed intercellular spaces which may be almost as large as the cells themselves. Yet outer plasmalemmas, which averaged $10.5 \mu\text{m}$ across for 13 cells, are dimensionally comparable to the polygonal areas; and it is likely that the latter are really the impressions of cells with their boundaries corresponding to the intercellular spaces. Notwithstanding this close fit, a pad of chitin, up to $4 \mu\text{m}$ or more thick, intervenes between the outer epithelium and the calcareous muscle scar, and is the culminating product of a series of changes that affect the secretory regime of cells as they become associated with the spreading muscle tissue. The changes can be traced in sequence inwards from the boundary of the muscle field (Pl. 3, fig. 5). Just beyond the boundary, outer epithelial cells which are laterally biconcave but as yet without tonofibrils cease depositing alternating layers of calcite

and protein so typical of the laminar secondary shell. Instead, as already inferred from consideration of the shell alone, the cells simultaneously secrete both calcite and a dense web of protein strands, between 5 and 10 nm. thick, in continuity with protein sheets interleaved with the underlying laminae. This is the deposit that thickens abruptly about 20 μm inwards of its first appearance to form the muscle scar and myotest proper. Indeed, it is at this stage that the polygonal areas and their boundaries become differentiated as impressions of the outlines of outer epithelial cells. The moulds persist with shell deposition and become preserved when shell thickening is terminated by the secretion of a protein sheet, about 5 nm. thick, to which is attached the organic web permeating the calcite of the scar. Immediately after, the cells, now heavily charged with glycogen, begin to secrete copious quantities of chitin, which may quickly form a layer. At the same time, fibrils, about 2 nm. thick, polymerize within the layer in dense haloes around the heads of tonofibrils which are now beginning to project through microvilli as they form within the cells. In this way, both shell and mantle are transformed to receive muscle bases.

With the exudation of chitin, changes in the secretory regime of the outer epithelium associated with the muscle tissue are complete. Yet the fact that the enlargement of adult muscle scars involves an outward shift in phase with the migration of muscle tissue away from the location of juvenile muscle fields, adds a complication. For deposition of orthodox secondary shell spreads outwardly in the wake of the migrating muscle fields as is shown by the transgression of laminar shell over medial areas of the muscle scars. This part of the succession is probably secreted by a secondary generative zone of outer epithelium developing within the inner edge of the muscle base, as well as by cells which, having exuded a layer of chitin, revert to laminar deposition.

The muscle scars in the pedicle valve are superficially like those of the brachial valve in that the microtopography of the mineral layer consists of raised or depressed polygonal areas bounded by well-defined troughs or ridges (Pl. 8, fig. 6). These features are also comparable in size being, on average, 10.6 μm across 10 polygonal areas and 2.6 μm across 10 boundaries, so that they, too, are probably the impressions of the outlines of outer epithelial cells underlying the muscle bundles. There, however, the similarity ends because the ventral muscle scars are fashioned out of the finely crystalline primary layer and not the laminar secondary shell. Consequently the difference in texture between the muscle scars and the rest of the pedicle valve is minor. The highly inclined crystallites characteristic of the primary layer persist into the muscle scar zone where they tend to be segregated into needles up to 400 nm. thick by numerous anastomosing canals usually less than 200 nm. in diameter, and are disposed more or less normal to growth surfaces. They may pass into nodules up to 8 μm in size which are distinguishable through their relatively low protein content and the coarser texture of their calcite constituents (Pl. 9, fig. 1). More commonly, however, they form thin layers alternating with well-developed films of protein which are interconnected by strands passing through the canals between the crystallites (Pl. 8, fig. 6). The calcite layers bearing polygonal impressions may be as thin as 2 μm . Finally it is noteworthy that a mineral base is not invariably developed beneath the ventral muscle tissue. Here and there within an otherwise normal scar, the chitin layer is secreted directly on top of the periostracum, a sequence which is consistent with the variable occurrence of primary shell on the valve floor.

Growth and morphology of caeca. During the deposition of both valves of *Crania*, branched extensions of the mantles become encased in primary and secondary shell. They differ in morphological detail from outgrowths penetrating the calcareous shell of some articulate brachiopods, although the term 'caeca' is appropriate for both types as is 'punctae' for all canals in the shell accommodating them. The structure and function of the caeca of *Crania* can best be described by outlining their formation in relation to the growth of the shell.

At the mantle edge, the first parts of the caeca to appear are a number of tubules between 75 and 150 nm. in diameter and up to 2 μm long (Pl. 2, fig. 1; Pl. 4, fig. 1). The tubules lie for most of their length on the inner surface of the periostracum but do not have any consistently arranged connections with that surface, only sporadically developed fibrils. They are generally aligned with the radial axis of the shell and may be directed posteriorly and anteriorly as are substantially thicker branches, 2 μm or more in diameter, to which they are joined. Hence the terminal branches of caeca are seen, especially in radial sections, to splay out beneath the periostracal layer and become embedded in this attitude within the primary layer as it is being deposited (Pl. 9, figs. 2, 3). This disposition is highly characteristic of the caeca of *Crania* as was first noted by Blochmann in 1892. Further shell secretion by surrounding outer epithelial cells causes a main stem to develop more or less normal to the zone of splayed terminal branches. As deposition proceeds, however, three or four adjacent stems converge ultimately to define the main trunk of a typical caecum, which may be up to 50 μm thick (text-fig. 13). In the brachial valve, branches up to the fourth or fifth order may contribute to the formation of a mature caecum, by which time the caecal bases are usually about 70 μm apart. Thus the density of punctae over the surface of a valve must vary with the thickness as well as the age of an individual, as is true of all brachiopods with arborescent punctae (Wright 1966, p. 552). This variation, however, does not account for a significant difference in the frequency of punctae on the internal surfaces of complementary valves. Counts of 56, 58, and 108 per mm^2 have been obtained for

EXPLANATION OF PLATE 9

Scanning electron micrographs of the shell of *Crania anomala*; Recent, Firth of Clyde and Raunefjord, Norwegian Sea.

Fig. 1. Section of the posterior adductor myotest of the pedicle valve; internal surface of valve towards the top ($\times 2700$).

Fig. 2. Section of the primary layer of the brachial valve to show the branches and tubules of a puncta filled with resin; external surface of the valve along the top margin ($\times 2600$).

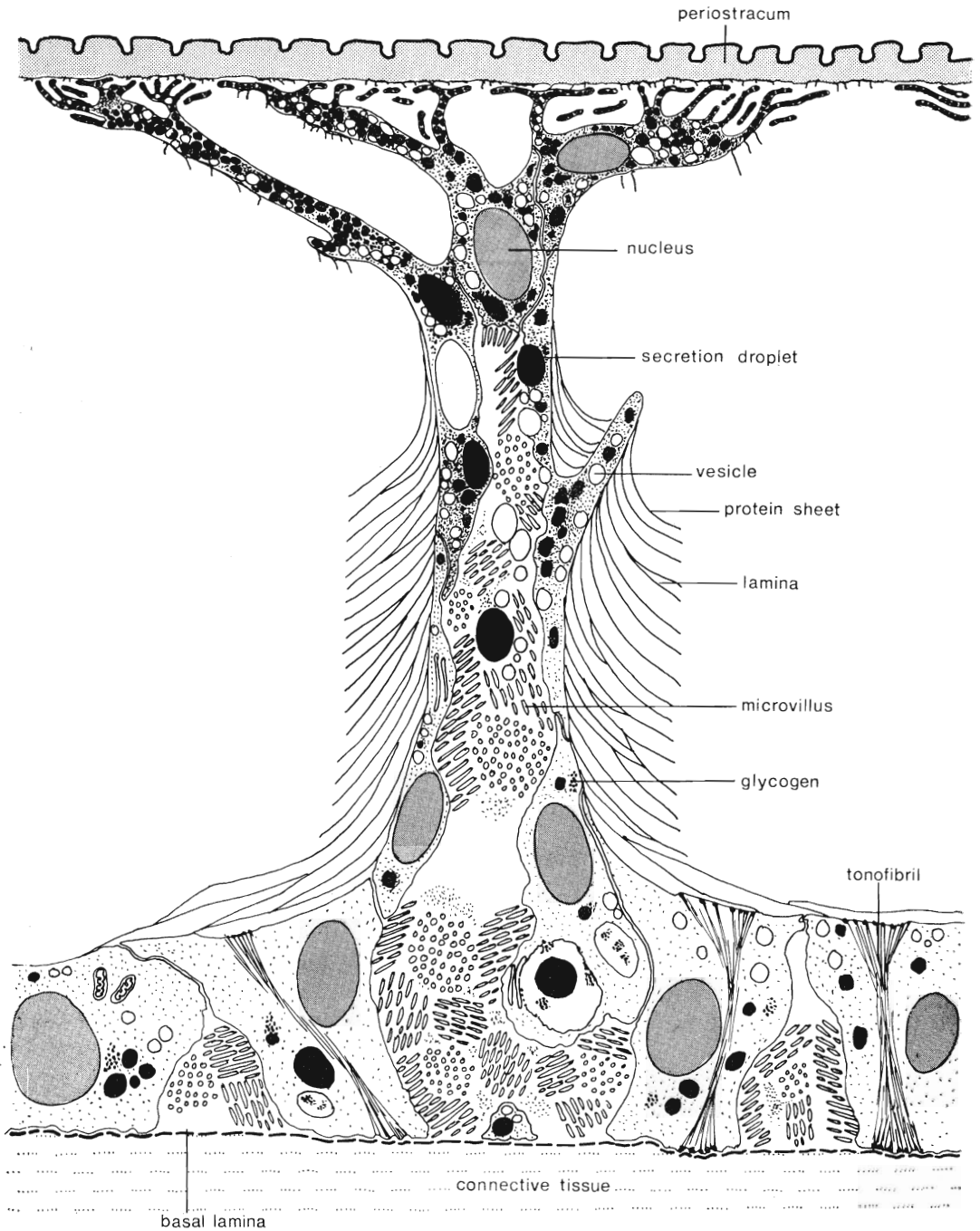
Fig. 3. Resin moulds of the terminal branches and tubules of some punctae seen after dissolving away the calcareous shell of the brachial valve ($\times 2500$).

Fig. 4. View of broken section of the secondary layer of the brachial valve showing the highly inclined disposition of laminae about a puncta ($\times 2600$).

Scanning electron micrographs of a brachial valve of *Isocrania egnabergensis*; Cretaceous (Senonian), Ignaberg, Sweden.

Fig. 5. Section showing the junction between the coarsely crystalline primary and the laminar secondary layer which curves from the left part of the top margin to the lower part of the right margin to accommodate a bulge of primary shell ($\times 1350$).

Fig. 6. View of an antero-lateral area of the internal surface showing the remains of secondary laminae ($\times 1350$).



TEXT-FIG. 13. Stylized diagram of a medial longitudinal section of a caecum showing its relationship to the periostracum and the dorsal mantle of *Crania*.

the pedicle valve compared with 132, 186, 188, and 208 per mm.² for the brachial valve. The estimates indicate that densities were twice as high in the dorsal interior; although, since the brachial is the thicker of the two valves, one would have expected it to have more widely spaced punctae bases.

The vertical extension of a caecum may involve some cell proliferation but the mode of branching alone confirms that fully differentiated outer epithelium must also contribute to the structure. In fact, it is not difficult to distinguish between the homologues of the core and peripheral cells making up the caecum of the articulate brachiopod (Owen and Williams 1969, p. 190). The terminal part of the caecum, principally that part embedded in the primary layer, is packed with rounded inclusions of variable electron-density, among which have been identified scattered lipid droplets and stellate clusters of glycogen. The commonest inclusions, however, are membrane-bound ellipsoidal bodies with a granular texture which vary in maximum diameter from 5 μm down to 100 nm. (Pl. 4, fig. 1). They also occur with fretted edges in intimate association with glycogen, or as traces within vesicles; and it is likely that they represent glycoprotein complexes in various stages of synthesis, storage, and breakdown. The cells composing the terminal zone of the caecum (Pl. 4, fig. 4), then, are similar to the caecal core cells of articulate brachiopods although they do not support a dense array of distal microvilli arranged in a brush. Moreover, these terminal cells also lead proximally into a lumen extending the length of the main caecal trunk, which is enclosed by flattened peripheral cells (Pl. 4, fig. 2) containing less densely distributed inclusions like those of the terminal cells. The flattened peripheral cells are clearly part of the outer epithelium which has been greatly stretched and brought into its present position by secondary shell accretion. They still carry out a limited amount of secretion, exclusively organic, along the wall of the punctae. The lumen likewise is simply an intercellular space of extraordinary size which extends outwards between the peripheral cells from the basal laminae bounding the connective tissue. This comparison is confirmed by the fact that the lumen is full of distinctive microvilli (Pl. 4, fig. 2) which are also found in the intercellular spaces of the outer epithelium and, more rarely, of the inner epithelium. The microvilli are about 40 nm. in diameter and pieces 1.6 μm long have been measured, although a complete microvillus must be much longer because connections with the cells are rare compared with the frequency of detached microvilli in any given section. Each microvillus is bounded by a fibrillar triple-unit membrane with a thickness of about 6.5 nm. and contains 8 or 9 regularly spaced fibrils, each about 3 nm. thick, which appear to extend throughout the entire length of the organelle (Pl. 4, fig. 3). In some transverse sections, the fibrils appear to be hollow and may be made up of interwoven helical coils. In any event, they are likely to have assisted in the activation of microvilli, groups of which are differently orientated in adjacent sectors or disposed in whorls around central spaces containing a moderately electron-dense substance like a polysaccharide.

There is, therefore, good evidence for believing that although the caeca of *Crania* differ in detail from those typical of articulate brachiopods, they, too, acted as repositories for foods, and that substances for their synthesis or the products of their breakdown did not, in natural circumstances, pass outwards through the periostracum but were freely circulated along microvillous intercellular passages leading into the base of the caecum and throughout the mantle (Pl. 4, fig. 5).

SHELL STRUCTURE OF FOSSIL CRANIACEANS

Apart from the impunctate, chitino-phosphatic *Eocomulus* which has been assigned to the superfamily for debatable reasons (see Rowell in Williams *et al.* 1965, p. H288), the craniaceans are a closely related group of brachiopods with a continuous history back to the Ordovician. Of the three genera represented by living species, only *Valdiviathyris* is unknown in the fossil state. The other two, *Craniscus* and *Crania* are first reported from the Jurassic and Carboniferous respectively. The geological range of the former seems to be reliable although only Recent specimens were available for study. The Carboniferous record of the latter genus is presumably based on species assigned to *Lissocrania* which has been tentatively classified as a subjective synonym of *Crania* by Rowell (in Williams *et al.* 1965, p. H290). Yet the description of *Lissocrania* given by its author J. S. Williams (1943, p. 70) indicates that it is much closer to *Petrocrania* than *Crania*; and the Carboniferous species '*Lissocrania*' *quadrata* (M'Coy) is undoubtedly a *Petrocrania* in the relative size of its adductor scars, the absence of a pustulose sub-marginal rim, and the structure of the pedicle valve. Consequently the fossil record of authentic *Crania* is here regarded as extending back only to the Cretaceous.

The remaining nine genera are represented solely by fossil species, although they differ from *Crania* only in minor morphological features, except for *Orthisocrania* and *Pseudocrania* which were unattached. Apart from *Philhedrella*, which appears to be closely related to *Petrocrania* (Kozłowski 1929, p. 40), specimens belonging to all those fossil genera as well as *Craniscus* have been examined, and descriptions of their shell structure are given below together with some intimation of the inferred relationship with *Crania*.

Isocrania. *Isocrania*, as represented by *I. egnabergensis* Retzius from the Senonian of Ignaberg, Sweden, and *Isocrania* sp. from the lower Senonian of Northfleet, England, is morphologically close to *Crania* and, equipped as it is with a tuberculate subperipheral rim in each valve, is barely distinguishable internally. Moreover, despite the prevalence of a skin of micrite on the shell surfaces, striking similarities can be seen in the shell fabric.

The primary shell of both brachial and pedicle valve (up to 50 μm and 20 μm thick respectively) is usually recrystallized into a mosaic with consertal boundaries; but here and there, patches of steeply stacked crystallites survive and may even be seen in the peripheral zone of the shell interior as radially disposed needles pointing outwards, up to 4 μm thick (Pl. 9, fig. 5; Pl. 10, fig. 5). Unlike living *Crania*, the secondary layer is present in both valves. Fifteen measured laminae in the brachial valve (Pl. 10, figs. 1, 2) had a mean thickness of 550 nm. and those in the pedicle valve were of the same order of size. Laminae too, can be found more or less unaltered on the internal surfaces of the shell (Pl. 9, fig. 6) and leave no doubt that they were deposited and grew in exactly the same way as in living *Crania*. The anterior margin of the pedicle valve of adult *Isocrania* tends to grow away from the substrate to form an upright rim. Such a feature can only develop through localized acceleration in shell deposition which is indicated by the secretion of clusters of long irregular crystallites up to 8 μm across, instead of laminae within the core of the rim (Pl. 10, fig. 6).

Modification of the calcareous skeleton to accommodate muscle systems also took place in the same way as in living *Crania*. The myotest is usually recrystallized, although not grossly enough, for example, to destroy the distinction at the surface between polygonal areas and their boundaries, which appear as discrete rhombic studs about 11 μm square (Pl. 10, figs. 3, 4).

As in *Crania anomala*, punctae coalesce to accommodate caecal branches in both valves of *Isocrania*, and are about 15 μm in diameter and 40 μm apart on the internal surface of the brachial valve just within the primary–secondary shell junctions.

Danocrania. Only pedicle valves of a Danian species from Ciply, Belgium were available for our study of *Danocrania* (Rosenkrantz 1964, p. 515), although this is the valve which exhibits the most distinctive features of the genus. In this stock mixoperipheral growth gave rise to a ventral pseudointerarea which, together with the anterior and even the lateral margins, grew away from the substrate so that only a postero-median patch of the valve formed the attachment area. This differential growth is reflected in the shell structure. Immediately above the area of attachment, the primary and secondary shell are orthodoxly developed with the former layer up to 40 μm thick and the latter composed of regular successions of laminae, ten of which averaged 370 nm. in thickness (Pl. 11, fig. 1). In contrast, secretion of the unattached parts of the valve was so accelerated as to preclude the development of a typical secondary layer. In the pseudointerarea and at the valve margins, the fabric of the secondary is significantly coarser (Pl. 11, fig. 3), and when groups of laminae can be identified, they may be up to 2 μm thick suggesting a sixfold increase in the rate of secretion.

The morphology of the junction between the secondary shell of the attachment area and that of the pseudointerarea is indicative of these differences in deposition. The regular laminae of the attachment area curve towards a persistent layer of calcite, about 10 μm thick, which separates the pseudointerarea from the rest of the valve (Pl. 11, fig. 2). At the junction with the layer of separation the laminae which are concave anteriorly pass into micritic rubble. The separation layer is more uniformly textured

EXPLANATION OF PLATE 10

Scanning electron micrographs of a brachial valve of *Isocrania egnabergensis*; Cretaceous (Senonian), Ignaberg, Sweden.

Fig. 1. Section through the lateral part of the valve showing the laminar structure of the secondary layer; exterior of valve towards the top ($\times 2700$).

Fig. 2. Section showing the disposition of laminae around a puncta in the secondary layer; exterior of valve towards the bottom ($\times 2600$).

Fig. 4. Section showing relationship between the crystalline myotest (in the bottom left-hand corner) and laminae in the secondary layer; interior of valve towards the bottom left-hand corner ($\times 1410$).

Scanning electron micrographs of a pedicle valve of *Isocrania* sp.; Cretaceous (Senonian), Northfleet, England.

Fig. 3. View of the internal surface showing recrystallized polygonal areas separated by depressed boundaries in the posterior adductor muscle scar ($\times 1350$).

Fig. 5. Section showing the ventral shell succession with the coarsely crystalline primary shell contained between the laminar secondary shell seen in the lower half of the micrograph and the substrate shown along the top margin of the micrograph ($\times 1400$).

Fig. 6. Section showing the coarse crystallites developed in place of laminae in the secondary shell; interior of valve beyond the top ($\times 2800$).

and bears no sign of banding. It may represent post-mortem calcification within a slot defined and maintained as a cavity with or without organic debris by the axis of a fold in the retreating outer epithelium that controlled the secretion of secondary shell lining the attachment area on one side and the pseudointerarea on the other. The separation layer persists anteriorly to intervene between the curved laminae of the attachment area and wedges of coarsely textured calcite which underlay the muscle bases in living animals. The layer ends abruptly, as does the regular secondary lamination characteristic of the attachment area, at the angle marking the change in growth of the ventral margin away from the substrate. Hence if account is also taken of the effects of muscle implantation on skeletal secretion, the secretion of relatively coarsely textured carbonate became prevalent over the entire surface of the pedicle valve in later stages of adult growth.

Ancistrocrania. Two species of *Ancistrocrania* have been examined: *A. parisiensis* DeFrance from the Maastricht sands of Ciplu, Belgium, and a new species from the Lower Senonian Chalk of Northfleet, England. The fully grown pedicle valve of the former species is like a truncated cone because its margin grew holoperipherally away from the substrate in adult stages of development. The pedicle valve of the latter, however, was adnate during growth and, consequently, remained more or less discoid throughout life. This difference in habit did not affect the basic skeletal fabric although it did modify the relationship between the primary and secondary shell.

The ultrastructure of the primary layer and the muscle scars is unexceptional. The primary layer varies between 30 and 60 μm in thickness in both valves and consists of coarse, elongate crystallites up to 10 μm thick, lying normal to the external surface (Pl. 12, fig. 1). The myotest is also composed of coarse crystallites disposed more or less normal to the internal surface (Pl. 11, fig. 6). The structure of the secondary layer of the pedicle valve, however, differs markedly from that of other craniaceans. In both valves, secondary laminae are consistently identifiable only in the vicinity of the punctae and even in those regions they are relatively coarse with an average thickness of 650 nm. for 20 laminae in the brachial valve and about the same order of thickness for those in the pedicle valve (Pl. 11, figs. 4, 5). The commoner constituents of the secondary layers of both valves are crystallites, 3 μm or more thick, disposed more or less in the same way as the laminae into which they grade. This fabric is the overwhelmingly dominant texture of the raised margins of the pedicle valve. However, the secondary layer of the margins as well as the rest of the valve is further characterized by being porous. In *A. parisiensis*, the pores are seen to be surface manifestations of unbranched canals about 80 μm wide (compared with about 15 μm for punctae) which form acute external angles with the primary layer. In the Northfleet species, the canals are much coarser, being up to 300 μm in diameter, and are so densely distributed as to be separated by partitions only 40 μm or so thick.

The nature and disposition of these canals indicate that in life they must have been at least partly occupied by evaginations of the mantle that became outwardly inclined during growth through the peripheral expansion of the pedicle valve. In the adnate Northfleet species they remained open (text-fig. 14d), but some canals occupying the core of the raised margins of the pedicle valve of *A. parisiensis* became closed by a cover of primary shell. Such reversals of growth could only have come about during

minor retractions of the mantle while it was being raised above the substrate by the excessive dorsal growth of the valve margins as shown in text-fig. 14 *a-c*. The function of the outgrowths accommodated by the canals is unknown. The grossness of lamination and the lack of any significant carbonate deposition within the canals during life suggests that the excessive proliferation of outer epithelium, which provided the mantle evaginations occupying the canals, was not, in itself, responsible for any abnormal thickening of the pedicle valve. These evaginations may simply have been storage centres in the same way as the long-established caeca and may even have represented a second but short-lived evolutionary development of punctation within the craniaceans.

Craniscus. Although *Craniscus* is first recorded from Jurassic rocks, only dried shells (BM 12510) of a Recent species collected off Korea have been examined. These have been classified as *Craniscus japonicus* (Adams) although certain morphological features suggest that the species could equally well have been identified as *Ancistrocrania*. The differences between *Ancistrocrania* and *Craniscus* are actually small. The brachial valves look alike in having unthickened margins and a pair of ridges bearing the anterior adductor scars, which diverge from a variably developed medial septum. Even the pedicle valves can be similar in general morphology because the margin of some species of *Ancistrocrania* remained attached to the substrate during adult stages of growth as in *Craniscus*. Moreover, the calcareous shell of the pedicle valve of the Korean species is permeated by unbranched canals like those found in the pedicle valve of *Ancistrocrania*. However, there is one important difference in shell structure of the pedicle valve which prompts us to retain the name *Craniscus* for the Korean species in the expectation that further investigations will show that this difference is consistently diagnostic of the genus.

The succession of the brachial valve of *C. japonicus* is like that of *Crania* in that the primary layer is about 25 μm thick and is made up of inclined, acicular crystallites and rarer impersistent platelets while the secondary layer consists of evenly developed

EXPLANATION OF PLATE 11

Scanning electron micrographs of a pedicle valve of *Danoocrania* sp.; Cretaceous (Danian), Ciply, Belgium.

Fig. 1. Section showing secondary laminae in the posterior part of the valve ($\times 2700$).

Fig. 2. Section showing the micritic rubble junction between the secondary laminae (above) and the separation layer shown by the relatively dark band across the lower part of the micrograph ($\times 1300$).

Fig. 3. Section showing the coarseness of fabric in the secondary layer of the pseudointerarea; internal surface towards the bottom ($\times 1300$).

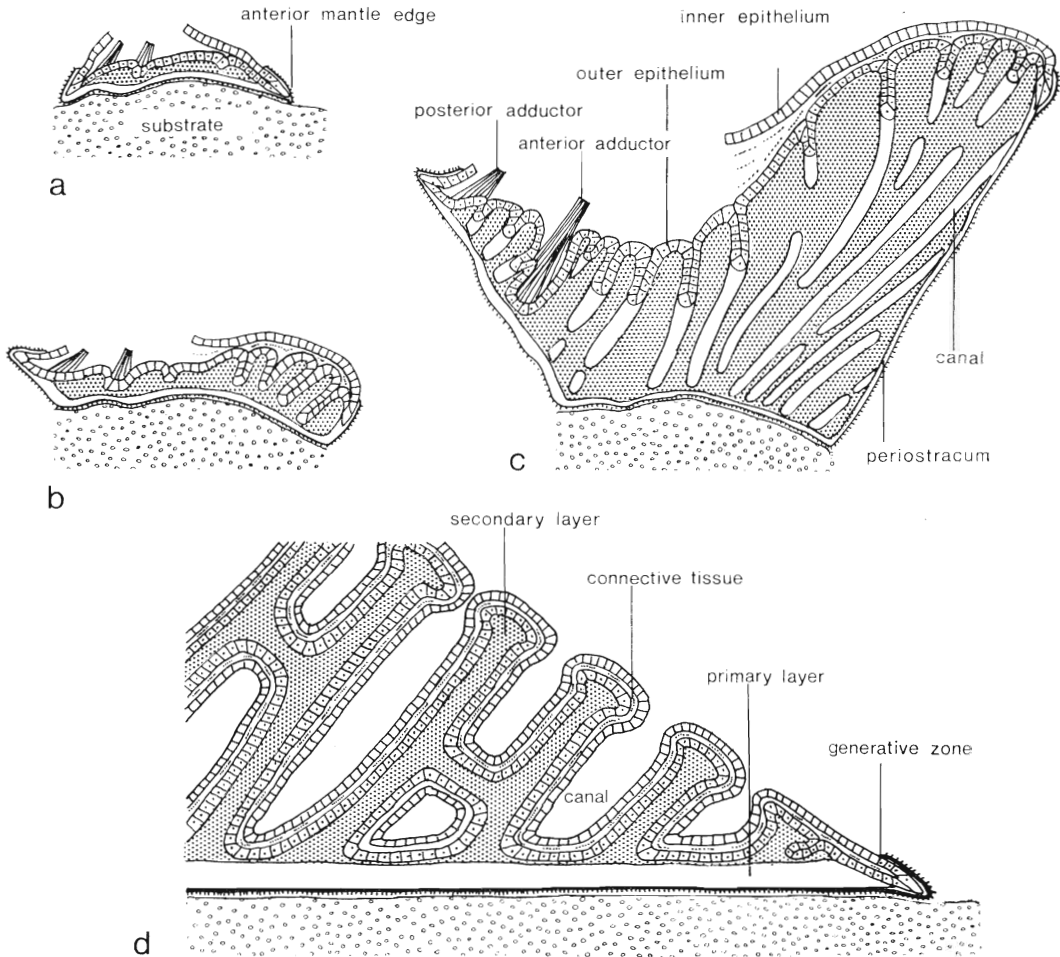
Scanning electron micrographs of the shell of *Ancistrocrania parisiensis*; Cretaceous (Maastrichtian), Ciply, Belgium.

Fig. 4. Section showing the laminar secondary shell in the mid-part of the brachial valve with an oblique view of a puncta branch in the top left-hand corner which is also the direction of the exterior ($\times 1500$).

Fig. 5. Section showing the disposition of laminae about a puncta (along the right margin) in the secondary shell underlying the myotest in the pedicle valve; exterior of valve towards the top ($\times 3000$).

Fig. 6. Section showing the junction between coarse laminae of the secondary layer and overlying myotest (consisting of vertically disposed crystallites) in the pedicle valve; interior of valve towards the top ($\times 1370$).

laminae about 230 nm. thick. Both layers are permeated by punctae, up to 15 μm across near their bases. The muscle scars of both valves are also orthodoxly differentiated into polygonal areas up to 15 μm in diameter, which become elongated into elliptical features arranged *en echelon* down the posterior surfaces of the ridges supporting the dorsal



TEXT-FIG. 14. Stylized longitudinal sections to show the structure and growth of the pedicle valve of *Ancistrocrania parisiensis* (a-c), and the structure of the edge of the pedicle valve of *Ancistrocrania* sp. (d).

anterior adductor bases. The calcareous layer of the pedicle valve, however, is like that of *Crania* in being composed exclusively of primary shell with a dominant acicular crystallite fabric, and like that of *Ancistrocrania* in being perforated by canals about 120 μm in diameter. Taking into account several other features, it seems reasonable to assume that *Craniscus* is more closely related to *Ancistrocrania* although secondary shell also failed to develop in this stock independently of *Crania*.

Philhedra. Contrary to some records (Rowell in Williams *et al.* 1965, p. H291), a costellate craniacean, congeneric with *Philhedra* at least in respect of its brachial valve, is known from the Oxford Clay of Boulonnais, France. Specimens at our disposal were partially silicified but a coarsely textured primary layer and a laminar secondary shell were identifiable here and there and confirm the orthodox development of the brachial valve of older *Philhedra*. These include the Devonian *Philhedra crenistria* (Hall) from the Hamilton, Arkona, Ontario, a Silurian species from the Eke Marl, Laubacke, Gotland, and an Ordovician species from the Rakvere beds (E), Estonia.

In the brachial valves of all three species, the ribbing is composed exclusively of primary shell which, therefore, varies greatly in thickness although the intercostellate thickness is between 30 and 40 μm . The primary layer typically consists of coarse elongate crystallites disposed more or less normal to the external surface (Pl. 12, fig. 4). The laminae of the secondary layer are also well defined with 10 laminae averaging 350 and 300 nm. thick in *P. crenistria* and the Silurian species respectively (Pl. 12, figs. 2, 3, 5, 6). Generally, however, recrystallization has united groups of laminae into thicker units and this may account for the significantly greater estimates obtained for 5 laminae of the Ordovician *Philhedra* which averaged 850 nm. in thickness (Pl. 13, fig. 1). The myotest, where seen, is characteristically coarsely crystalline and the punctae in all three species appear to be unbranched, at least within the secondary layer, and between 20 and 30 μm in diameter.

Only specimens of *P. crenistria* were attached to the substrate and so afforded an opportunity of examining the complete shell. However, no trace of a pedicle valve was found although one shell was 14 mm. across, well in excess of the diameter at which calcification of the pedicle valve takes place in *Crania*. It is therefore assumed that the pedicle valve of this species was exclusively organic, consisting of no more than a periostracum with a thickened inner protein boundary.

Acanthocrania. A complete specimen of *Acanthocrania* sp. attached to a *Rafinesquina* from the Cincinnati, Cincinnati, Ohio, was used to determine the skeletal ultra-

EXPLANATION OF PLATE 12

Scanning electron micrograph of a pedicle valve of *Ancistrocrania* sp.; Cretaceous (Senonian) Northfleet, England.

Fig. 1. Section showing coarse crystallites of the primary layer lying normal to the junction with the substrate in the lower right-hand corner ($\times 1400$).

Scanning electron micrographs of a brachial valve of *Philhedra crenistria*; Devonian (Hamilton); Arkona, Ontario.

Fig. 2. Section showing the relationship between the punctae and laminae of the secondary layer; exterior of valve towards the top ($\times 750$).

Fig. 3. Section showing the laminar secondary layer ($\times 1400$).

Fig. 4. Section showing the junction between the laminar secondary shell and the coarsely crystalline primary shell in the top left-hand corner, which is also the direction of the exterior of the valve ($\times 2900$).

Scanning electron micrographs of a brachial valve of *Philhedra* sp.; Silurian (Eke Marl), Laubacke, Gotland.

Fig. 5. Section showing the laminae of the secondary shell ($\times 2600$).

Fig. 6. Section showing the relationship between a puncta and the laminae of the secondary shell; exterior of valve towards the top ($\times 1350$).

structure of this stock. The brachial valve is orthodoxly developed with a primary layer about $4\ \mu\text{m}$ thick composed of coarse crystallites aligned normal to the surface; and a secondary shell made up of layers of laminae (ten of which averaged 316 nm. in thickness) alternating with layers of lath-like crystallites (Pl. 13, fig. 2). These crystallites are usually about $1.5\ \mu\text{m}$ wide and are stacked in variably defined rows at high angles to the bounding surfaces of the layers (Pl. 13, fig. 3). It is evident that the amounts of organic material within these layers, as represented by the protein coats of the laminae and laths, would have differed significantly in the unaltered shell. Moreover the layers themselves form isochronous growth surfaces so that they were probably differentiated seasonally. The fact that a similar layering is found in shells of *Petrocrania scabiosa* (Hall) attached to the same *Rafinesquina* specimen lends credence to this interpretation.

The brachial valve is also typically permeated by punctae up to $25\ \mu\text{m}$ in diameter. The most distinctive feature of *Acanthocrania* is the spine-like surface ornamentation of the brachial valve. The spines are hollow but the canals, which are about $40\ \mu\text{m}$ in diameter, do not penetrate much below the primary-secondary junction. They were therefore formed by superficial variation in shell deposition and were lined by periostracum not outer epithelium.

No pedicle valve of *Acanthocrania* has yet been recorded. But in the specimen sectioned, which was a mature individual 8 mm. in diameter, a lenticle of coarsely crystalline calcite, about $500\ \mu\text{m}$ long and $4\ \mu\text{m}$ high, occurred just within the edge of the brachial valve and was separated from the *Rafinesquina* host by a normal micritic coat (Pl. 13, fig. 4). This is the expected profile and position of an anterior rim that may have developed through incipient calcification of the pedicle valve. It is therefore possible that, although the pedicle valve of *Acanthocrania* was normally entirely organic, an arc of primary shell representing a thin impermanent submarginal rim may have developed anteriorly in some specimens.

Petrocrania. Three species of *Petrocrania* were examined: *P. quadrata* (M'Coy) from the Carboniferous Limestone Group, Carlisle, Scotland, *P. scabiosa* from the Ordovician, Cincinnati, Ohio, and *Petrocrania* sp. from the Devonian Silica Shale, Sylvania, Ohio. All three were represented by complete specimens while pedicle valves of the first two were also available for inspection, although only those of *P. quadrata* were sufficiently well preserved to reveal the finer detail of their internal morphology.

The structure of the brachial valves of all three species is quite normal in that the calcareous shell is fully differentiated into primary and secondary layers pervaded by punctae. The primary layer is only about $10\ \mu\text{m}$ thick in *P. quadrata* compared with about $50\ \mu\text{m}$ in the Devonian species and even $80\ \mu\text{m}$ in *P. scabiosa*, although it invariably consists of a coarse mosaic indicating a recrystallized condition. In contrast, the fine lamination of the secondary shell generally survives as a thin impermanent layering averaging 200 nm., 280 nm., and 350 nm. in thickness for 10 laminae of *P. quadrata*, *P. scabiosa*, and *Petrocrania* sp. respectively (Pl. 13, fig. 5; Pl. 14, fig. 2). As already stated, brachial valves of *P. scabiosa* are characterized by layers of laminae interleaved with those of lath-like crystallites stacked in rows at high angles to the layering (Pl. 14, fig. 2). The punctae, which have not been seen to coalesce within sections of brachial valves examined by us, are about $10\ \mu\text{m}$ wide at their bases. Judging from their distribution on the slightly abraded external surface near the edge of a brachial valve of

P. quadrata they are regularly spaced at intervals of about 25 μm (93 were counted within an area of 0.0625 mm.²). It may not be arithmetically precise to compare this density with that determined for punctae occurring on the internal surface of the brachial valve of *Crania anomala* at the primary–secondary junction (31 within 0.0625 mm.²); yet it is likely that the punctae of *P. quadrata* were more densely distributed than those of *C. anomala*, and that they accommodated simple caeca with no more than a spray of terminal branches beneath the periostracum.

The calcareous shell of the pedicle valve of adult *Petrocrania* is not only thin but was secreted relatively late in life; in *P. scabiosa*, for example, calcite secretion did not generally take place until the shell was more than 7 mm. in diameter. Nonetheless both primary and secondary layers are readily identifiable (Pl. 14, fig. 3). The former is about 20 μm thick in *P. quadrata* (Pl. 13, fig. 6) and is made up of a coarse recrystallized mosaic, while the latter is composed of laminae of about the same thickness as those in the complementary brachial valves. However, unlike other fossil stocks in which the skeletal succession of the pedicle valve is complete, there is no undoubted trace of punctation in either layer. Punctae were seen permeating some of the shell forming a margin of one specimen of *P. scabiosa*, but this was almost certainly an adherent patch of brachial valve. In all other sections as well as the interiors of four well preserved pedicle valves of *P. quadrata* examined by us, no punctae were found, thus confirming the views of John Young (see Davidson 1880, p. 269).

Coarsely crystalline calcite lenses of myotest, commonly with cleavage set at high angles to their transgressive junctions with laminae, also occur within the secondary shell of both valves of *P. quadrata* (Pl. 14, fig. 1) and crop out at the internal surfaces as muscle scars. Even polygonal areas, like those associated with the muscle systems of living *Crania* are sporadically preserved in the muscle scars of *P. quadrata*; and although these have not been seen in the older species, the myotest, as observed in section, must have been identical.

EXPLANATION OF PLATE 13

Scanning electron micrograph of a brachial valve of *Philhedra* sp.; Ordovician (Rakvere Beds), Rakvere, Estonia.

Fig. 1. Section showing recrystallized laminae of the secondary shell ($\times 1400$).

Scanning electron micrographs of the shell of *Acanthocrania* sp.; Ordovician (Cincinnati), Cincinnati, Ohio.

Fig. 2. Section of the secondary layer of the brachial valve showing punctae and the alternating layers of laminae and lath-like crystallites; exterior of valve towards the bottom ($\times 650$).

Fig. 3. Section of the secondary layer of the brachial valve showing the structure of lath-like crystallites; exterior of valve towards the top ($\times 6000$).

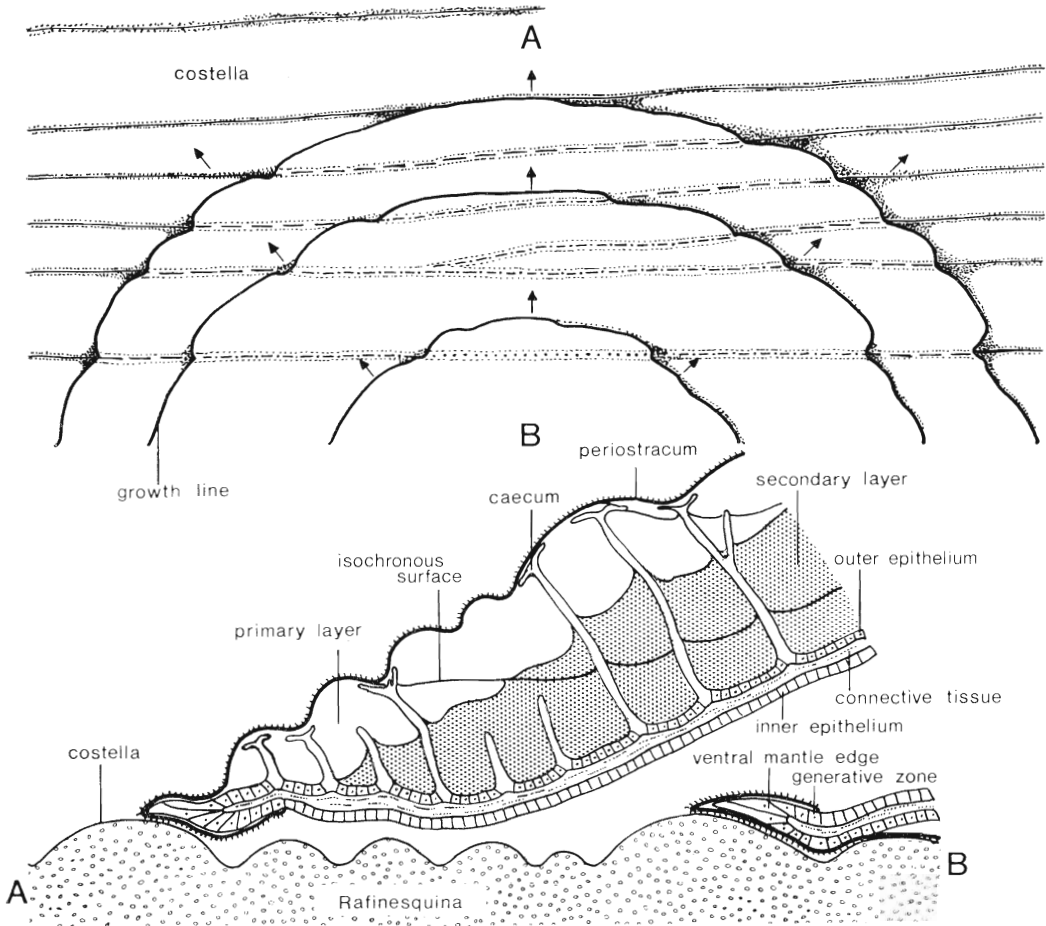
Fig. 4. Section showing a lenticle of darker, more compact calcite inferred to be the anterior sub-peripheral rim of the pedicle valve attached to a rafinesquinid shell in the bottom right-hand corner ($\times 550$).

Scanning electron micrographs of the shell of *Petrocrania quadrata*; Carboniferous (Carboniferous Limestone Series), Carlisle, Scotland.

Fig. 5. Section of the brachial valve showing laminar secondary shell; exterior of valve towards the top right-hand corner ($\times 1600$).

Fig. 6. Section of the pedicle valve showing laminar secondary (top left-hand corner) and coarsely crystalline primary shell in relation to substrate in the bottom right-hand corner ($\times 2600$).

One of the most characteristic features of *Petrocrania* is that it usually reproduced the detailed topography of the substrate on the external surface of the brachial valve. *P. scabiosa*, which frequently settled on *Rafinesquina* and replicated the parvicostellate ornamentation of that stock with remarkable clarity, is probably the best-known form



TEXT-FIG. 15. Stylized external view (above) and longitudinal section (below) of the edge of the brachial valve of *Petrocrania scabiosa* to show how details of substrate topography are reproduced on the dorsal external surface.

(text-fig. 15), although such mimicry was prevalent among all species referred to the genus and indicates a noteworthy sensitivity of the dorsal mantle edge. Three factors combined to promote this particular mode of growth. First, the calcareous shell of the pedicle valve, when it was secreted, tapered to a wafer-thin edge instead of forming a blunt limbus and/or a high submarginal rim which would have precluded convergence of the dorsal mantle towards the substrate. Secondly, the dorsal mantle consistently extended well beyond the boundary of the mineral part of the pedicle valve, and so

made contact with the substrate. Thirdly, the stiffening of the mineral layers of the brachial valve by amalgamation of calcite crystallites must have constantly taken place as both the inner and outer surfaces of the mantle edge were being moulded to the substrate without the intervention of a fringe of setae. In this way, the expanding mantle made a periostracal mould of the substrate and then filled in the mould with calcite which survived as a mineral cast long after the organic cover had disappeared.

Pseudocrania and *Orthisocrania*. Both *Pseudocrania* and *Orthisocrania* differ from all other craniaceans in that they did not live attached to a substrate. Consequently the pedicle valve was as well developed morphologically as the brachial, and this should be reflected in the ultrastructure of the shell. The poorly preserved *Orthisocrania divaricata* (M'Coy) from Longvillian mudstones, Kildare, Ireland (Wright 1970), examined for this study, gave no more indication of shell fabric than that lamination within the secondary layer was characteristic of at least one of the valves. However, through the kindness of Dr. Valdar Jaanusson, many fine specimens of *Pseudocrania* sp. from the *Vaginatum* Limestone, Hälludden, Öland, were available and show how alike the valves were. In both, a full calcareous succession of identical texture was secreted. The primary layer in each valve was about 50 μm thick and consisted of roughly equidimensional crystallites with consertal boundaries. The laminae of the secondary layer are normally recrystallized into thicker units but ten, which were identifiable as not having been so affected, had an average thickness of 400 nm. (Pl. 14, fig. 4). Caeca, about 5.5 μm in diameter, were also equally developed in both valves as were patches of coarsely crystalline myotest (Pl. 14, fig. 5).

EXPLANATION OF PLATE 14

Scanning electron micrograph of a pedicle valve of *Petrocrania quadrata*; Carboniferous (Carboniferous Limestone Series), Carluke, Scotland.

Fig. 1. Section showing the relationship of a coarsely crystalline lens of myotest to laminae in the secondary layer; exterior of valve towards the bottom ($\times 2500$).

Scanning electron micrographs of the shell of *Petrocrania scabiosa*; Ordovician (Cincinnatian), Cincinnati, Ohio.

Fig. 2. Section of the secondary layer of the brachial valve showing the alternating layers of laminae and lath-like crystallites ($\times 1300$).

Fig. 3. Section of the pedicle valve showing the secondary and primary shell in relationship to the underlying substrate seen in the bottom margin of the micrograph ($\times 1200$).

Scanning electron micrographs of the shell of *Pseudocrania* sp.; Ordovician (*Vaginatum* Limestone), Hälludden, Öland.

Fig. 4. Section of the brachial valve showing the disposition of laminae around a puncta; exterior of valve towards the top left-hand corner ($\times 1450$).

Fig. 5. Section of the pedicle valve showing the junction between the coarsely crystalline myotest towards the top and the laminar secondary shell towards the bottom, which is also the direction of the valve exterior ($\times 1500$).

Scanning electron micrograph of the shell of *Craniops implicata*; Silurian (Mulde Marl), Mulde, Gotland.

Fig. 6. Section of the pedicle (?) valve showing the laminar structure of the secondary shell; interior of valve towards the bottom ($\times 1250$).

SHELL STRUCTURE OF THE CRANIOPSIDAE

The craniopsids are three (or four) closely related genera which, despite such craniacean characteristics as a calcareous exoskeleton and lack of pedicle, are currently classified as lingulaceans because their shell is impunctate and bears muscle scars resembling those of lingulids. One species of *Craniops* has been available for study, *C. implicata* (J. de C. Sowerby) from the Wenlockian Mulde Marl, Mulde Brick-yard, Gotland, and from unspecified Silurian strata, Gotland; both samples are characterized by the shell structure described below.

The *Craniops* shell is composed mainly of well-defined laminae, disposed parallel with the shell surface so that they are more or less flat-lying in section, and averaging 0.3 μm in thickness (the mean for 20 laminae (Pl. 14, fig. 6)). The fabric is generally well preserved, and is immediately recognizable, even when recrystallization *in situ* may give rise to bands up to 4 μm thick with consertal lateral boundaries, because such replacements are disposed in the same way as individual laminae. It seems, therefore, that this layer is so like the secondary laminar one of *Crania* that it, too, must have been secreted as discrete plates of calcite growing by screw dislocation and separated from one another by protein sheets. Differences in attitude of the laminae arise from the punctation of the *Crania* shell which causes the laminae in that stock to be disposed in a series of outwardly facing concave arcs. Unaltered laminae have not been seen on the internal surfaces of the valves of *Craniops* because they have been either obscured by a coating of micritic particles about 1 μm in size, or recrystallized into comparatively large thick tablets.

There are also traces of a non-laminar primary layer in *Craniops*, although it is not always distinguishable from the rock matrix because the original state of the external surface of a valve is more difficult to interpret than the internal. In better-preserved shells, a variable thickness of microcrystalline calcite may intervene between undoubted matrix and the laminar part of the shell, but grain growth tends to blur the outer surface of the zone so that no sharp contact is readily and consistently identified. The shell of *Craniops*, however, is strongly lamellose, a condition brought about by periodic retraction of the mantle, and it is in the interlamellar spaces that one would expect to find wedges of primary shell preserved. Such wedges of non-laminar calcite, up to 10 μm thick, do occur (Pl. 15, fig. 1). They are usually parallel with the laminae forming their inner boundaries and slightly oblique to those along their outer boundaries. In such confined spaces as those subtended by overlapping lamellae, any wedge of rock matrix is most likely to be either a drusy growth or a granular cementation, characterized by increases in grain size inwards away from its boundaries. Variation of this kind has not been seen; on the contrary, the wedges are usually featureless except for grooves up to 0.5 μm long developed at irregular intervals, more or less normal to their boundaries. Such wedges separating laminar layers have, therefore, been interpreted as recrystallized primary shell; and although no trace of the original ultrastructure has been found, the fact that the fabric has been so completely destroyed by recrystallization suggests that it was originally composed of very fine crystallites with little organic matrix.

Like the rest of the shell interior, the muscle scars in both valves are covered by micrite. Sections, however, show that the scars in each valve represent surface outcrops

of wedge-like myotest buried within the laminar secondary shell. The myotest thickens away from a postero-median area which must have been the site of the first-formed muscle attachments and has variably developed junctions with the laminae of the secondary shell. The outer junctions are usually not strongly demarcated because adjacent laminae, over which they grew, curve into the myotest to lose their own boundaries gradually within the mosaic (Pl. 15, fig. 2). The inner junctions, on the other hand, are normally sharply defined by subparallel laminae which cover only the inner ends of the myotest and were deposited by regenerated outer epithelium in the wake of the spreading muscle bases. Thus muscle systems of the craniopsids were attached to parts of the calcareous skeleton that underwent a continuous modification which was co-ordinated with the migration of muscle bases in the manner of living brachiopods like *Crania*. Moreover, recalling the effects of recrystallization on the muscle pads of stocks like *Isocrania* which were closely related to *Crania*, it is possible that the craniopsid muscle pads were also secreted as crystallites disposed more or less normal to the surface of attachment.

SHELL STRUCTURE OF THE OBOLELLIDA

Although specimens of *Bicia* and *Obolella* (including *O. congesta* Poulsen) were available for study, only *Trematobolus pristinus bicostatus* Goryansky from the Lower Cambrian (Lensky Stage) of the Rassokha River Basin, E. Siberia afforded any clue to the shell fabric of the order.

The Russian material, which was most generously provided by Dr. Goryansky, consists of disarticulated valves preserved in a pale green marl. The rock is quite rich in organic fragments down to 25 μm in size, although these are usually scattered throughout the marl which has undergone a patchy replacement by grain growth mosaic. The valves must also have been affected by recrystallization but remnants of the enveloping periostracum and mantle seem to have survived long enough after the burial of most specimens to promote permanent grain boundaries between the rock matrix and the

EXPLANATION OF PLATE 15

Scanning electron micrographs of the shell of *Craniops implicata*; Silurian (Mulde Marl), Mulde, Gotland.

Fig. 1. Section of brachial (?) valve showing coarsely crystalline primary shell of a lamella extending from the top left-hand corner to the bottom right-hand corner of the micrograph and lying between two laminar secondary layers ($\times 2700$).

Fig. 2. Section of brachial (?) valve showing the relationship of myotest to laminar secondary shell in the lower part of the micrograph; exterior of valve towards the bottom ($\times 1300$).

Scanning electron micrographs of a brachial valve of *Trematobolus pristinus bicostatus*; Cambrian (Lensky Stage), Rassokha River Basin, E. Siberia.

Fig. 3. Section showing the junction between the coarsely crystalline primary shell above and the laminar secondary shell below ($\times 2500$).

Fig. 4. Section showing nodules of calcite in relation to the laminar secondary layer, exterior of valve towards the top ($\times 2500$).

Fig. 5. Section showing amalgamated nodules of calcite in relation to the laminar secondary layer; exterior of valve towards the top ($\times 2500$).

Fig. 6. Section showing laminae disposed about a nodule; exterior of valve towards the top ($\times 6500$).

mineral part of the skeleton. The bulk of the shell itself is remarkably well preserved with fully differentiated primary and secondary layers and a strongly developed myotest.

The primary layer, which was periodically extended anteriorly to form the concentric lamellae ornamenting the exterior of *Trematobolus*, is about 35–40 μm thick between lamellae, and consists of coarse recrystallized grains with consertal boundaries (Pl. 15, fig. 3). The primary–secondary junction is quite sharp with fully developed laminae marking the boundary. These laminae are the chief constituents of the secondary shell. They are lenticular in section and about 10 μm across and 480 nm. thick (an average for 10 units) (Pl. 15, figs. 4, 5, 6). The laminae are essentially flat-lying and, despite the masking effects of recrystallization and other complications referred to below, there is little doubt that they were separated from one another by protein sheets and grew as a series of screw dislocations in the same way as those making up the secondary shell of living *Crania*.

One new feature in *Trematobolus* is the occurrence of nodules, either hemispherical or, more rarely, lenticular in shape, which are regularly arranged at intervals of about 25 μm , throughout much of the laminar secondary shell (Pl. 15, fig. 4). The nodules, which are about 8 μm wide and high and only rarely amalgamated laterally into bodies up to 40 μm across (Pl. 15, fig. 5), are composed of coarsely crystalline calcite. The convex surfaces of the great majority of nodules face externally, the planar surface internally; and, since the surrounding laminae are disposed parallel to these surfaces (Pl. 15, fig. 6), both laminae and nodules (or at least the hemispherical spaces they now occupy) must be syngenetic. Morphologically, the nodules are very like the lenses developed in association with the main myotest of *Crania* although the orientation is reversed. Consequently a nodule is regarded as marking the site of a cell which, unlike those depositing lenses within the secondary layer of living *Crania*, temporarily ceased secreting secondary shell although deposition by neighbouring cells continued. Subsequently, the depression formed in this way became filled with coarse crystallites deposited relatively quickly by the same cell before it reverted to normal secondary secretion which resulted in the growth of more or less flat-lying laminae across the top of the nodule. Despite the inferred differences in epithelial activity, the cells that gave rise to nodules may also have functioned as muscle ties, like those responsible for the secretion of lenses in *Crania*. Alternatively, they may have been temporary evaginations of the outer epithelium accommodating intercellular secretion droplets, a precursory stage in the development of permanent caeca (text-fig. 16).

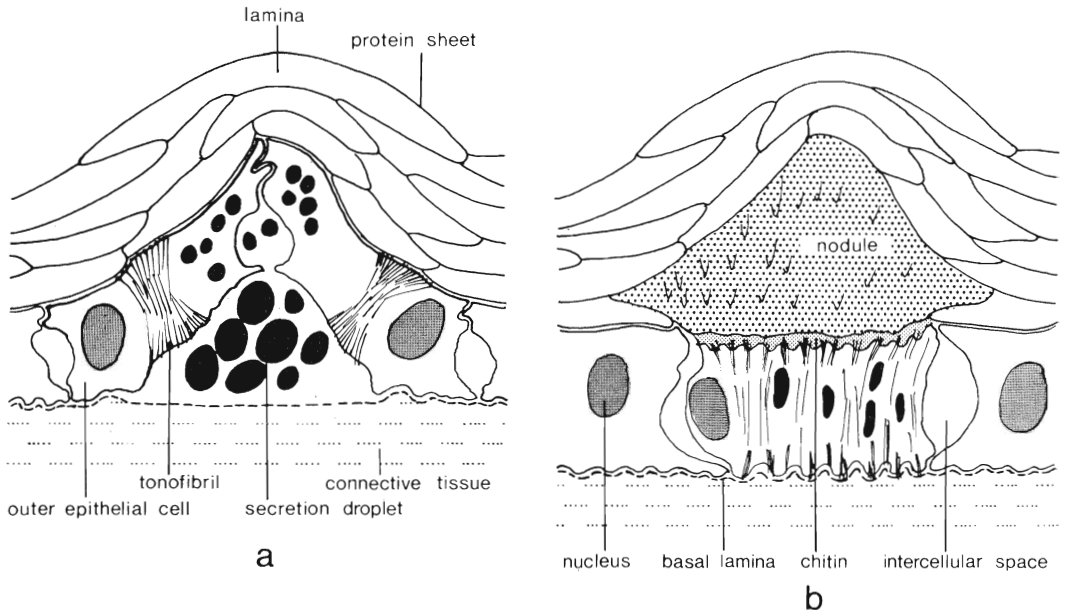
The myotest of *Trematobolus* is also easily identifiable. It forms a wedge extending anteriorly from the umbo beneath coarsely laminar secondary shell. The latter deposit, with laminae up to 4 μm thick lying more or less parallel to the inner surface, represents secondary shell secreted in the wake of the migrating muscle fields. It contrasts with the myotest which consists of strong, coarse crystallites, typically about 75 μm long and 10 μm wide, which are disposed normal to the outer surface of the valve.

CONCLUSIONS

Any reconstruction of the structural evolution of the craniacean shell must be founded on the contrasting variability of the skeletal succession in the brachial and pedicle valves. The difference is so profound as to hint at the original fabric of the prototypic

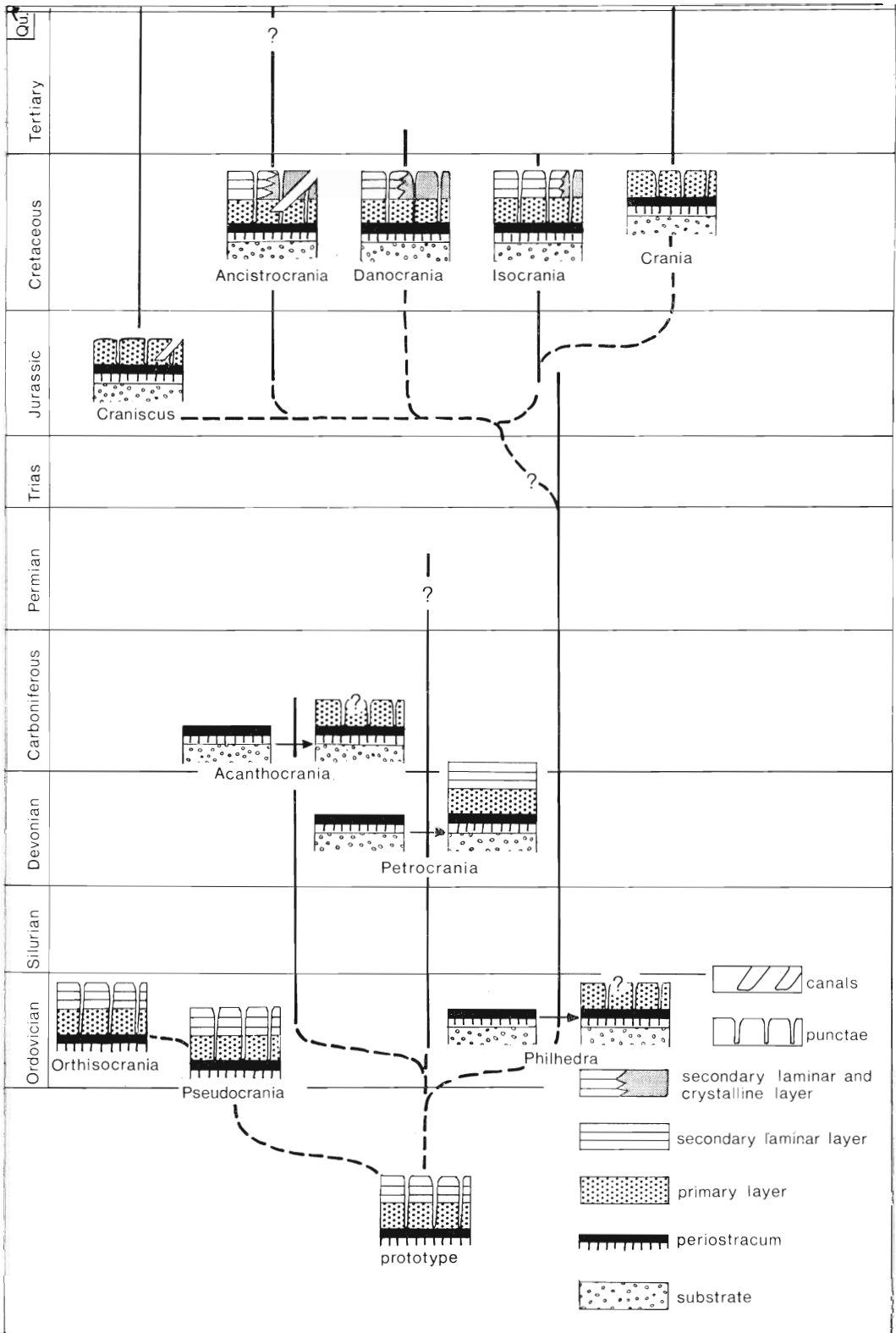
shell on the one hand, and to illustrate a surprisingly wide range of pedomorphic and gerontomorphic changes on the other (text-fig. 17).

From the known beginning of the group, as represented by the five genera recovered from the Ordovician, the brachial valve has always been composed of orthodoxly developed primary and secondary calcareous layers permeated by punctae and extensively modified only in the formation of the myotest. So constant is this pattern that



TEXT-FIG. 16. Diagrammatic reconstruction in section of part of the mantle and secondary shell of *Trematobolus pristinus bicostatus* to show that nodules originated either as diagenetic infillings of hollows which previously accommodated intercellular secretion bodies (a), or as syngenetic structures supporting cellular muscle ties (b).

even the average thickness of laminae of representative Ordovician species of *Petrocrania*, *Acanthocrania*, and *Pseudocrania*, which varies from 280 to 400 nm., compares closely with the 260 nm. average for living *Crania*; and, despite a coarsening of laminae in Cretaceous species, which may be partly attributable to recrystallization, the carbonate phases of the secretory regime of the brachial valve are evidently long-established, stable operations. The organic constituents of the shell do not survive for any length of geological time as identifiable morphological features. Yet, bearing in mind the antiquity of the fibrillar outer bounding membrane (Williams 1968, p. 283), it is likely that the periostracum too has not greatly changed over the last 500 million years. It may, therefore, be assumed that the secretory regime of the brachial valve of the craniacean ancestor did not differ importantly from that of living *Crania*, and that it involved the sequential deposition of a periostracum consisting of a mucopolysaccharide film, an outer bounding membrane, a mucopolysaccharide layer and an inner protein boundary, and a calcareous shell comprising a primary layer of crystallites usually acicular in habit, and a secondary layer of laminae.



TEXT-FIG. 17. Inferred phylogeny of the ventral skeletal successions of the Craniacea.

In contrast to the structural stability of the brachial valve, the fabric of the pedicle valve has been subject to profound changes throughout craniacean history although the greatest range in development is exhibited by the earliest members of the superfamily. Despite these changes, the secretory regime of the prototypic pedicle valve can be confidently deduced. Structural modification of the pedicle valve was undoubtedly initiated by cementation of that valve to the substrate following the loss of pedicle by the craniacean prototype. Had the pedicle valve remained unattached, one would expect its fabric to have been identical with that of the complementary brachial valve. The expectation is confirmed by the structural similarity of both valves of *Pseudocrania* which lacked both a pedicle and the means of cementing the pedicle valve to the substrate. *Pseudocrania planissima* (Eichwald) from the Lasnamagi (C_{1b}) beds of Estonia, the oldest known species of *Pseudocrania*, is only marginally younger than the earliest recorded *Petrocrania*, *P. prona* (Raymond) from the Marmor formation of the U.S.A. Consequently *Pseudocrania*, and the closely related *Orthisocrania*, may be regarded as the least modified descendants of the craniacean prototype, the pedicle valve of which probably consisted of periostracum and primary and secondary shell arranged in the same way as is found in the brachial valve of living *Crania*.

The onset of a biochemical change which rendered the ventral mucopolysaccharide film sufficiently adhesive to induce cementation of the pedicle valve, initially had a dramatic effect on the secretory regime of that valve (text-fig. 17). Three attached genera are recorded from the Ordovician but as far as is known no ventral calcareous exoskeleton has yet been identified with certainty in any species belonging to *Philhedra* and *Acanthocrania*. Indeed according to Rowell (in Williams *et al.* 1965, pp. H290-1), the pedicle valve of *Acanthocrania* is unknown and that of *Philhedra* is 'thin, commonly not calcified', although both stocks persisted into the Carboniferous. Our own researches indicate that there might have been a negligible development of the anterior rim through the secretion of primary shell in adult *Acanthocrania*, and we have assumed (text-fig. 17) that the sporadically calcified pedicle valves of *Philhedra*, which have been reported from time to time, were also composed solely of primary shell. Hence all immature as well as the great majority of adult pedicle valves of species of *Acanthocrania* and *Philhedra* were exclusively organic. In terms of the standard secretory regime this condition implies that deposition never proceeded beyond the exudation of the inner protein boundary. Thus the organic exoskeleton may have consisted of a normally developed periostracum and a grossly thickened inner boundary representing a steady increment of protein which had not been segregated into sheets by concomitant secretion of calcite crystallites and laminae. A predominantly organic layer approaching this condition survives within the central area of the pedicle valve of living *Crania*.

Petrocrania was the third attached craniacean to appear in the Ordovician, but unlike the other two cemented stocks, both primary and secondary layers were fully differentiated in adult pedicle valves. It is, therefore, probable that the secretory regime of the ventral mantle of *Petrocrania* was as complete as that responsible for the development of the complementary brachial valve or that inferred for the ancestral pedicle valve. Yet it is unlikely that the ventral skeletal succession of the craniacean prototype was inherited unmodified by the *Petrocrania* stock because immature shells (those of *P. scabiosa*, for example, which are less than 7 mm. in diameter) show no sign of a calcified pedicle valve. This condition suggests that young pedicle valves of

Petrocrania were exclusively organic like those of *Acanthocrania* and *Philhedra*, and that the full potential of the standard secretory regime was inherited by the ventral mantles of all three stocks from the ancestor although its translation into skeletal deposition was either partly suppressed or, at least, significantly delayed. Whether the delay was diminished during the evolution of *Petrocrania* remains to be seen, although the smaller size of specimens of *P. quadrata* equipped with a calcified pedicle valve suggests that it was.

Despite the full development of the *Petrocrania* pedicle valve, it remains unique in craniacean history in its lack of punctation. There is no ready explanation for this condition. Compared with the frequency in the brachial valve, the density of punctation in the pedicle valve of living *Crania* is significantly reduced, but without indication of any morphological difference except that terminal branches of the ventral caeca appear to be more extended parallel to the external surface, than the dorsal ones. Since craniacean caeca appear to be relatively unspecialized extensions of a microvillous outer epithelium, it may well be that their development was reduced or even inhibited when shell secretion, which traps and encases the evaginations making up the caeca, became slow or negligible.

Although caution is prompted by the notoriously unreliable records of extinction and diversification for the Permo-Triassic periods, the occurrence of five new craniacean stocks in Jurassic-Cretaceous successions must be taken as reflecting a second radiation. All five genera *Ancistrocrania*, *Crania*, *Craniscus*, *Danocrania*, and *Isocrania*, are sufficiently alike in morphology as well as shell fabric to suggest that they were monophyletically derived. According to known geological occurrences the choice of immediate ancestor of these stocks is restricted to either *Philhedra* which persists into the Jurassic, or *Petrocrania* which is reported from the Permian. Assuming that the potentiality of secreting a fully developed pedicle valve was present in both genera (although realized only in *Petrocrania* so far as is known) *Philhedra* is the more likely ancestor because pedicle valves of all Mesozoic craniaceans are punctate.

Isocrania, which, like *Ancistrocrania* and *Craniscus*, is known from the Jurassic, appears to have the most generalized ventral succession and is probably nearest to the ancestral stock. Most of the valve is attached to the substrate; and in this part a primary layer with highly inclined acicular crystallites and a secondary laminar shell are fully developed and are, presumably, the mineral remnants of the standard secretory regime. However, in the margins of the adult pedicle valve, which grew away from the substrate especially antero-medially, the secondary laminar shell was replaced by long, thick crystallites indicative of accelerated secretion. The feature is of some evolutionary significance in that it is the first known occasion in the history of attached craniaceans when the pedicle valve became as large as, or even larger than, the brachial valve. This morphological trend was continued in *Danocrania* and *Ancistrocrania*. In the former, the posterior margin also extended antero-dorsally to define a pseudointerarea. In the latter, the growth of the entire margin away from the substrate was commonly so marked as to transform the pedicle valve into a truncated one. The trend was not always maintained in *Ancistrocrania* because the pedicle valves of some species remained adnate. Yet adults of all three genera are characterized by excessively developed ventral margins in which the principal constituents of the secondary shell are long, thick crystallites, a texture that is not obscured by the system of large canals permeating the valves of all species of *Ancistrocrania*. In terms of the skeletal succession, then, the

introduction of this zone of coarse crystallites in the adult pedicle valve represents a gerontomorphic modification of the shell fabric, although it could only have been brought about by a paedomorphic substitution of crystallite for laminar deposition in the standard secretory regime.

The derivation of *Crania* poses a problem because, although it is obviously related to *Isocrania*, no laminar shell is deposited in the pedicle valve of living representatives. It is possible that the ventral calcareous succession of *Crania* is a correlative of both the primary layer and the non-laminar secondary layer of *Isocrania*. But the fabric of the latter layer is unlike any found in the ventral mineral succession of *Crania*, which is best regarded as being entirely primary shell. Now *Crania s.s.* is not reliably recorded in rocks older than the Cretaceous (Senonian according to Rosenkrantz 1964, p. 518). Hence, although *Crania* could conceivably be ancestral to *Isocrania* which became different by secretion of a ventral laminar secondary shell, it is more likely to have been derived out of *Isocrania* by a neotenus suppression of secondary shell secretion. In this way, the shell structure of immature living *Crania* has come to resemble that of the earliest attached craniaceans.

The relationship of *Craniscus* to other Mesozoic craniaceans is not entirely clear in that, like *Crania*, it lacks a laminar layer in the pedicle valve. Other features, however, including the presence of canals in the pedicle valve, suggest that *Craniscus* is much more closely related to *Ancistrocrania* and that non-deposition of the secondary shell came about independently of that condition in *Crania*.

Not much more can be said than is already known about the relationship between the craniaceans and other inarticulates with calcitic shells. On the whole, the Craniopsidae do not seem to have been derived from the same ancestral stock as the Craniacea. Rowell (in Williams *et al.* 1965, p. H273) has listed important differences between the two groups including the impunctate nature of the craniopsid shell. This condition may, of course, have been inherited from a common ancestor from which the craniaceans diverged through the development of caecal outgrowths of the mantle. Moreover, the very strong likeness between the recrystallized primary layer and the laminar secondary layer of the craniopsids, and the calcareous succession of contemporaneous craniaceans, suggests a close structural affinity. Yet the discovery that the shell of obolellides, which are too far removed in time to be related to either stock, was also differentiated into a crystalline primary layer and a laminar secondary layer diminishes the significance of fabric likeness. Instead it suggests that the synthesis of a structurally sound skeleton by secretion of solidly packed crystallites (primary layer) on an organic membrane (periostracum) as a foundation for a laminated organic-mineral secondary layer was a widespread phenomenon at least in the brachiopod phylum.

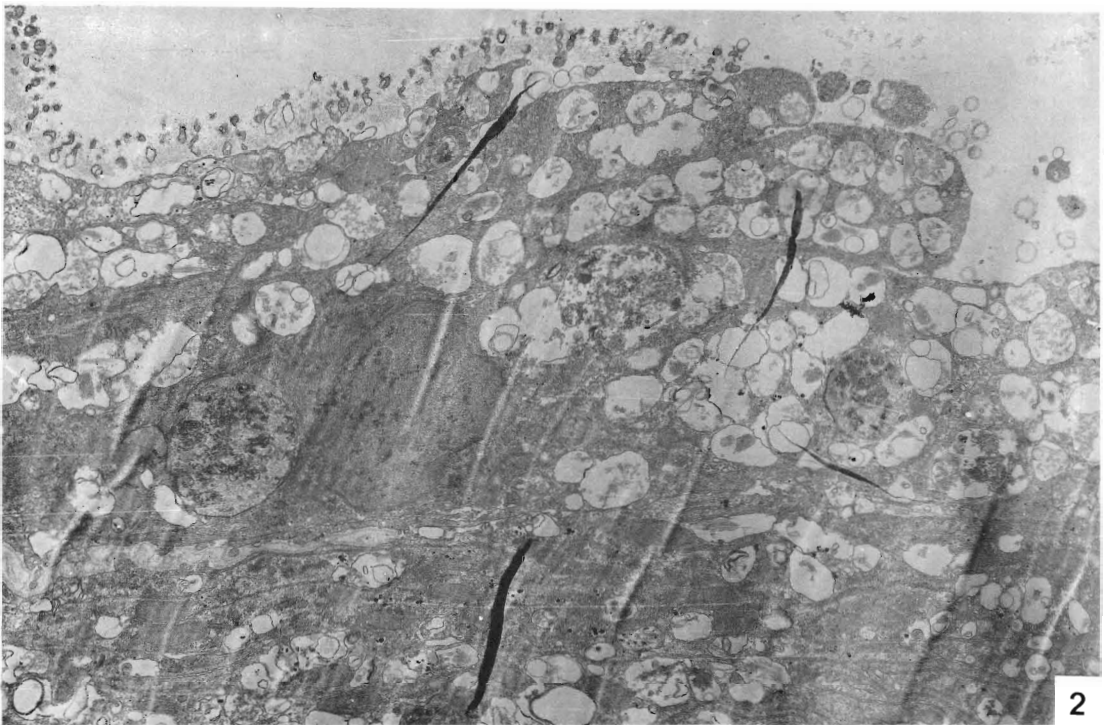
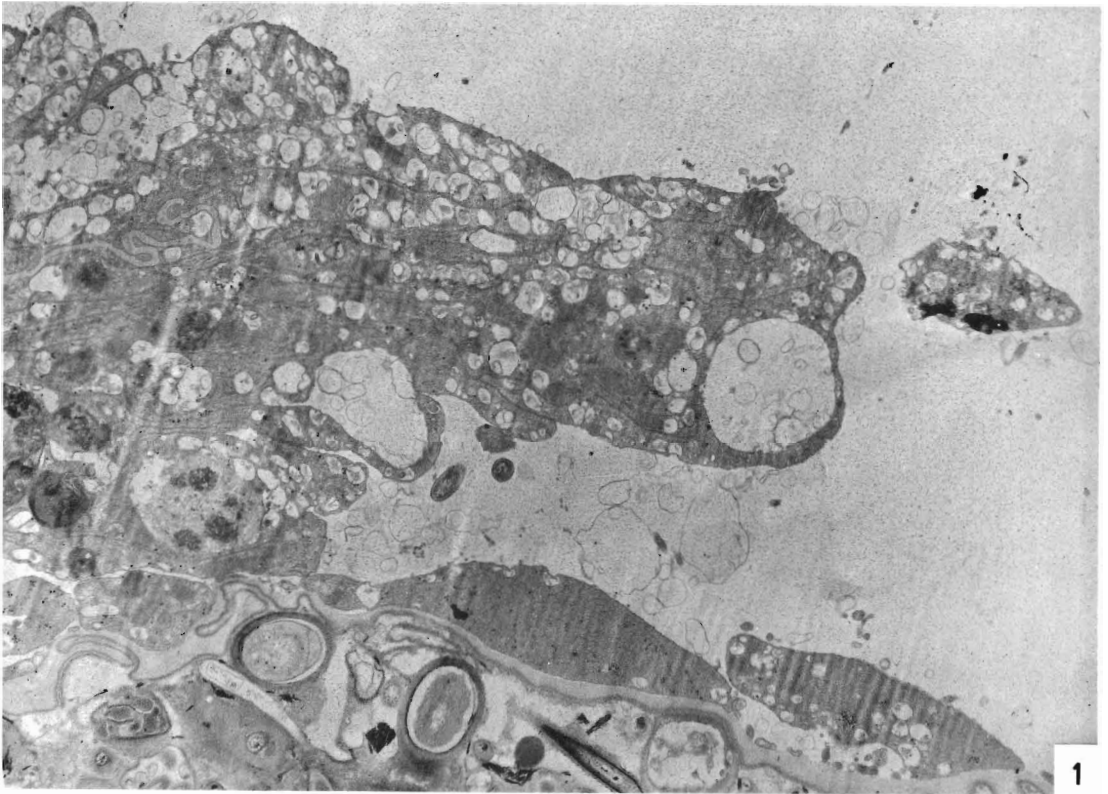
Acknowledgements. We are indebted to many people for providing specimens for sectioning and for invaluable advice on problems arising from this study. However, special mention must be made of Mr. C. Bang of the Biological Station, Blomsterdalen for providing living specimens of *Crania anomala* and Dr. H. Brunton of the British Museum of Natural History for arranging loans of several fossil inarticulates; and of Dr. V. Yu Goryansky of Leningrad, Dr. V. Jaanusson of the Natural History Museum, Stockholm and Dr. A. J. Rowell of the University of Kansas, Lawrence for sending specimens of *Trematobolus*, *Pseudocrania* and *Philhedra*, and *Bicia* and *Obolella* respectively. We also wish to thank Dr. Jean Graham and Dr. Katharine McClure, research assistants in the Department of Geology of the Queen's University, Belfast, for their help in the preparation of illustrations and some of the sections figured herein.

REFERENCES

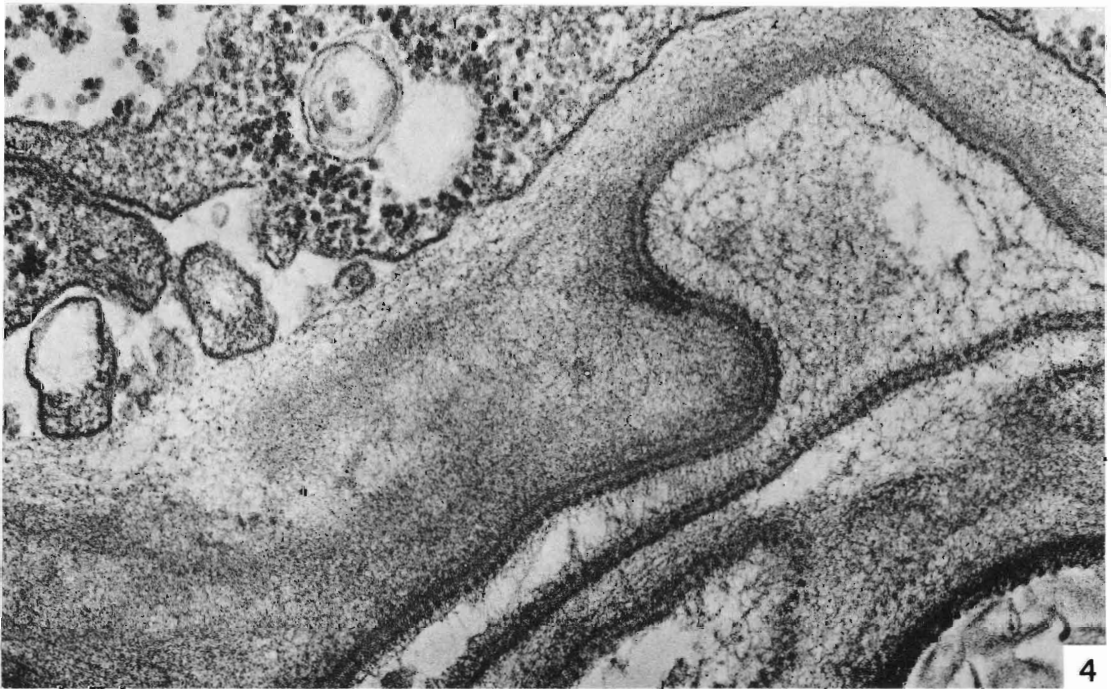
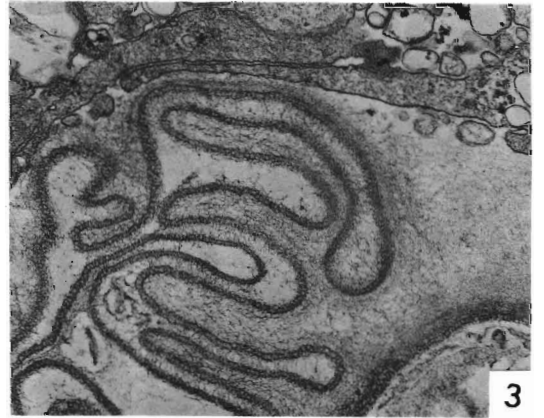
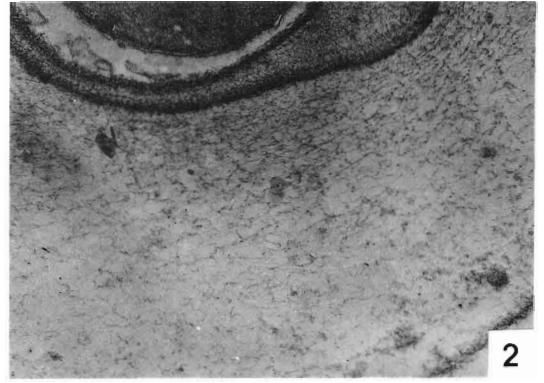
- BLOCHMANN, F. 1892. *Untersuchungen über den Bau der Brachiopoden*. Pt. 1, 1–65. Jena.
- DAVIDSON, T. 1880. *British Fossil Brachiopoda: Supplement to the Permian and Carboniferous species*, 4, pt. 3, 243–316. Palaeontogr. Soc. (Monogr.).
- JAANUSSON, V. 1966. Fossil brachiopods with probable aragonitic shell. *Geol. Fören. Förhandl.* **88**, 279–81.
- KOZŁOWSKI, R. 1929. Les brachiopodes gothlandiens de la Podolie Polonaise. *Palaeont. Polon.* **1**, 1–254.
- KRANS, T. F. 1965. Études morphologiques de quelques spirifères dévoniens de la Chaîne Cantabrique (Espagne). *Leidse Geol. Med.* **33**, 73–148.
- OWEN, G., and WILLIAMS, A. 1969. The caecum of articulate Brachiopoda. *Proc. Roy. Soc.* **172B**, 187–201.
- ROSENKRANTZ, A. 1964. Note on some crania from Central Poland. *Acta Palaeont. Polon.* **9**, 513–38.
- ROWELL, A. J. 1960. Some early stages in the development of the brachiopod *Crania anomala* (Müller). *Ann. Mag. Nat. Hist.* ser. 13, **3**, 35–52.
- WILLIAMS, A. 1968. Evolution of the shell structure of articulate brachiopods. *Palaeont. Assn. Spec. Pap.* **2**, 1–55.
- 1968a. A history of skeletal secretion among articulate brachiopods. *Lethaia*, **1**, 268–87.
- 1970. Comments on the growth of the shell of articulate brachiopods. *Smithson. Misc. Coll.*
- *et al.* 1965. *Treatise on Invertebrate Paleontology* (ed. MOORE, R. C.). Part H, Brachiopoda, **1**, H1–H521. Lawrence.
- WILLIAMS, J. S. 1943. Stratigraphy and Fauna of the Louisiana Limestone of Missouri. *U.S. Geol. Surv. Prof. Pap.* **203**, 1–133.
- WRIGHT, A. D. 1966. The shell punctation of *Dicoelosia biloba* (Linnaeus). *Geol. Fören. Förhandl.* **87**, 549–57.
- 1970. The stratigraphic distribution of the Ordovician inarticulate brachiopod *Orthisocrania divaricata* (M'Coy) in the British Isles. *Geol. Mag.* (in press).

ALWYN WILLIAMS and ANTHONY D. WRIGHT
 Department of Geology,
 The Queen's University,
 Belfast,
 Northern Ireland

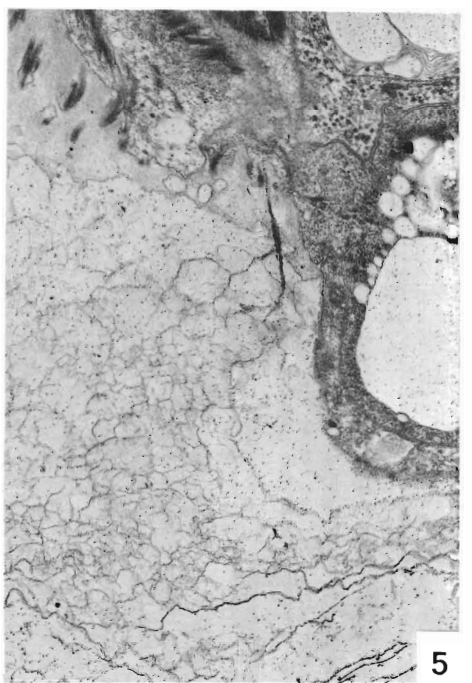
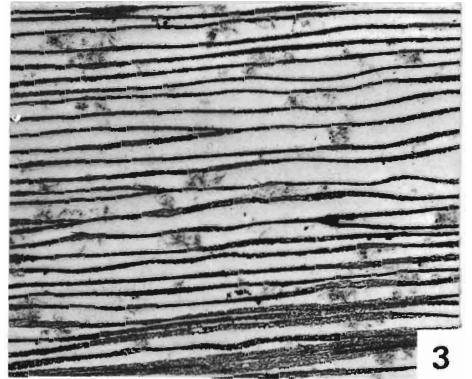
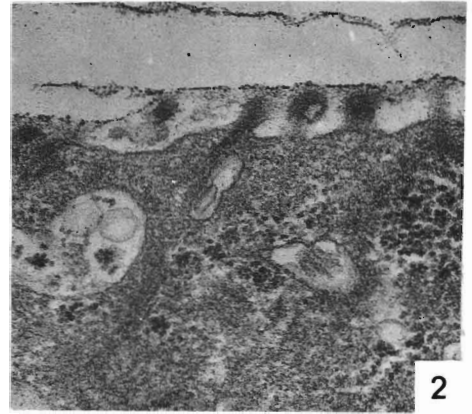
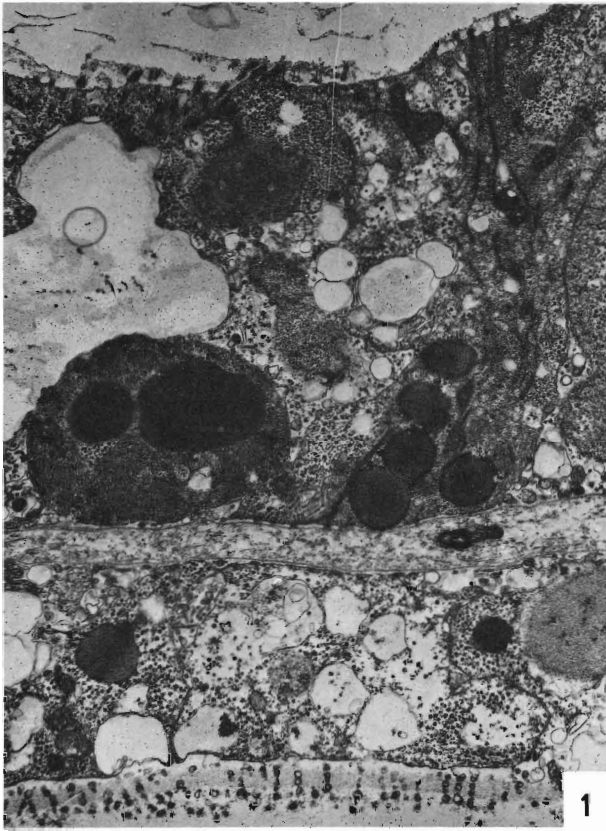
Typescript received 7 July 1969



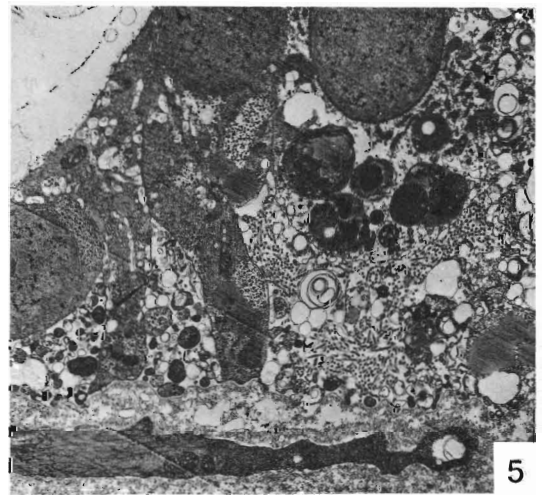
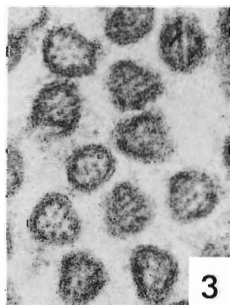
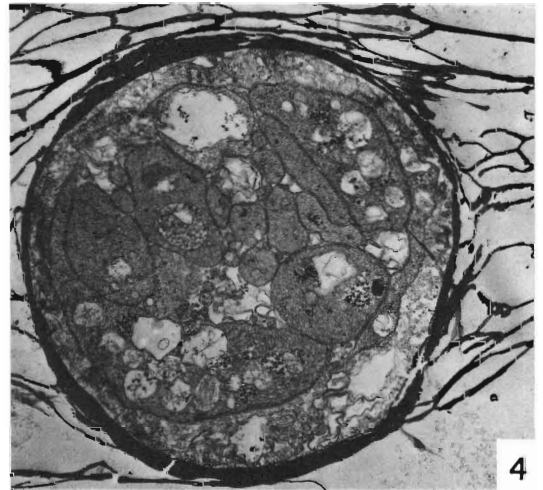
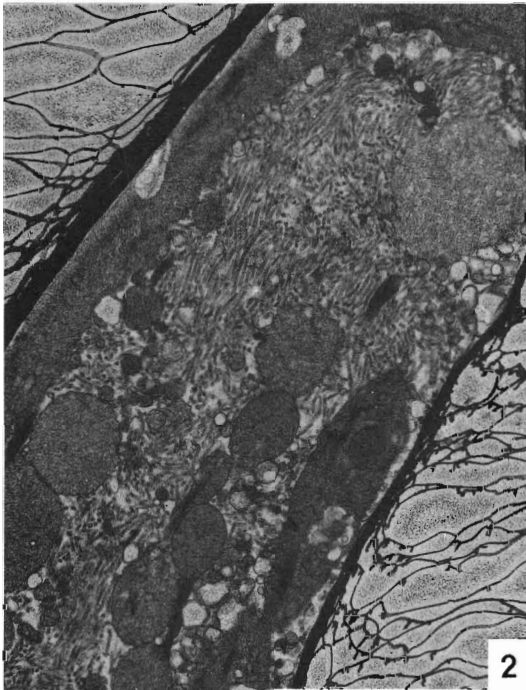
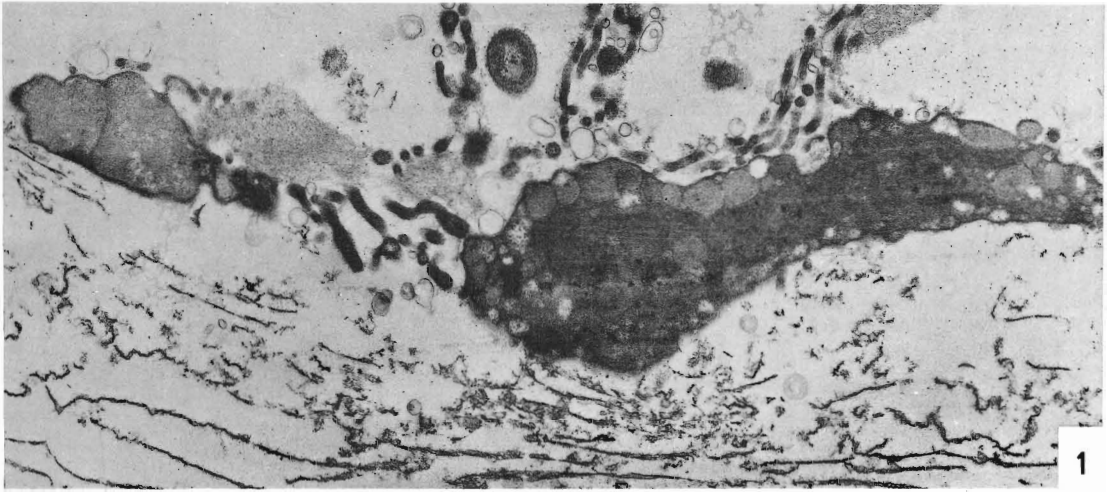
WILLIAMS and WRIGHT, Shell structure of calcareous inarticulate Brachiopoda



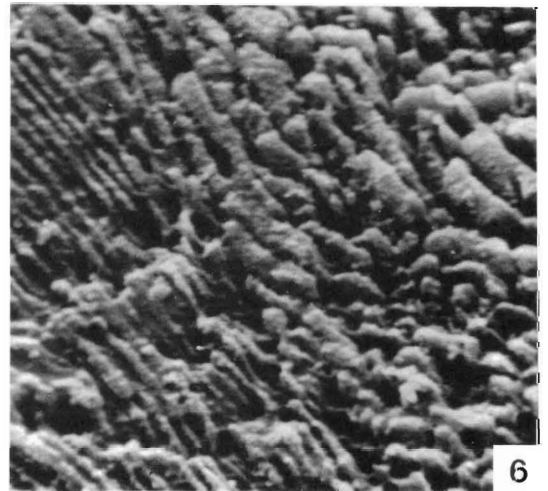
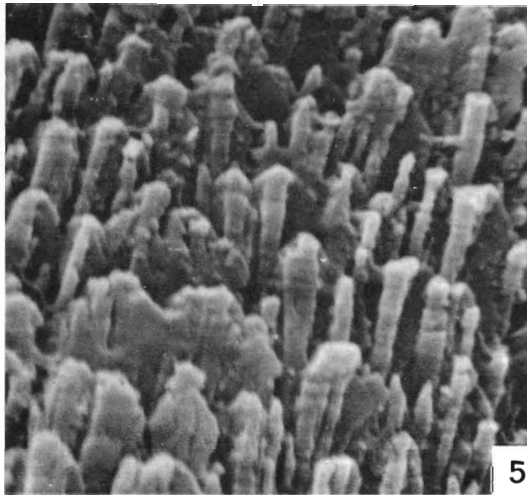
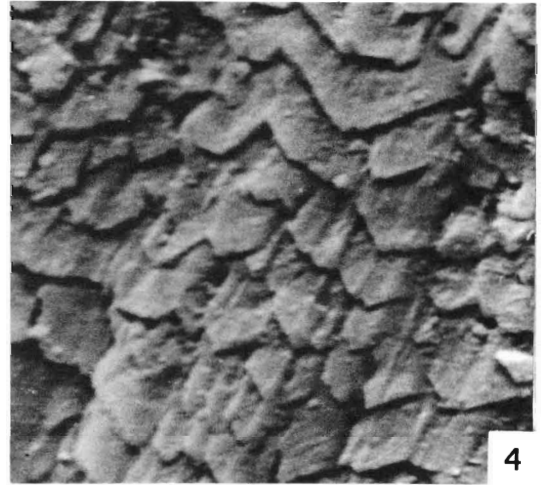
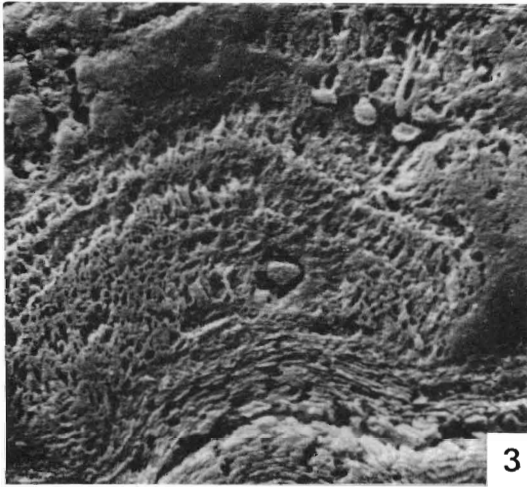
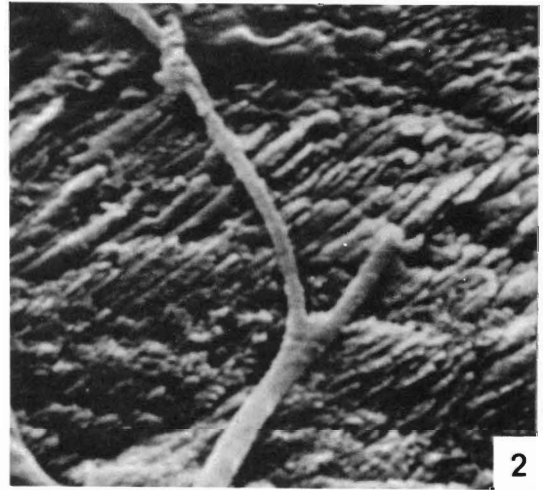
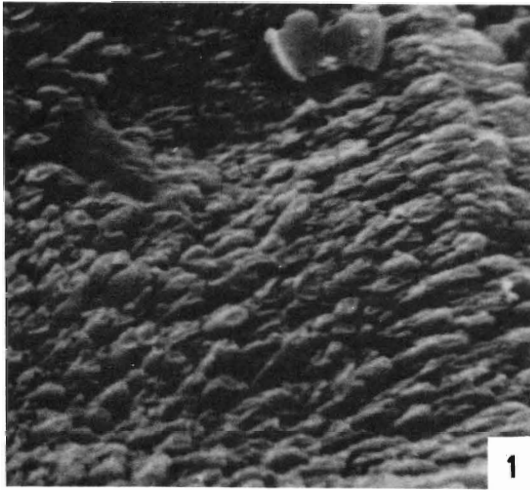
WILLIAMS and WRIGHT, Shell structure of calcareous inarticulate Brachiopoda



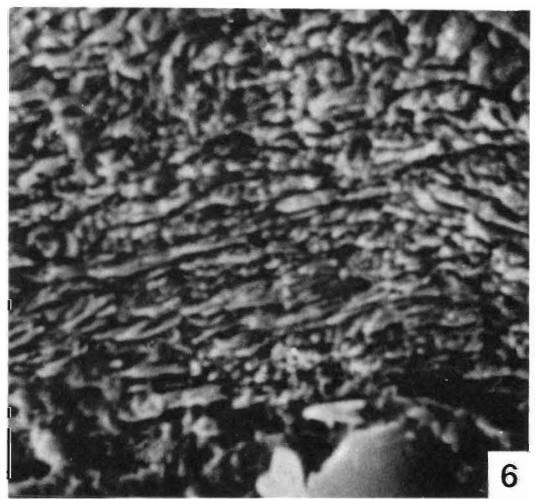
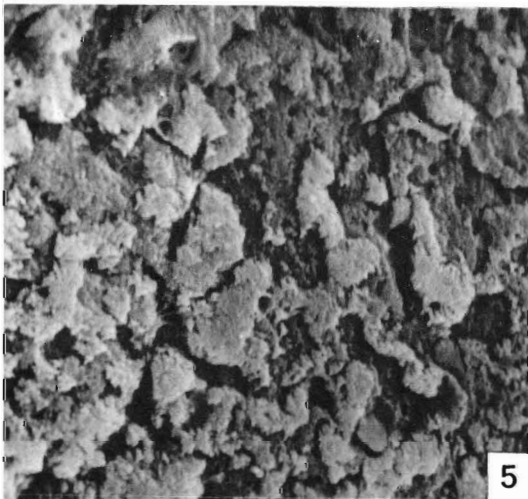
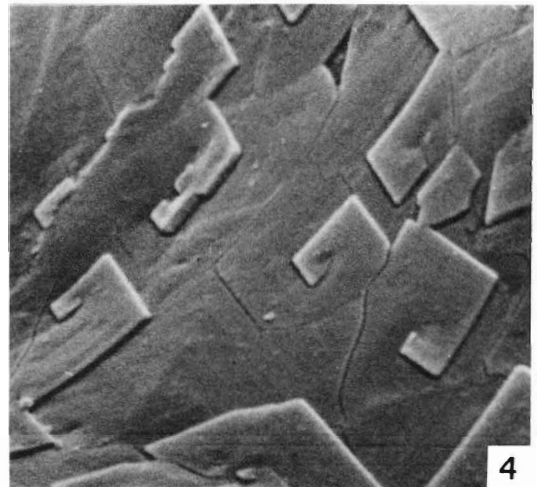
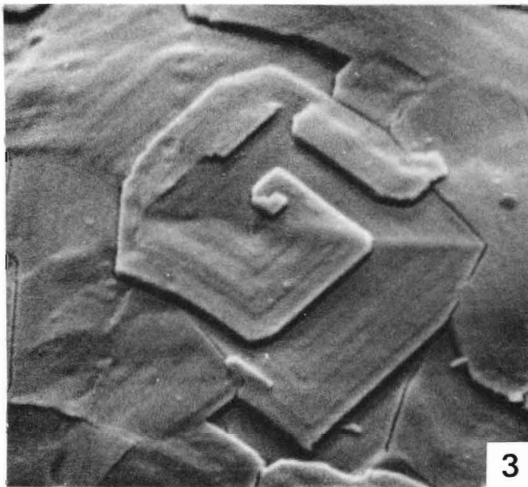
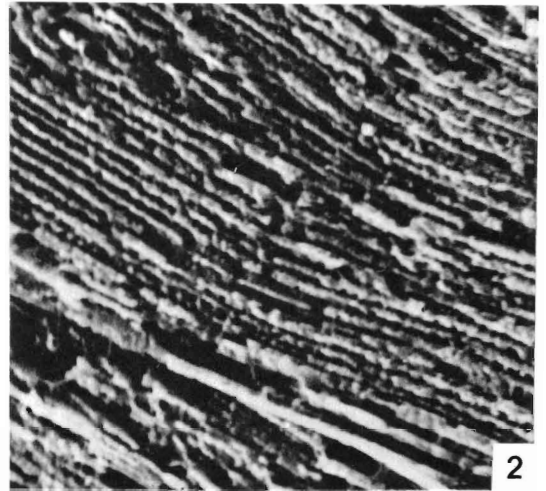
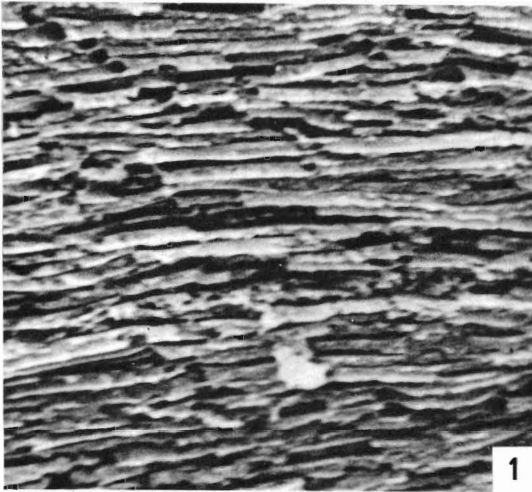
WILLIAMS and WRIGHT, Shell structure of calcareous inarticulate Brachiopoda



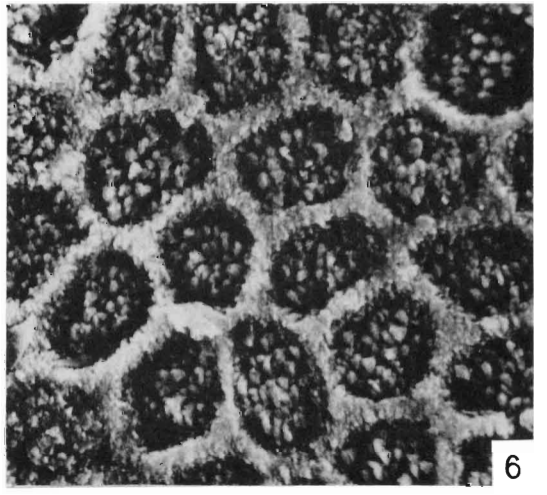
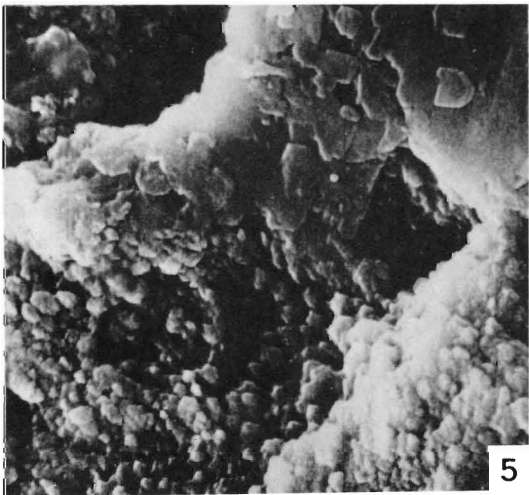
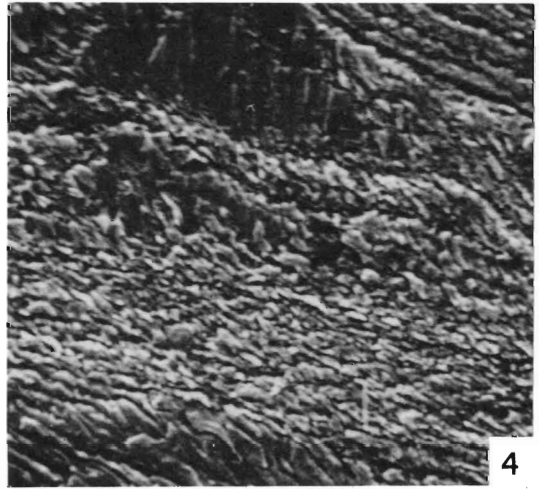
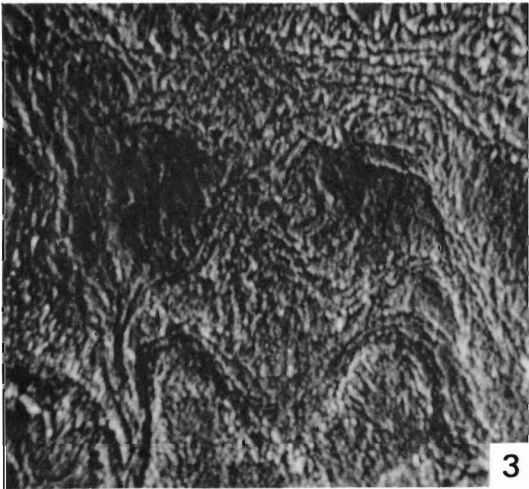
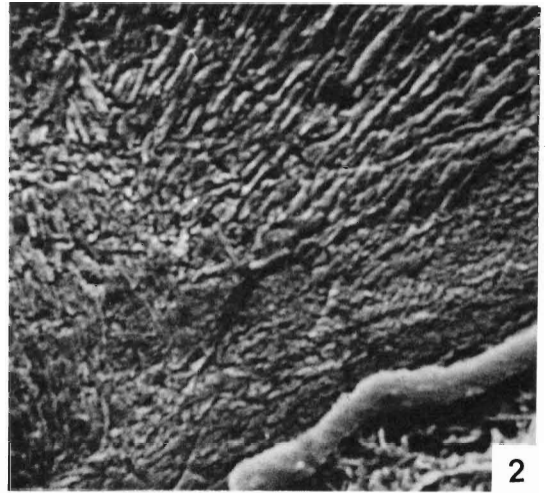
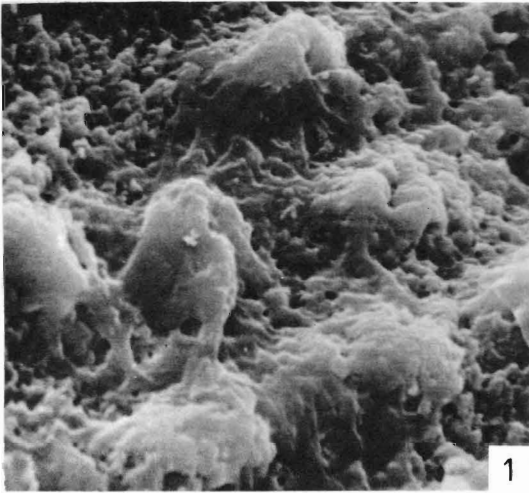
WILLIAMS and WRIGHT, Shell structure of calcareous inarticulate Brachiopoda



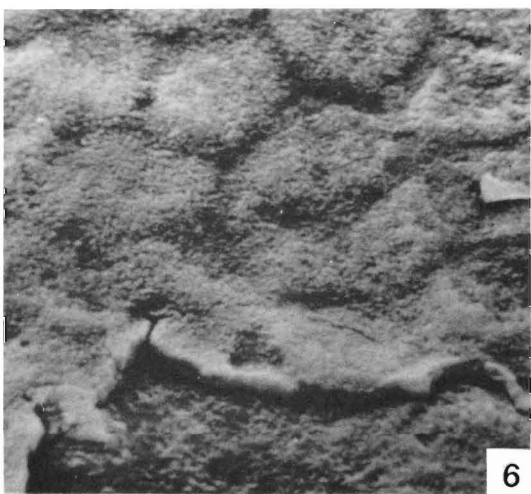
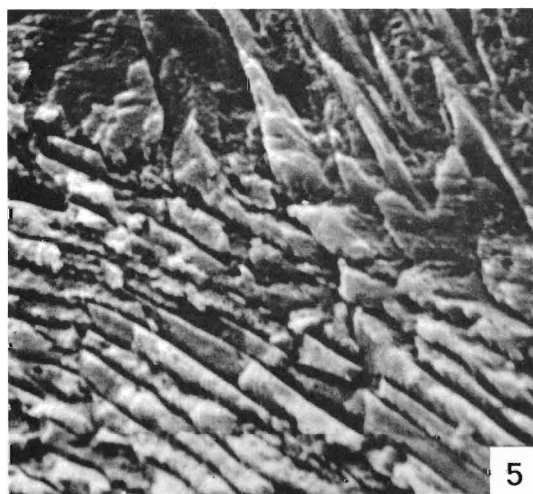
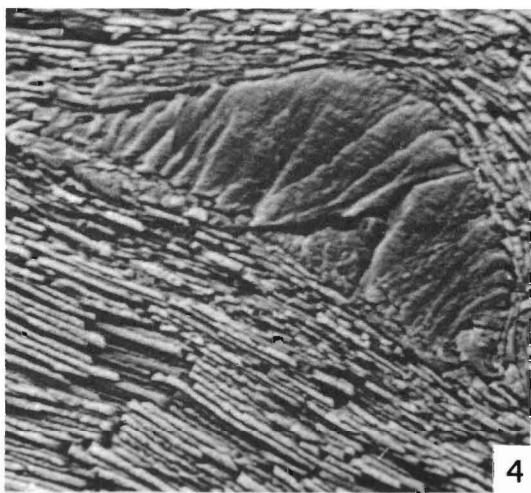
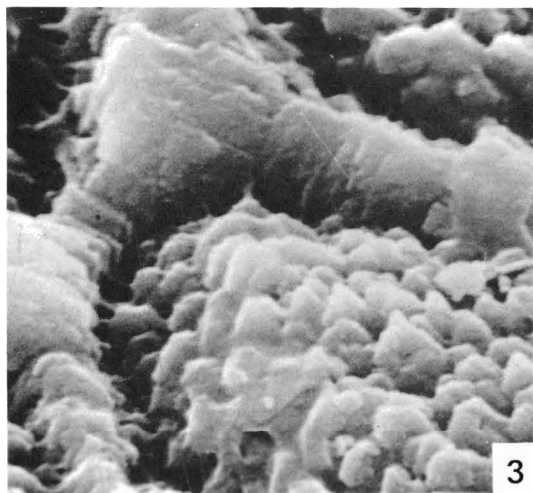
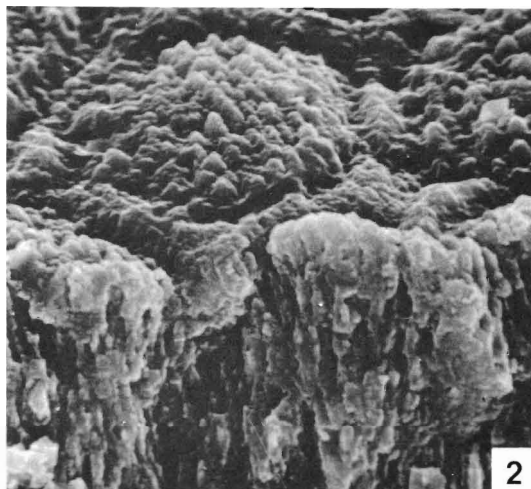
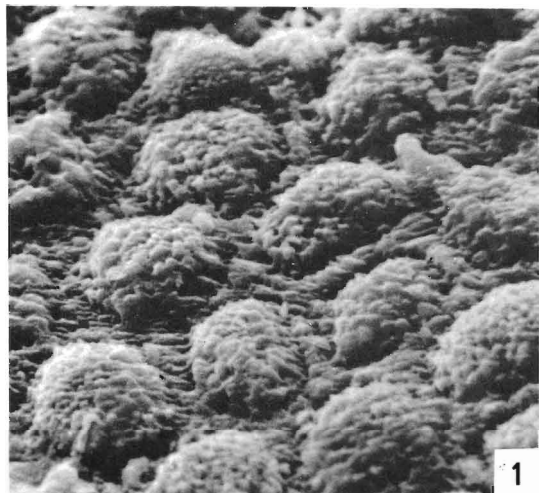
WILLIAMS and WRIGHT, Shell structure of calcareous inarticulate Brachiopoda.



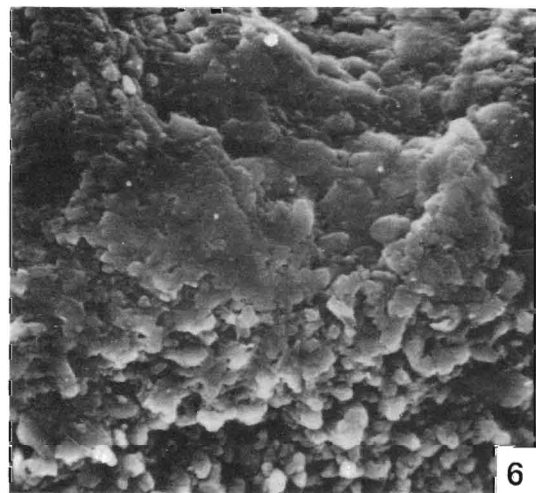
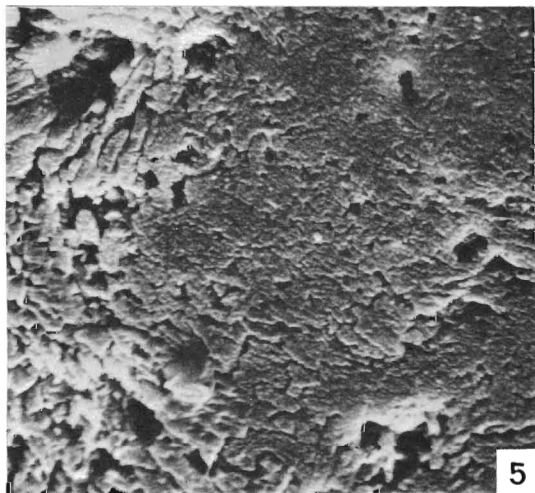
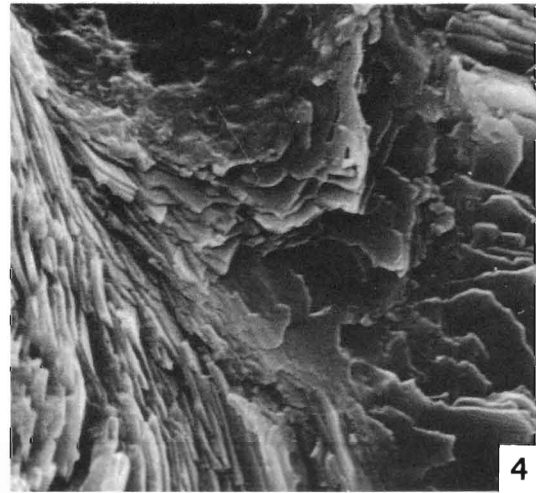
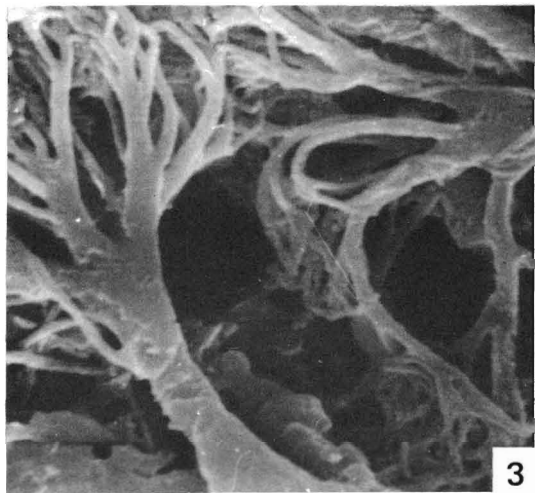
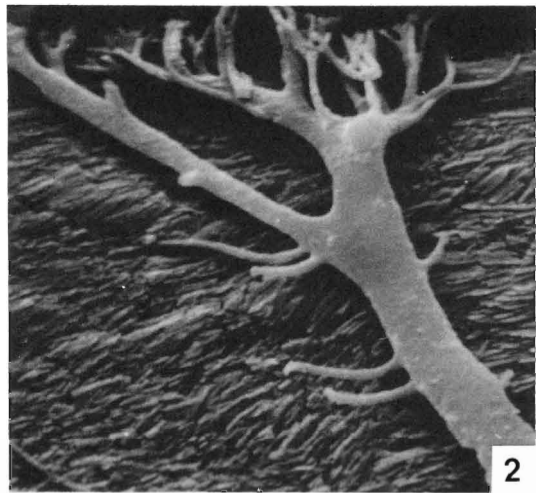
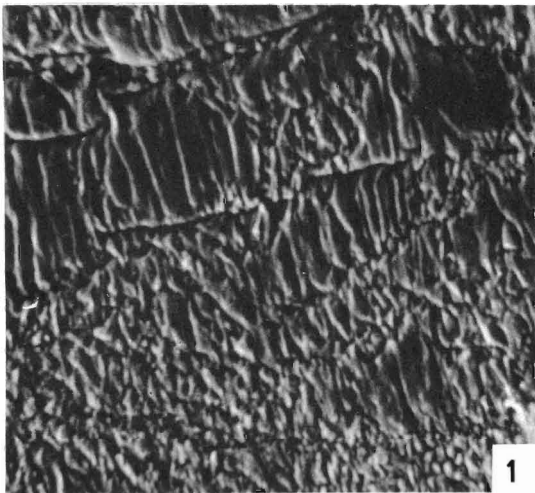
WILLIAMS and WRIGHT, Shell structure of calcareous inarticulate Brachiopoda



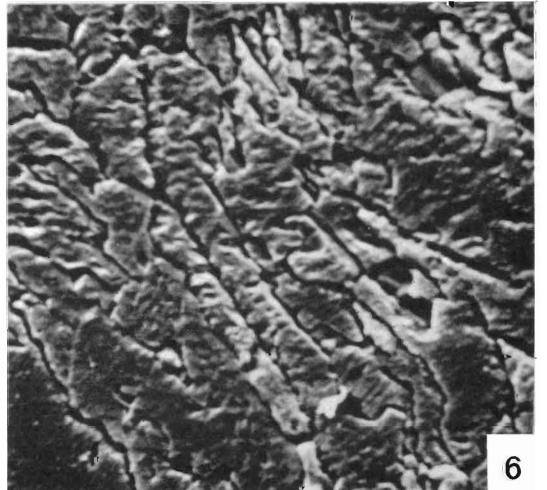
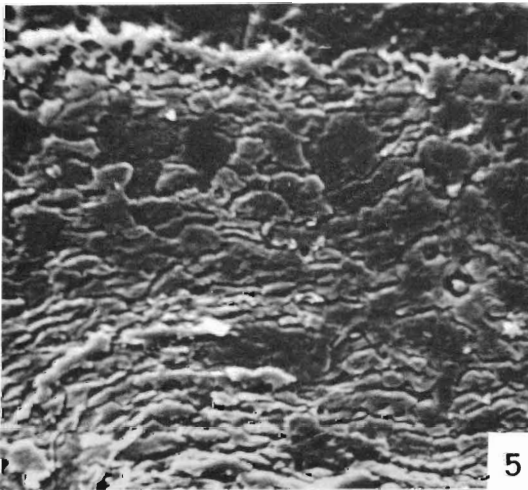
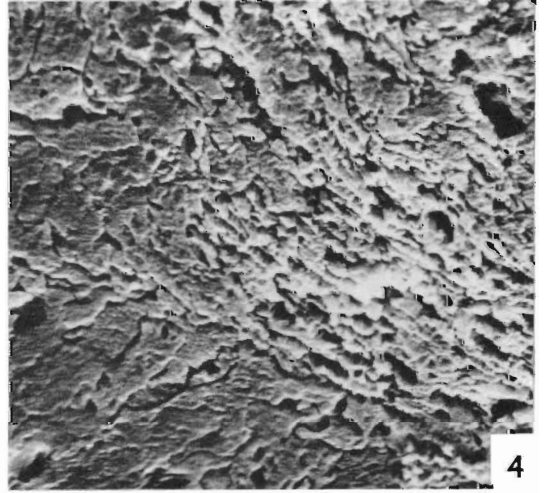
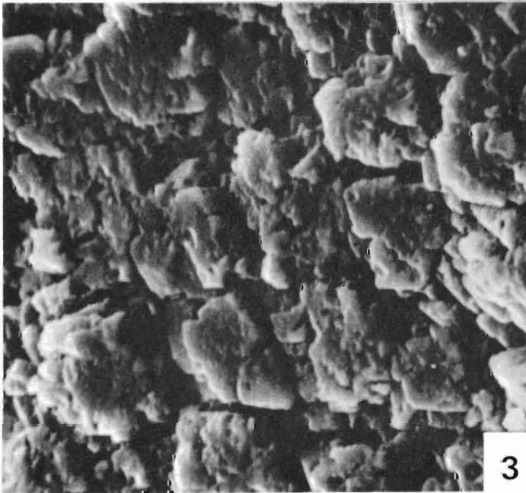
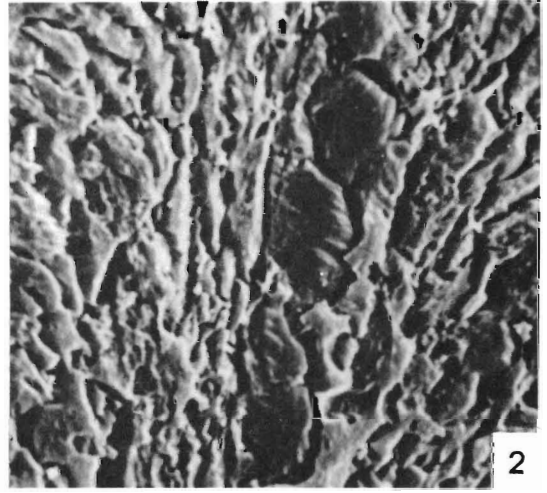
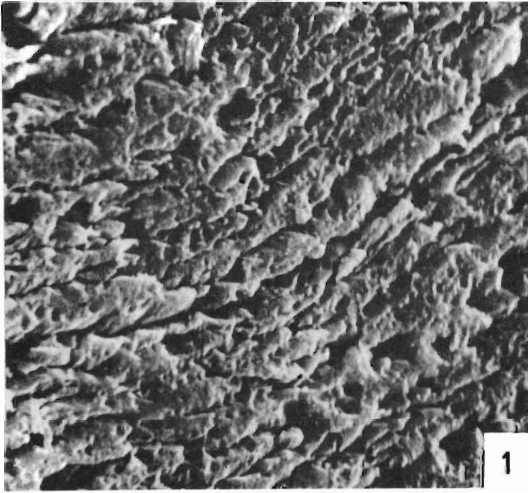
WILLIAMS and WRIGHT, Shell structure of calcareous inarticulate Brachiopoda



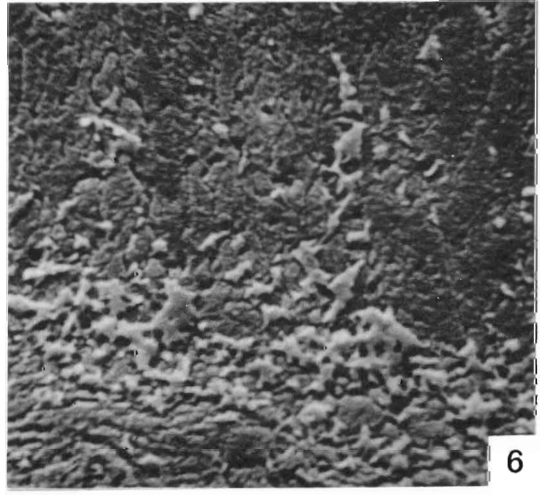
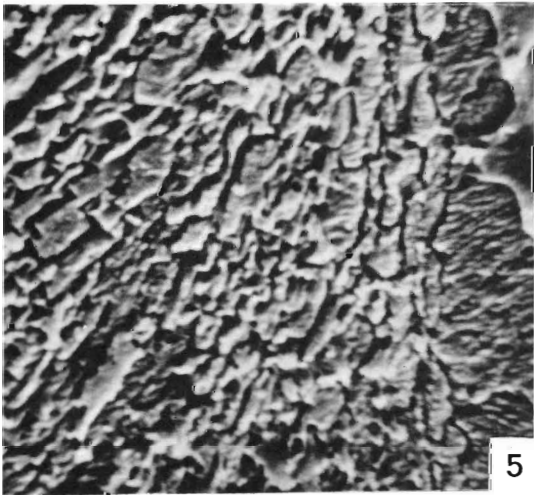
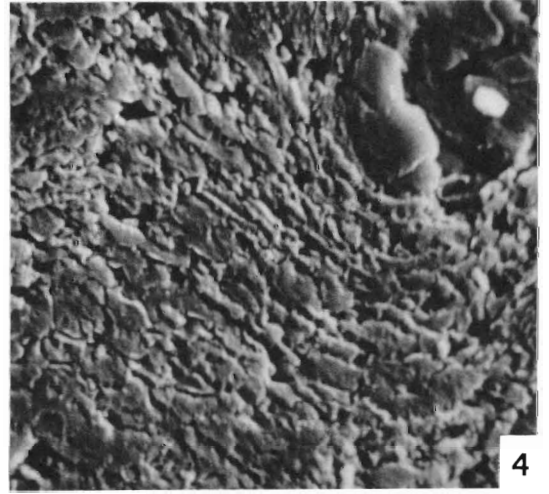
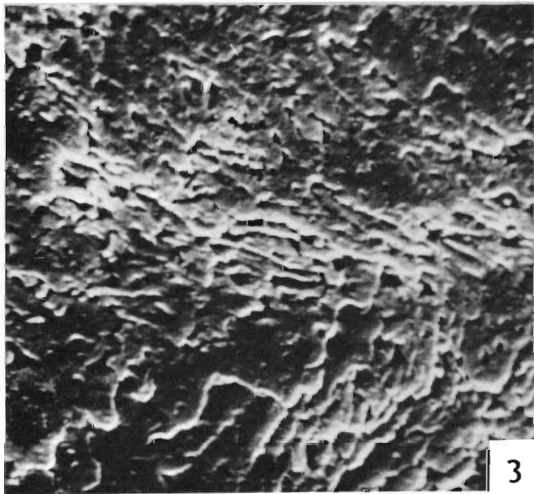
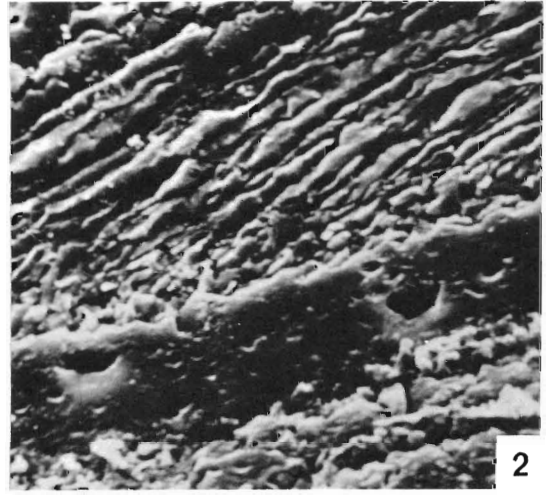
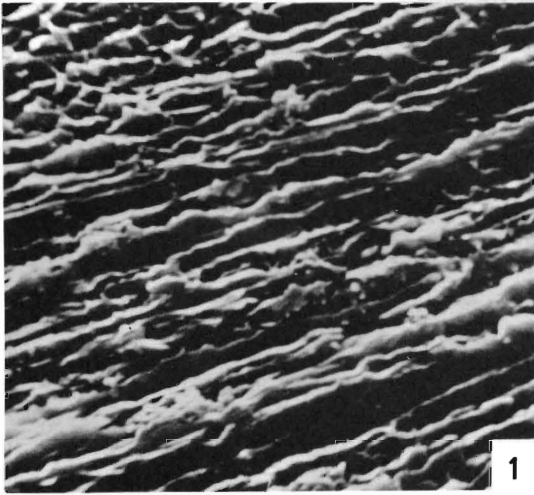
WILLIAMS and WRIGHT, Shell structure of calcareous inarticulate Brachiopoda



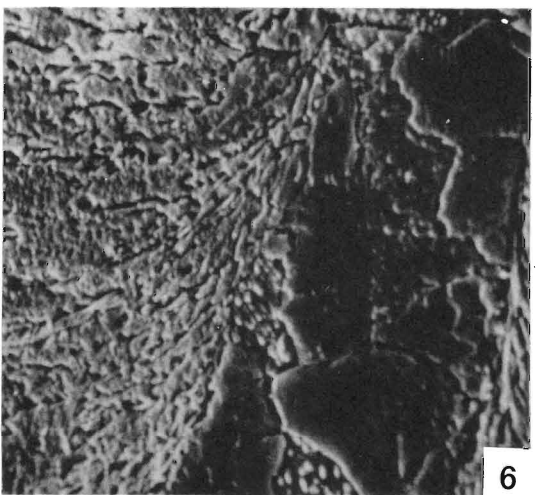
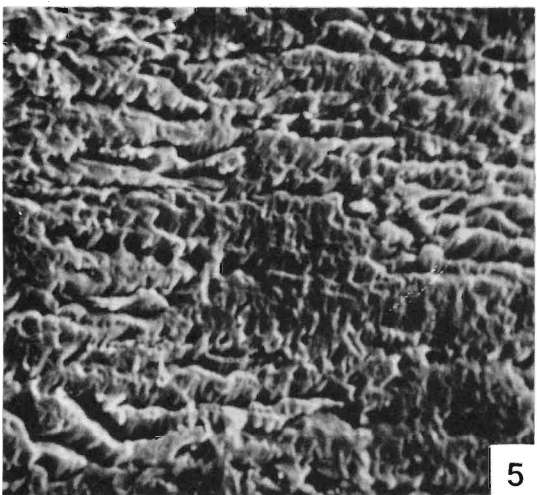
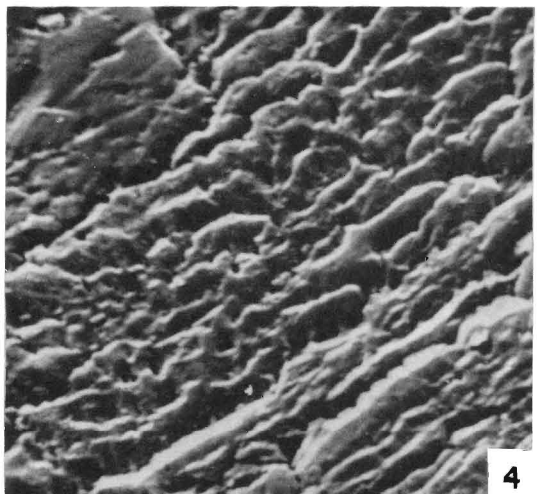
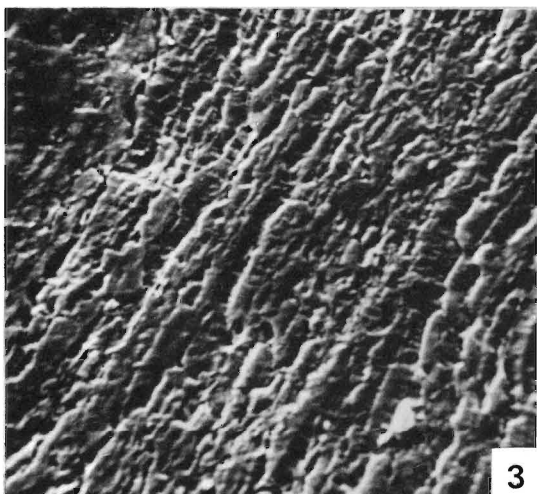
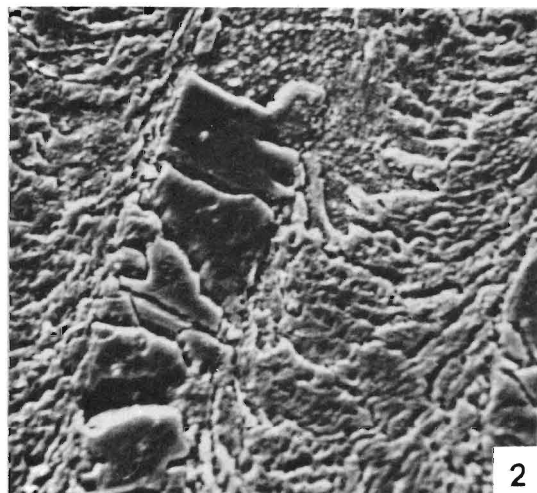
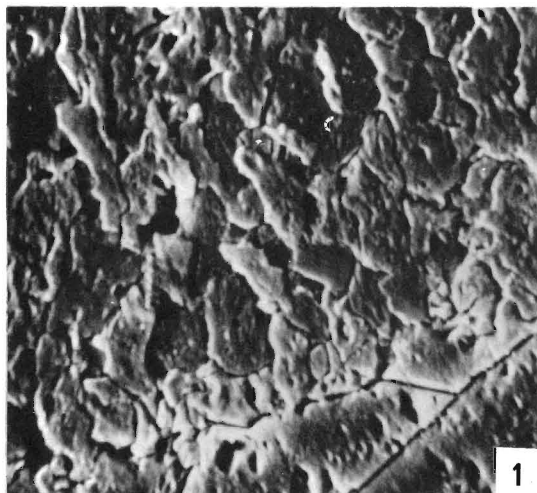
WILLIAMS and WRIGHT, Shell structure of calcareous inarticulate Brachiopoda



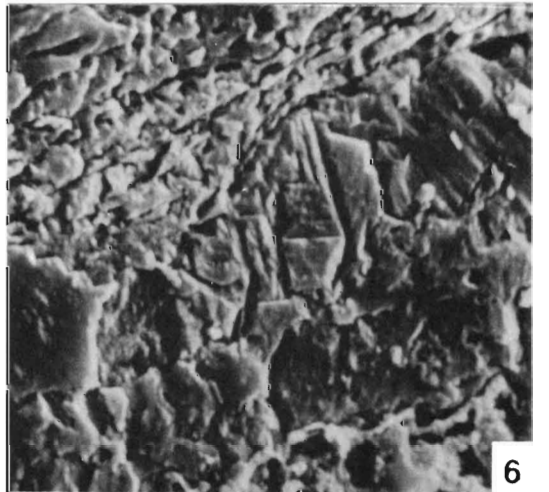
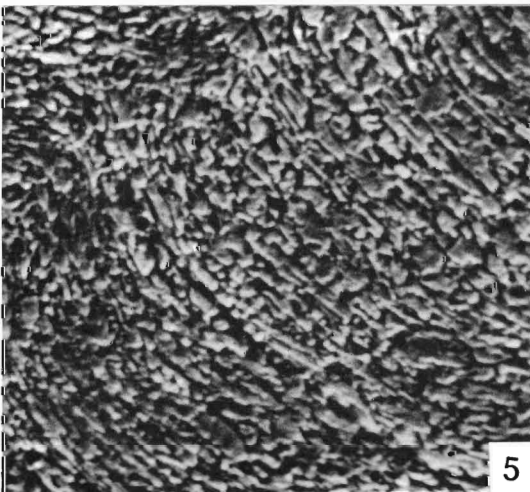
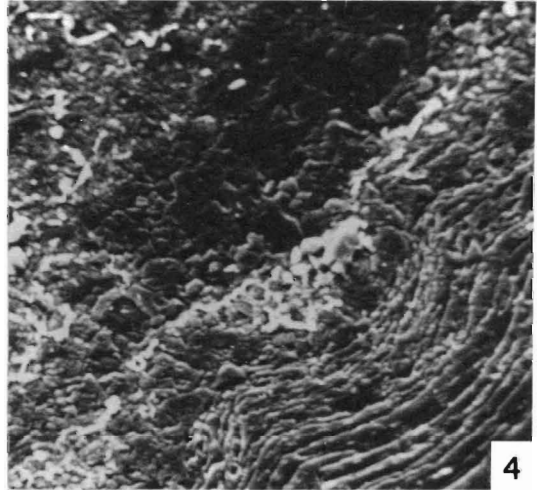
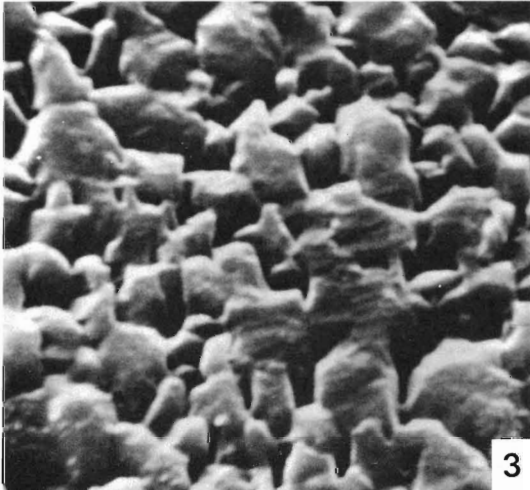
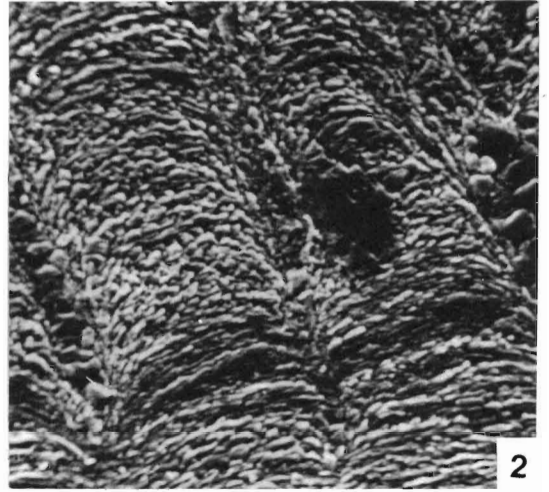
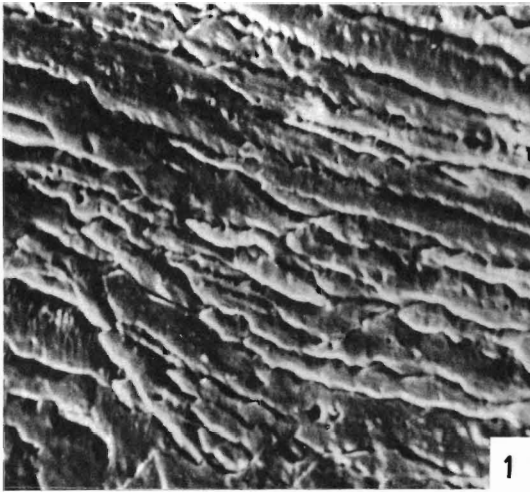
WILLIAMS and WRIGHT, Shell structure of calcareous inarticulate Brachiopoda



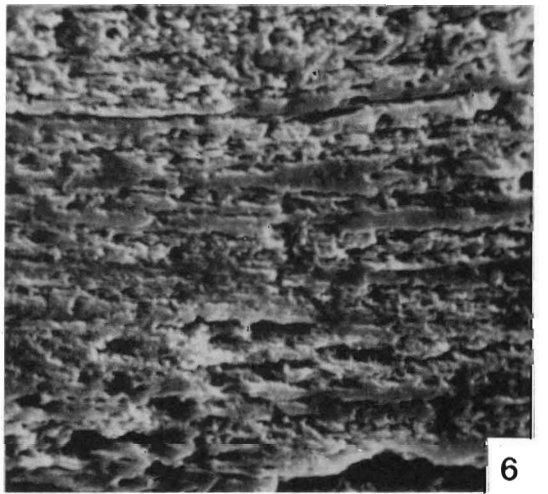
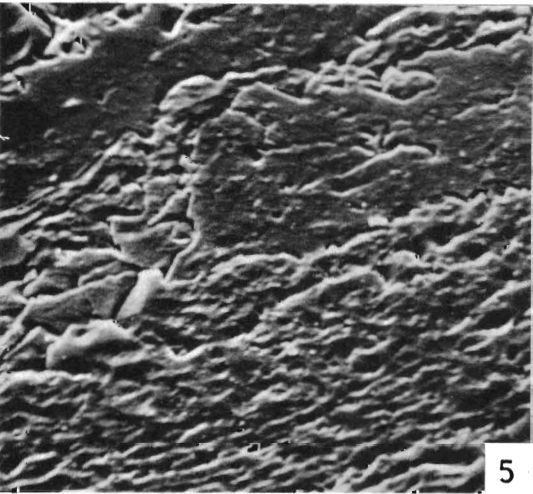
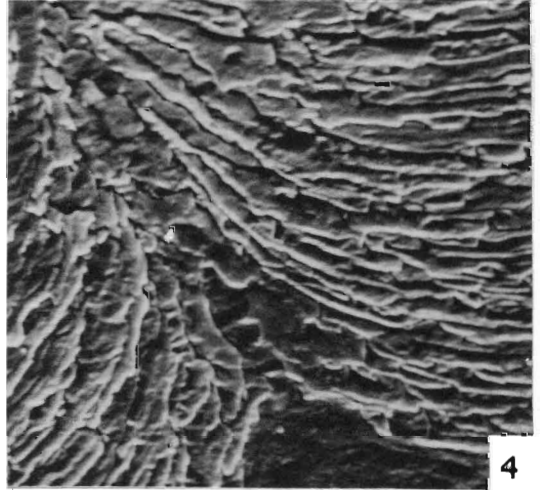
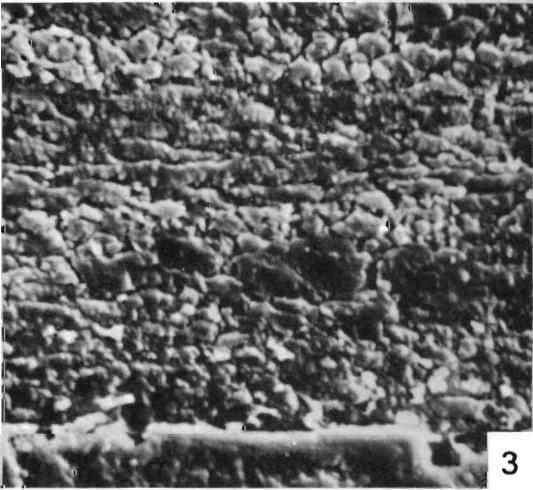
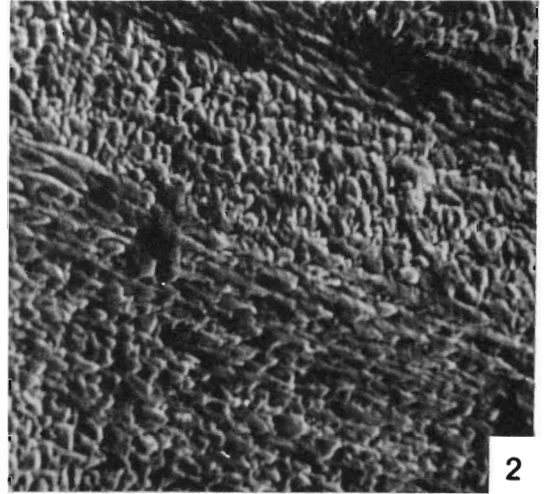
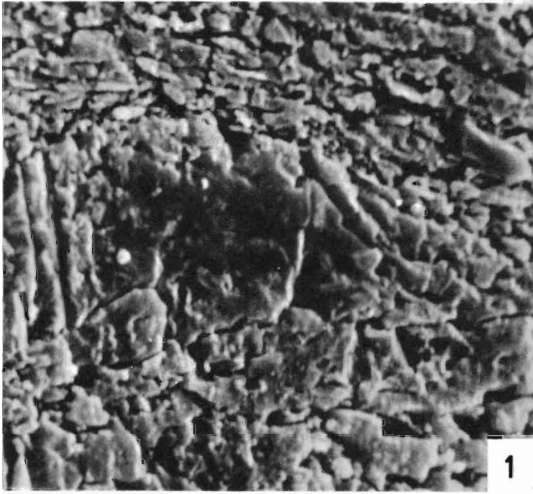
WILLIAMS and WRIGHT, Shell structure of calcareous inarticulate Brachiopoda



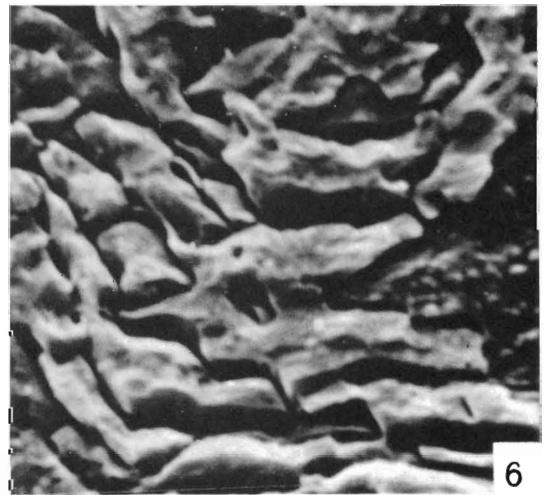
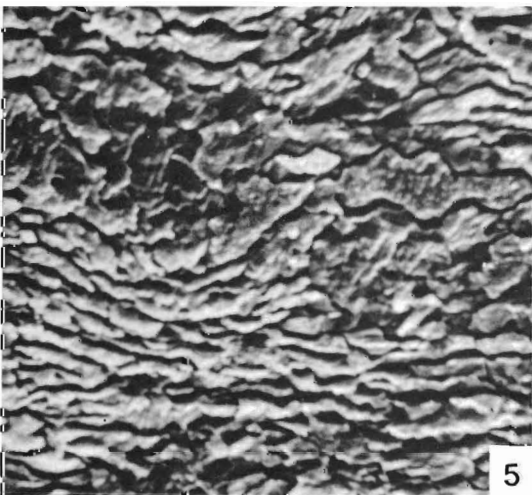
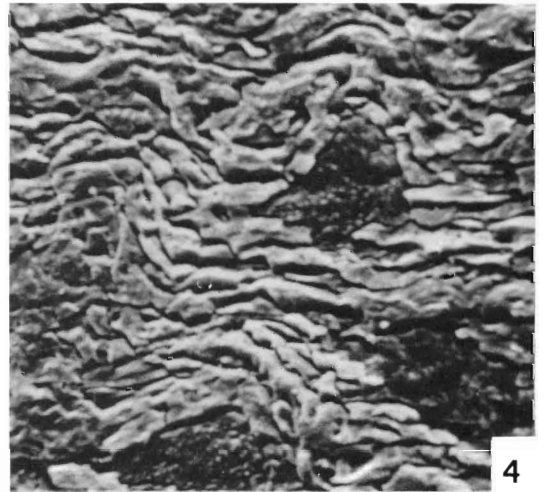
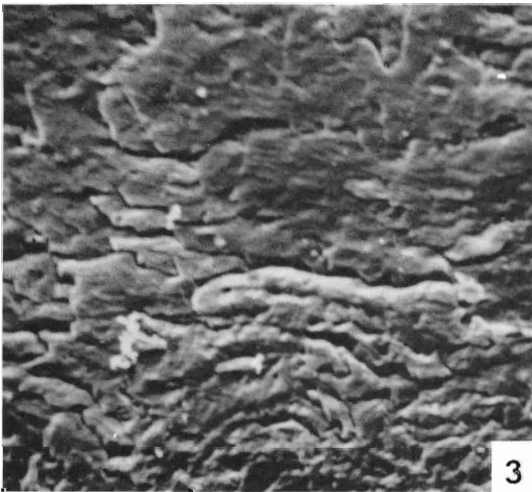
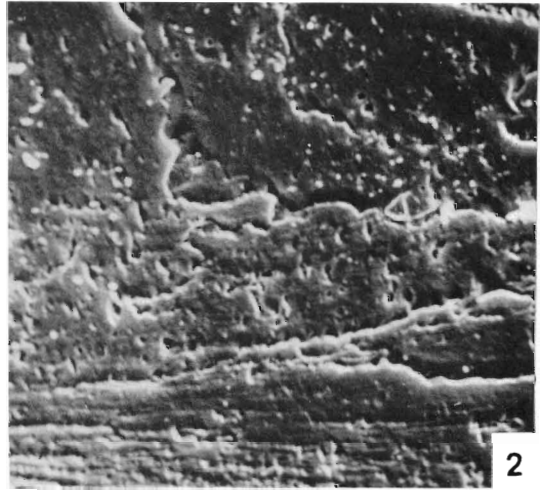
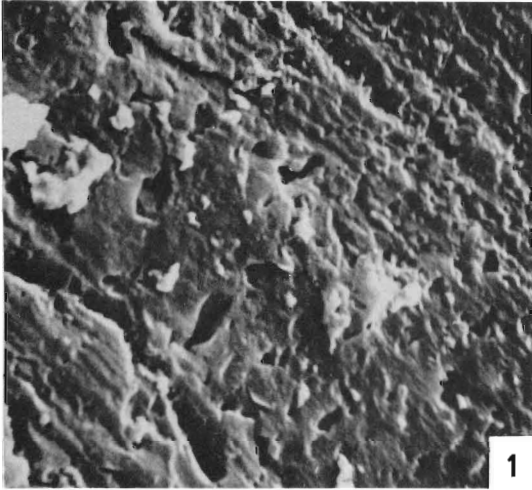
WILLIAMS and WRIGHT, Shell structure of calcareous inarticulate Brachiopoda



WILLIAMS and WRIGHT, Shell structure of calcareous inarticulate Brachiopoda



WILLIAMS and WRIGHT, Shell structure of calcareous inarticulate Brachiopoda



WILLIAMS and WRIGHT, Shell structure of calcareous inarticulate Brachiopoda